Evaluation of lipid-based formulations of poorly water-soluble drugs in the gastro-intestinal tract using in vitro tests

Yvonne Elisabeth Arnold

aus Schlierbach (LU), Schweiz

Basel, 2011

Genehmigt von der Philosophisch-Naturwissenschaftlichen Fakultät
auf Antrag von

Herrn Prof. Dr. Georgios Imanidis (Fakultätsverantwortlicher)

Herrn Prof. Dr. Theodor Güntert (Korreferent)

Basel, den 15. November 2011

Prof. Dr. Martin Spiess

Dekan

Damit das Mögliche entsteht,

muss immer wieder das Unmögliche versucht werden.

Hermann Hesse (1877-1962)

creative commons

Namensnennung-Keine kommerzielle Nutzung-Keine Bearbeitung 2.5 Schweiz

Sie dürfen:

das Werk vervielfältigen, verbreiten und öffentlich zugänglich machen

Zu den folgenden Bedingungen:

Namensnennung. Sie müssen den Namen des Autors/Rechteinhabers in der von ihm festgelegten Weise nennen (wodurch aber nicht der Eindruck entstehen darf, Sie oder die Nutzung des Werkes durch Sie würden entlohnt).

Keine kommerzielle Nutzung. Dieses Werk darf nicht für kommerzielle Zwecke verwendet werden.

Keine Bearbeitung. Dieses Werk darf nicht bearbeitet oder in anderer Weise verändert werden.

- Im Falle einer Verbreitung müssen Sie anderen die Lizenzbedingungen, unter welche dieses Werk fällt, mitteilen. Am Einfachsten ist es, einen Link auf diese Seite einzubinden.

- Jede der vorgenannten Bedingungen kann aufgehoben werden, sofern Sie die Einwilligung des Rechteinhabers dazu erhalten.

- Diese Lizenz lässt die Urheberpersönlichkeitsrechte unberührt.

Quelle: http://creativecommons.org/licenses/by-nc-nd/2.5/ch/   Datum: 3.4.2009

ABSTRACT

Novel active pharmaceutical ingredients are often poorly water-soluble. Such compounds may only partially dissolve or may precipitate during intestinal passage, potentially leading to incomplete drug absorption. Despite the importance of the process, the underlying in vivo as well as in vitro drug-precipitation mechanisms remain poorly understood. Several formulation principles, including lipid-based formulations, have been introduced to prevent drug precipitation in the gastro-intestinal tract. However, in vitro performance testing of these formulations is a topic of ongoing scientific discussions. Reliable in vitro tests as well as suitable monitoring tools to better analyze in vitro solubilization, precipitation, as well as lipolysis processes in the gastro-intestinal tract are required.

In the present thesis, dispersion, dissolution, precipitation, and lipolysis processes are discussed. We compared the results obtained with a paddle apparatus with those from a physiologically motivated flow-through cell taking lipolysis into consideration, using lipid-based formulations of a weakly acidic drug (Biopharmaceutics Classification System Class II). We tested pure indomethacin and the drug-containing self-microemulsifying drug delivery system (SMEDDS) using pure aqueous buffers and biorelevant media. The results of these dispersion/precipitation tests showed generally increased solubility of indomethacin in the SMEDDS compared with the solubility of the pure drug. One of the SMEDDS was superior compared to the others regarding the solubilizing capacity. This was demonstrated only in the flow-through test and dispersion in hydrochloric acid (0.1 N HCl). However, these results must be interpreted in the light of the lipolysis test showing that the observed differences in solubilization were not based on lipolysis. We concluded that suitable characterization

of SMEDDS involving an acidic drug should include a physiologically motivated flow-through test or dispersion/precipitation test in acidic environment, together with a lipolysis test.

We studied the effects of polysorbate 80 (PS80) on fenofibrate precipitation in the simulated intestinal medium using focused beam reflectance measurement (FBRM). We dissolved three different quantities of fenofibrate in six different mixtures of PS80 and ethanol (EtOH). After adding these formulations to biorelevant media, we evaluated the effects of micelles in the simulated medium in combination with PS80 on fenofibrate solubility and precipitation. Endogenous micelles in combination with PS80 micelles enhanced drug solubility and therefore reduced supersaturation. Compared to pure water, micelles of biorelevant media accelerated drug-precipitation kinetics. Addition of increasing amounts of PS80 to the biorelevant media prolonged nucleation time slightly and reduced the number of particles. We successfully introduced FBRM as a monitoring tool in biorelevant media.

In another drug precipitation test, we simulated the transfer from the stomach to the intestine using simulated gastric and intestinal media. We used online dynamic image analysis and inline Raman spectroscopy. Further, we analyzed concentration profiles of the model drug dipyridamole in the simulated intestine by high-performance liquid chromatography (HPLC), and we developed a kinetic nucleation and growth model that was fitted to the experimental data. Dynamic image analysis revealed a complex structure of the precipitated dipyridamole particles. These precipitated upon transfer to the intestinal medium and were described as star-like crystals or aggregates of elongated primary particles. Furthermore, Raman spectroscopy allowed the

monitoring of precipitation over time. By fitting the model to the data, nucleation and growth exponents were obtained. These were consistent with data published in the literature and provided perfect agreement between the model and data.

The last part of the work described in this thesis focused on in vitro lipolysis of lipid-based drug delivery systems. Dispersion and digestion processes mainly govern the fate of such systems. We studied concentration effects of six poorly water-soluble drugs on in vitro lipolysis rate of medium-chain triglycerides (MCT), and we compared the results with drug effects on oil viscosity and surface tension. First, we characterized the drugs by molecular modeling and determined an apparent in vitro lipolysis rate in biorelevant medium by potentiometric titration.

The different drugs exhibited varying effects on oil viscosity and surface tension. However, all drugs significantly lowered the apparent lipolysis rate of the oil. This effect was very similar among the different compounds and did not correlate with the effects on oil viscosity and surface tension. Orlistat was the exception in that it practically blocked lipolysis by direct inhibition. The other drugs affected lipolysis kinetics most likely by different mechanism(s). In the light of the obtained results, drug effect on oil viscosity or surface tension appeared to play a minor role in reducing lipolysis rate. The lipolysis kinetics were not affected by the drug load, which was deemed advantageous from a pharmaceutical viewpoint. Different dose strengths are therefore not assumed to alter lipolysis kinetics, which is beneficial for limiting the variability of in vivo drug release.

Moreover, we studied the digestibility of 10 excipients often used in lipid-based drug delivery systems. We introduced a mathematical model to describe in vitro lipolysis

kinetics, and we defined the relative half-lipolysis time that was independent of the set-up of the lipolysis test using Miglyol®812 as the reference excipient. The results indicated two classes of excipients. Some additives were partially hydrolyzed, while others displayed complete lipolysis. For the latter class, we used the lipolysis extent X as a function of time in a simplified mathematical model that provided a good first approximation of initial lipolysis kinetics. The relative half-lipolysis time was obtained from the model with Miglyol®812 as the reference and seemed to be a promising tool for comparing results of in vitro tests employing different experimental conditions.

In conclusion, the analytical tools and mathematical models provided new insights into in vitro solubilization, precipitation, as well as lipolysis in the gastro-intestinal tract. A more complete understanding already at an early stage of drug development allows the formation of new, much more efficient lipid-based drug delivery systems that minimize drug precipitation.

ACKNOWLEDGEMENTS

Ganz herzlich danken möchte ich allen guten Geistern im Hintergrund, die für einen stets reibungslosen Ablauf des Alltages gesorgt haben. Dieser Dank geht an der Hochschule für Life Sciences an Petra Eckert, Andreas Hauser und Christof Jeiziner. An der ETH Zürich gilt mein besonderer Dank Prisca Rohr.

Herzlich danke ich allen Kolleginnen und Kollegen des Instituts für Pharma Technology der Hochschule für Life Sciences, sowie allen Kolleginnen und Kollegen der Safety and Environmental Technology Group der ETH Zürich für die stets gute Atmosphäre und die unvergesslichen Momente innnerhalb als auch ausserhalb des Labors.

Mein besonderer Dank gebührt aber auch allen, die mich auf dem Weg zur Promotion in irgendeiner Form begleitet haben. Herzlich danken möchte ich Frau Rosemarie Bieri für Ihre langjährige, äusserst wertvolle Unterstützung. Ein spezielles Dankeschön für die stete, freundschaftliche Begleitung während meiner ganzen Dissertationszeit geht an Christine und ihre Familie. Last but not least geht mein ganz besonderer Dank an Irene, die mich während der Abschlussphase unermüdlich unterstützt hat und mir immer motivierend zur Seite gestanden ist.

TABLE OF CONTENTS

LIST OF FIGURES

LIST OF TABLES

LIST OF PEER-REVIEWED PUBLICATIONS

The following peer-reviewed publications were extracted from this thesis:

Arnold Y, Bravo Gonzalez R, Versace H, Kuentz M (2010). Comparison of different in vitro tests to assess oral lipid-based formulations using a poorly soluble acidic drug. **J Drug Del Sci Tech** 20(2):143-148.

Arnold YE, Imanidis G, Kuentz MT (2011). Advancing in-vitro drug precipitation testing: new process monitoring tools and a kinetic nucleation and growth model. **J Pharm Pharmacol** 63(3):333-341.

Arnold YE, Imanidis G, Kuentz MT (2011). Study of drug concentration effects on *in vitro* lipolysis kinetics in medium-chain triglycerides by considering oil viscosity and surface tension. **Eur J Pharm Sci** 44(3):351-358.

Arnold YE, Imanidis G, Kuentz MT. In vitro digestion kinetics of excipients for lipid-based drug delivery and introduction of a relative lipolysis half life. **Drug Dev Ind Pharm**, accepted.

LIST OF ABBREVIATIONS

A	Projected area
ANOVA	Analysis of Variance
API	Active Pharmaceutical Ingredient
ASD	Artificial Stomach Duodenal Model
BCS	Biopharmaceutics Classification System
c_g	Solubilized drug concentration in FaSSGF
c_i	Solubilized drug concentration
c_{sat}	Saturation concentration
Caco-2	Human colonic carcinoma cell line
CCD	Charge-coupled device
CLC	Chord Length Distribution
CMC	Critical Micelle Concentration
CNT	Classical Nucleation Theory
D	Diffusion coefficient
EHM	Estimated Hydrolysis Maximum
F_{tr}	Transfer rate
FaSSGF	Fasted State Simulated Gastric Fluid
FaSSIF	Fasted State Simulated Intestinal Fluid
FaSSIF V2	Fasted State Simulated Intestinal Fluid, Version 2
FBRM	Focused Beam Reflectance Measurement
FDA	American Food and Drug Administration
FeSSGF	Fed State Simulated Gastric Fluid
FeSSIF	Fed State Simulated Intestinal Fluid
FeSSIF V2	Fed State Simulated Intestinal Fluid, Version 2

ΔG	Total free energy
ΔG^*	Activation energy for nucleation
ΔG_s	Free energy change for the surface formation
ΔG_v	Free energy change for the phase transformation
gr	Particle growth exponent
h	Lipolysis half life
h_{rel}	Relative lipolysis half life
HCl	Hydrochloric acid
HIV	Human Immunodeficiency Virus
HLB	Hydrophilic-Lipophilic Balance
HPLC	High-Performance Liquid Chromatography
k_1	Hydrolysis reaction constant
k_{-1}	Hydrolysis back reaction constant
k_b	Boltzmann constant
k_{gr}	Particle growth constant
$K_m{'}$	Michaelis-Menten constant
k_{nu}	Nucleation constant
KCl	Potassium chloride
LCT	Long-Chain Triglyceride
LFCS	Lipid Formulation Classification System
ln	Natural logarithm
log P	Logarithm of the partition coefficient
LSD	Least significant difference
M_{pr}	Precipitated amount of drug
M_{sol}	Solubilized amount of drug

MCT	Medium-Chain Triglyceride
n	Nucleation exponent
NaCl	Sodium chloride
NaOH	Sodium hydroxide
NaTC	Sodium taurocholate
no wt	Unweighted mode
P	Lipolysis product molecule
p_0	Bubble pressure base value
p_{max}	Maximal bubble pressure
PBPK	Physiologically-Based Pharmacokinetic Model
PDI	Polydispersity Index
PEG	Polyethylene glycol
PhD	Doctor of philosophy
Ph.Eur.	European Pharmacopeia
pK_a	Dissociation constant
PLS	Partial Least Square
PS80	Polysorbate 80
Q	Lipolysis product molecule
r	Capillary radius
R	Hydrodynamic radius
r_c	Critical particle radius
RMSE	Root Mean Square Error
RMSEC	Root Mean Square Error of Calibration
rpm	Revolutions per minute
RSD	Relative Standard Deviation

S	Drug concentration
[S]	Concentration of ester bonds at a given time point
$[S]_0$	Concentration of ester bonds at the start of lipolysis
S_{eq}	Equilibrium solubility
SE	Standard Error
SEDDS	Self-Emulsifying Drug Delivery Systems
SGF	Simulated Gastric Fluid
SIF	Simulated Intestinal Fluid
SMEDDS	Self-Microemulsifying Drug Delivery Systems
sqr wt	Square-weighted mode
SS	Supersaturation
std	Standard deviation
t	Time
T	Absolute temperature
t_{gr}	Start time of particle growth
t_{nu}	Start time of nucleation
TBU	Tributyrin Units
USP	United States Pharmacopeia
UV/Vis	Ultraviolet visible spectroscopy
V_i	Volume at time point t
V_{i0}	Volume at time point 0
v_m'	Maximal rate
V_M	Molecular volume of precipitating drug
WDD	Waddle Disk Diameter
WHO	World Health Organization

X   Lipolysis degree

X_E Lipolysis degree, plateau value

LIST OF SYMBOLS

γ_{ns} Interfacial energy per unit area

η Viscosity

π Mathematical constant equal to 3.14159

σ_d Dynamic surface tension

1 INTRODUCTION AND OBJECTIVES

1.1 Introduction

Poor water solubility is a main reason for low bioavailability of new active pharmaceutical ingredients after oral intake. Poor solubility in gastro-intestinal fluids leads to slow and incomplete dissolution of drugs from solid dosage forms. For solubilized drugs, this can result in precipitation that leads to limited drug absorption with high inter- as well as intrasubject variabilities. Several formulation approaches to enhance drug solubility under physiological conditions have been described (Brewster, 2008; Kohri et al., 1999; Loftsson and Brewster, 2010; Rabinow, 2004; Veiga, 1998). One of them is the lipid-based drug delivery systems (Pouton, 1985). Bioavailability of poorly water-soluble drugs may be improved by dissolving them in lipid systems, including colloidal dispersions, lipid emulsions, and self-emulsifying drug delivery systems (SEDDS). However, the fate of a drug or formulation principle in the gastro-intestinal tract depends on various factors. The presence of food or excipients, changes in gastro-intestinal motility, as well as pH in the gastro-intestinal tract can affect drug solubilization in different ways, depending on the physicochemical properties of the active pharmaceutical ingredient. Improved understanding of such influences on drug solubilization is important for formulation development.

In vitro tests to evaluate drug and formulation behavior under simulated physiological conditions are essential for efficient drug development. Although a number of in vitro tests to predict the fate of a drug and formulation in the gastro-intestinal tract exist, some tests only mimic the environment in the stomach or in the intestine, while others simulate the whole gastro-intestinal passage including transfer from the acidic

conditions in the stomach into the more neutral conditions in the intestine (Gu et al., 2004; Kobayashi et al., 2001; Kostewicz et al., 2004; Vatier et al., 1998). However, the performance of drugs trapped in lipid-based delivery systems does not only depend on dispersion and/or dissolution. Additionally, digestion of the formulation components can significantly influence drug solubility. Therefore, lipolysis tests simulating digestion in the intestine were introduced (Fernandez et al., 2009; MacGregor et al., 1997; Reymond and Sucker, 1987; Zangenberg et al., 2001). Existing results revealed the high complexity of lipolysis processes.

In early work, in vitro tests were usually performed in simple buffer solutions. To increase the predictability of in vitro tests, biorelevant media for mimicking physiological conditions were introduced. More than 10 years ago, Galia et al. proposed fasted state as well as fed state media simulating the stomach and gut (Galia et al., 1998). More recently, Jantratid introduced improved media that allow a more realistic simulation of drug solubilization in the gastro-intestinal tract, since they contain substances of physiological relevance such as bile salts and phospholipids (Jantratid et al., 2008).

Despite the considerable efforts applied to biopharmaceutical research, the processes following oral administration of lipid-based formulations remain insufficiently understood. Once the formulation is in contact with the aqueous medium of the gastro-intestinal tract, complex processes are initiated. These are strongly influenced by the physiological conditions in the gastro-intestinal tract as well as the formulation properties.

1.2 Objectives

The goal of this PhD research was to gain new insight into the behavior of poorly water-soluble drugs in the gastro-intestinal tract using lipid-based formulations. This included the following parts:

1) Study of dispersion, dissolution, precipitation, and lipolysis of these drug formulations.
2) Implementation of novel analytical tools to monitor drug precipitation with respect to particle number and size and shape of the precipitates/aggregates.
3) Comparison of different in vitro tests used to evaluate drug formulations.
4) Where appropriate, establishment of theoretical models to describe the relevant processes.

As model compounds we selected poorly water-soluble drugs, including weak acids, weak bases, and neutral substances. The formulations consisted of pure oil, pure excipients, or SEDDS, including mixtures of oils, surfactants, and cosurfactants. We performed the experiments in acidic solutions or phosphate buffer, and in biorelevant media simulating the physiological conditions.

2 THEORETICAL SECTION

2.1 Biopharmaceutics Classification System

Modern techniques, such as high-throughput screening or combinatorial chemistry, facilitate the speedy identification of new, highly potent chemical entities. Very often new compounds exhibit higher molecular weights and lower water solubility compared to drugs already on the market (O'Driscoll, 2008). Substances in development are categorized by means of the Biopharmaceutics Classification System (BCS), introduced by Amidon et al. in 1995. This system is a valuable tool and forms part of the regulatory guidance issued by the American Food and Drug Administration (FDA) as well as World Health Organization (WHO) (Dahan et al., 2009). The system categorizes drugs into four classes depending on their solubility and permeability (Figure 2-1). Class I drugs exhibit high solubility and high permeability, Class II drugs show low solubility and high permeability, Class III substances demonstrate high solubility and low permeability, and finally, in case of Class IV drugs, both characteristics are low.
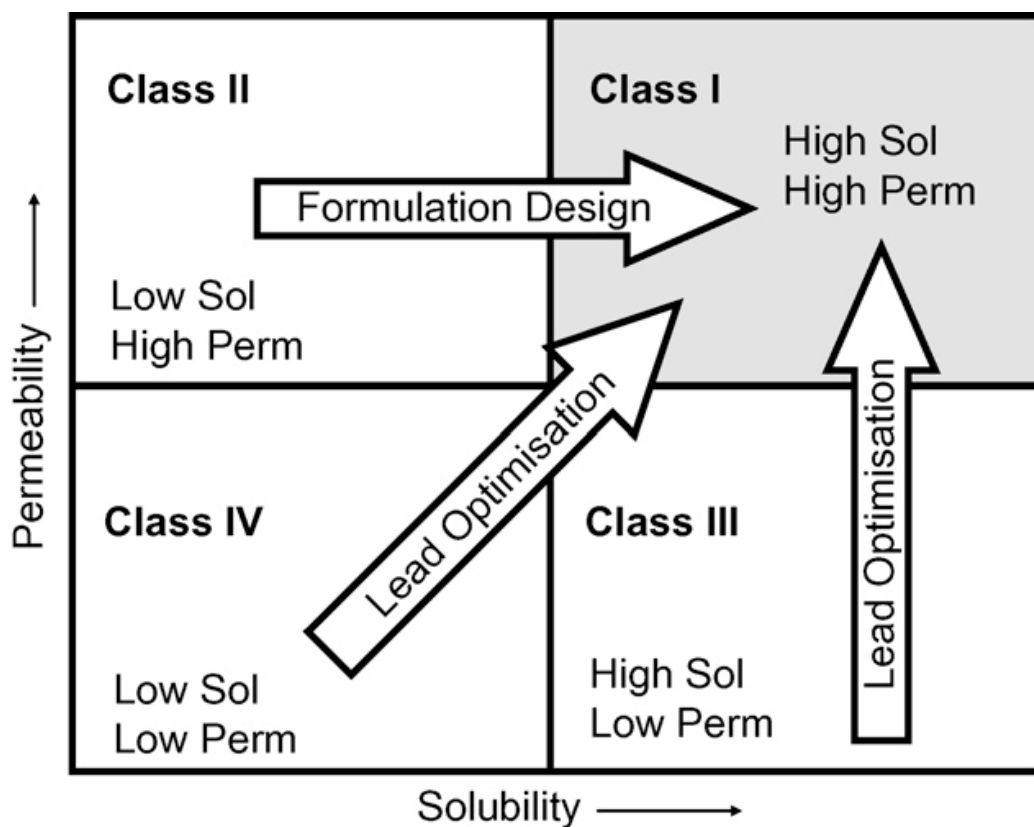
Figure 2-1: Biopharmaceutics Classification System (Pouton, 2006)

The BCS II substances present the greatest challenge in the field of pharmaceutical technology. If membrane permeability is good, the rate-limiting step is solubility that can be altered by formulation principles. As indicated in Figure 2-1, it would be possible to convert a BCS II drug into a BCS I drug, using a suitable formulation. Since only the dissolved fraction of drug is available for absorption, it is of prime importance to keep the drug in a solubilized state during the whole gastro-intestinal passage. Otherwise, the drug would exhibit poor and variable bioavailability.

2.2 Drug solubility in the gastro-intestinal tract

The FDA recommendations stipulate that drug solubility is determined by dissolving the highest unit dose of the compound in 250 ml buffer in the range between pH 1.0 and 8.0. A drug is considered highly soluble if the solubility volume is less than, or equal to, 250 ml. Solubility of a compound in the gastro-intestinal tract depends on various factors that change along the tract. The physicochemical parameters of the active pharmaceutical ingredient primarily define solubility. Substance properties such as pK_a, diffusivity, lipophilicity, surface area, hydrogen bonding, particle size, as well as crystal form can influence the solubilization behavior.

Moreover, the environment in the gastro-intestinal tract significantly affects solubility. Physiological as well as pathological processes can influence the environment in the stomach and intestine. Under physiological conditions in the fasted state, drugs undergo a marked pH change during gastro-intestinal passage. After the acidic conditions (pH 1.5-2) in the stomach, drugs are exposed to a more neutral environment (pH 4.9-6.4) in the intestine (Fleisher et al., 1999). This change is relevant for drug delivery, since many compounds are weak acids or weak bases. In such cases, pH affects ionization and therefore also the solubilization behavior of drugs. As an example, the weak base dipyridamole, $pK_a = 6.4$ (www.roempp.ch), is readily soluble in the acidic environment of the stomach. In the upper intestine, the pH is higher so that drug solubility decreases due to deprotonation. As a consequence, the base will precipitate. The opposite situation occurs with poorly water-soluble acids. They exhibit low solubility in the stomach and higher solubility in the gut.

Under fed conditions, the pH characteristics are different. In the early days, food in the gastro-intestinal tract was regarded as a barrier to absorption. It was recommended to take drugs on an empty stomach (Wagner, 1977; Welling, 1977). These days, it is

generally accepted that food typically influences the solubility of a drug and therefore can impact on oral bioavailability (Fleisher et al., 1999). Depending on the type of meal, the pH in the stomach increases and therefore precipitation of drugs in the stomach is different in the fed than the fasted state. In addition, gastric emptying varies, since the emptying rate is associated with the pH, volume of the content, calories, viscosity, and osmolarity (Fleisher et al., 1999; Shafer et al., 1985). As an example, the rate of gastric emptying decreases if the gastric pH increases and the other way round if gastric pH decreases. Under fed conditions, secretion of endogenous solubilizing components in the small intestine is enhanced. As reported by Persson et al., total bile salt concentration in the jejunum is 2 ± 0.2 mM in the fasted state but is as high as approx. 8 ± 0.1 mM in the fed state (Persson et al., 2005). These authors also reported that phospholipid concentrations increase by a factor of 15, from 0.2 mM under fasted conditions to 3 mM under fed conditions (Persson et al., 2005). Thus, the increased concentration of colloidal substance improves the solubility of poorly soluble drugs. Bakatselou et al. showed that the higher concentration of bile salts under fed conditions improves the solubility of steroids (Bakatselou et al., 1991). Moreover, concomitant intake of food increases the bioavailability of fenofibrate (which is approx. 30% when taken without food) by approximately 35% to 65% (Guay, 1999). Another factor affecting the solubility of drugs is the age of treated subjects. Studies have shown that 10% of individuals over 65 years of age have a gastric pH greater than pH 6 in the fasted state (Russell et al., 1994).

Apart from physiological factors, disease states may affect the solubilizing capacity in the gastro-intestinal tract. For example, subjects suffering from human immunodeficiency virus (HIV) tend to have a higher gastric pH, and cystic fibrosis

patients have a lower gastric pH (Herzlich et al., 1992; Youngberg et al., 1987). Furthermore, gastric pH can be influenced by concomitant treatment with other drugs. Blum et al. for example showed that an increase of the pH due to antacids lowers the bioavailability of the antifungal drugs fluconazole and ketoconazole (Blum et al., 1991).

In view of the complexity of the physiological conditions, it remains a challenge to keep the drug in a dissolved state during the entire gastro-intestinal passage, particularly since the conditions in the two parts of the gastro-intestinal tract are completely different. Therefore, development of efficient formulation principles that avoid drug precipitation requires a better understanding of drug precipitation processes. The following chapter gives an introduction into precipitation processes.

2.3 Precipitation

Poorly water-soluble drugs may precipitate in the gastro-intestinal tract. Precipitation is a complex process based on three steps. In a first, essential step, supersaturation has to be reached. This means that the concentration of the solubilized drug is above the saturation solubility. Equation 2.1 expresses the degree of supersaturation:

$$SS = \frac{S}{S_{eq}} \tag{2.1}$$

where S represents the actual concentration and S_{eq} is the equilibrium solubility. In a supersaturated system, the drug solution is thermodynamically unstable and will return to the equilibrium state by drug precipitation. Ostwald introduced the terms "metastable" and "labile" supersaturation (Ostwald, 1897). In case of metastable supersaturation, precipitation does not occur spontaneously, but in the presence of crystal seeds, nucleation and particle growth appear. In the labile zone, precipitation occurs in every case.

After supersaturation is reached, the process continues with nucleation. As shown in Figure 2-2, different types of nucleation exist. If a system does not contain any crystals, the process is named primary nucleation. Primary nucleation is subdivided into homogeneous and heterogeneous nucleation, depending if nucleation occurs spontaneously or if it is induced by foreign particles. In case of nucleation induction by crystals, the process is referred to as secondary nucleation.

Nucleation

primary

secondary
(induced by crystals)

homogeneous
(spontaneous)

heterogeneous
(induced by foreign particles)
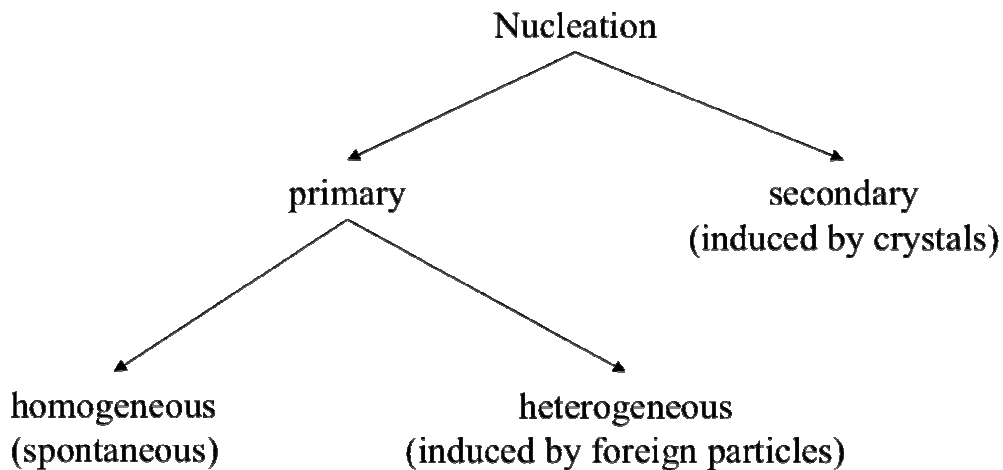
Figure 2-2: Nucleation nomenclature (adapted from Mullin, 2001)

Today, different models exist for describing nucleation processes (Erdemir et al., 2008; Vekilov, 2010). The most widely used theory is the Classical Nucleation Theory (CNT) developed by Gibbs (Gibbs, 1948). In this thermodynamic approach (see Figure 2-3), ΔG is the driving force of the nucleation processes. On the one side, there is the free energy change for the phase transformation ΔG_v, which favors particle growth, and on the other side there is the free energy change for the surface formation ΔG_s, which prefers particle dissolution. With small particles, ΔG_s causes an increase in total free energy. After reaching an energy maximum at the critical size r_c, total free energy decreases and nucleus formation can start. With heterogeneous nucleation, the free energy maximum at the critical size of the radius is lower than that with homogeneous nucleation.
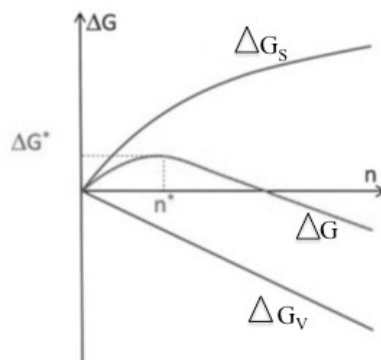
Figure 2-3: Free energy diagram for nucleation (Vekilov, 2010)

In case of homogeneous primary nucleation, the formation of stable nuclei is based on assumptions. It probably results from a sequence of bimolecular additions of molecules until the critical size is reached. Further addition of molecules leads to nucleation and particle growth (Mullin, 2001). The number of molecules in a stable nucleus varies from ten to several thousands. However, formation of critical nuclei is a dynamic process. As explained above, several steps are required before the critical size is reached and nucleation processes as well as particle growth can continue. The many subnuclei formed are labile and therefore redissolve rapidly.

In reality, homogeneous nucleation occurs rarely. Most nucleation processes are based on heterogeneous nucleation, since it is rather difficult to eliminate all foreign particles in a solution (Mullin, 2001).

Because lipid-based formulations were of primary interest in this PhD research, I discuss this formulation principle in detail below.

2.4 Lipid-based drug delivery systems

Based on the positive effects of food on bioavailability, lipid-based drug delivery systems were introduced in which the drug is solubilized (Hong et al., 2006; Porter et al., 2008). Thus, solid-liquid phase transition is avoided (Charman et al., 1992). Lipid-based drug delivery systems include lipid suspensions, lipid emulsions, or SEDDS. The latter is of special interest in this work. In 1985, Pouton established SEDDS (Pouton, 1985). At this time, solid-phase formulations were much more important than SEDDS but the successful marketing of the first lipid system changed this situation. Sandimmun[®] (cyclosporine A) proved the suitability of lipid-based drug delivery systems. Today, several lipid-based formulations are commercially available (Strickley, 2004; Strickley, 2007).

Lipid-based systems range from simple oils to complex mixtures (Pouton, 2006). In 2000, Pouton introduced the Lipid Formulation Classification System (LFCS), which takes the composition of the formulations as well as the fate of formulations in the gastro-intestinal tract into account (Pouton, 2000). Table 2-1 shows the classification system encompassing five types of formulations and their characteristics.

Excipients	Content of formulation (%, w/w)				
	Type I	**Type II**	**Type IIIA**	**Type IIIB**	**Type IV**
Oils	100	40-80	40-80	< 20	-
Water-insoluble surfactants (HLB < 12)	-	20-60	-	-	0-20
Water-soluble surfactants (HLB > 12)	-	-	20-40	20-50	30-80
Hydrophilic cosolvents	-	-	0-40	20-50	0-50

HLB: hydrophilic-lipophilic balance

Table 2-1: Lipid Classification System (Pouton, 2006)

The hydrophilic fraction increases from type I to type IV. Type I formulations contain only oil and require digestion to free fatty acid and 2-monoglycerides. These degradation products build colloidal dispersions within bile salt-lecithin mixed micelles. Due to its simplicity, type I formulations are the type of choice for drugs with a $\log P > 4$. Addition of lipophilic surfactants (Hydrophilic-Lipophilic Balance [HLB] < 12) to oils leads to type II formulations. Since they emulsify in aqueous solutions under gentle agitation, they are named "self-emulsifying drug delivery systems" (SEDDS). They are thermodynamically stable if there is a relatively small volume of the dispersed oil phase and a narrow range of droplet size distribution (Shah et al., 1994). The amount of surfactant should be in the range of 20% to 60% (w/w). Starting from a surfactant concentration of 25%, self-emulsification occurs. At concentrations around 65%, depending on the surfactant, the self-emulsifying process is slowed by a viscous liquid crystalline gel, formed at the oil-water interface. Such a

system is able to build a stable emulsion, but for emulsifying processes, energy is needed. Type III formulations contain hydrophilic surfactants (HLB > 12) and/or cosolvents such as EtOH, propylene glycol, or polyethylene glycol. They form very fine particles and are therefore named "self-microemulsifying drug delivery systems" (SMEDDS). Such microemulsion preconcentrates are of substantial interest to the pharmaceutical industry as well as academic research. Some recent articles reported the use of SMEDDS to formulate itraconazole (Woo et al., 2007), fenofibrate (Mohsin et al., 2008), vinpocetine (Chen et al., 2008), and oridonin (Zhang et al., 2008). Since the hydrophilic fraction can influence precipitation, type III formulations are subdivided into type IIIA and type IIIB formulations. The latter contains higher amounts of hydrophilic substances that enhance the risk of drug precipitation (Pouton, 2000).

In 2006, Pouton introduced an additional type IV formulation that solely contains hydrophilic surfactants and cosolvents (Pouton, 2006). Type IV formulations are used for drugs that are hydrophilic but not lipophilic. A disadvantage of these formulations is the tendency of high local surfactant concentrations that may cause irritations (Attwood and Florence, 1983). Therefore, if this formulation is used on a regular basis, it might not be well tolerated.

2.4.1 Oils

In lipid-based oral formulations, medium-chain triglycerides (e.g. coconut oil, palm seed oil, Miglyol) or long-chain triglycerides (LCT) (e.g. peanut oil, sesame oil, olive oil) are commonly used. Triglycerides enhance drug solubility in the gastro-intestinal tract. On the one hand, they stimulate secretion of bile salts and phospholipids. On the other hand, the degradation products after digestion form mixed micelles together with the endogenous bile salts and phospholipids (Hernell et al., 1990). To promote

drug solubilization, mixed glycerides are often incorporated into formulations (Pouton and Porter, 2008).

Efforts were made to test the solubilizing potential of the medium as well as long-chain triglycerides. It was shown that digestion of oils depends on the length of fatty acids (Porter at al., 2004; Sek et al., 2002). Digestion of a medium-chain triglyceride to a 2-monoglyceride and two fatty acids is faster than digestion of a long-chain triglyceride. This difference is of prime importance for a drug dissolved in oil. If digestion of triglycerides is slow, a poorly water-soluble drug can stay in the undigested oil for a longer time period. In case of faster digestion, the drug can be dispersed into the aqueous phase, or precipitation can occur.

Recently, a novel class of excipients for lipid-based drug delivery systems was tested (Holm et al., 2011). They compared an indigestible semi-fluorinated alkane, 1-perfluorohexyloctane, with a long-chain triglyceride and a medium-chain triglyceride. Since the results showed no clear benefits, the usefulness of semi-fluorinated alkanes as inherent part of lipid-based drug delivery systems is still uncertain.

2.4.2 Surfactants

Further components of lipid-based drug delivery systems are surfactants. They are amphiphilic molecules consisting of a polar head and a nonpolar tail, composed of saturated or unsaturated fatty acids. Depending on the properties of the head group, anionic, cationionic, amphoteric, or nonionic surfactants exist. At low concentrations, surfactants adsorb on surfaces or interfaces, reducing surface or interface tension. As shown in Figure 2-4, micelles are formed above the critical micelle concentration (CMC) of the surfactant.
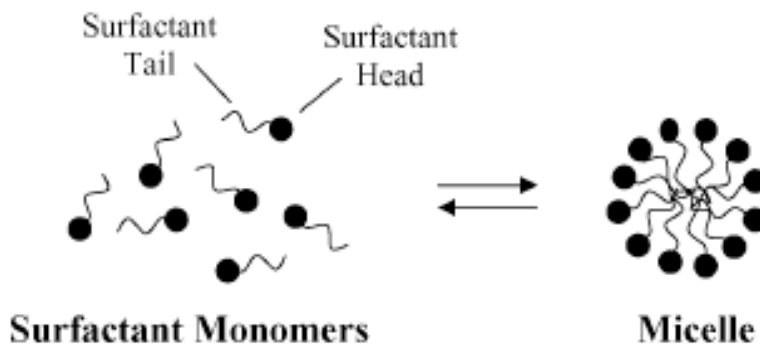
Figure 2-4 : Micelle formation (Rangel-Yagui et al., 2005)

The hydrophilic heads build the surface of the micelles, whereas the hydrophobic tails accumulate in the core of the micelle. Formation of micelles is based on intermolecular forces such as hydrogen bonds, van der Waals forces as well as hydrophobic, steric, and electrostatic forces. In addition, HLB values of the surfactants play an important role. Previous studies showed that the most efficient surfactants considering micelle formation are those with HLB values ranging from 12 to 15 (Thi et al., 2009). Regarding the inner, hydrophobic part of micelles, we can distinguish between two regions: one outer phase still containing water and an inner phase completely free of water. This is important for the solubilization capacity of micelles, i.e. the main advantage of this system.
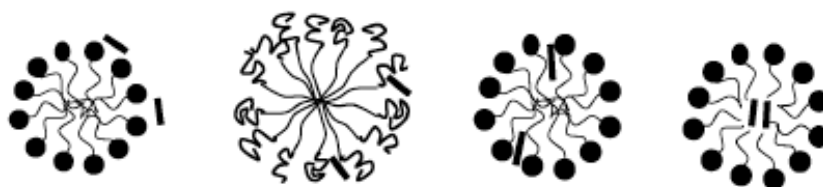
Figure 2-5: Possible locations of drugs in micelles (Rangel-Yagui et al., 2005)

Figure 2-5 shows different locations of drugs (**I**) in the micelles, depending on the drug properties. A nonpolar drug accumulates in the core of the micelle. Drugs with intermediate hydrophilicity/hydrophobicity accumulate in an intermediate position in

the micelle (Torchilin, 2001). In general, the position of the drug moves in the direction of the surface of the micelle with increasing polarity of the drug.

Nonionic surfactants are excellent solubilizing agents. They exhibit lower CMC values than the other surfactants. This is of main importance with respect to the physiological conditions in the gastro-intestinal tract. Micelles undergo marked dilution first in the stomach and afterwards in the intestine. It is known that only those micelles that consist of surfactants with low CMC values still exist after dilution in large volumes (Yokoyama, 1992). Micelles composed of surfactants with high CMC values dissociate after dilution, and the probability of drug precipitation increases immediately. In addition, nonionic surfactants show a good safety profile because they cause less mucosal irritation in the gastro-intestinal tract. However, nonionic surfactants can cause reversible changes in intestinal mucosal permeability leading to facilitated absorption of the co-administered drug (Gursoy and Benita, 2004).

2.4.3 Cosolvents

Cosolvents, e.g. EtOH, glycerol, polyethylene glycol, propylene glycol, or transcutol are used to facilitate dispersion of the surfactants and to increase solvent capacity (Pouton, 2006). For the latter purpose, high concentrations of cosolvents are needed. This increases the risk of precipitation, since cosolvents lose their solvent capacity in case of dilution in the gastro-intestinal tract (Pouton and Porter, 2008). Moreover, cosolvent concentrations have to be chosen carefully due to potential incompatibility with capsule shells (Cole et al., 2008).

A plethora of different lipid-based formulations can be constructed, and, depending on the drug, the behavior of each formulation may be different. Chambin et al. demonstrated that the polarity of a drug influences wettability, thermal behavior,

microscopic aspects, as well as the release properties of the lipid-based formulation (Chambin et al., 2009). However, in vitro tests for an early assessment of the fate of the formulation in the gastro-intestinal tract are of prime importance.

2.5 In vitro tests

In vitro tests for reliable prediction of the solubilization behavior of a drug/formulation under physiological conditions are indispensible. Such tests should predict the fate of a drug in the gastro-intestinal tract already at an early stage of development. Experiments in animals as well as humans could be minimized, thus lowering the costs and saving time. The following chapter gives an overview of the established in vitro tests.

2.5.1 Biorelevant media

The purpose of an in vitro test is to mimic physiological conditions as close to reality as possible. For dissolution testing, experiments are usually performed in water, aqueous hydrochloric acid, or aqueous buffer solutions (pH 4.4-8.0). However, these aqueous buffer solutions do not simulate physiological conditions. Efforts were made to develop test media simulating physiological conditions. At the beginning, media contained artificial surfactants without physiological relevance or they included physiological substances at concentrations different from the physiological concentrations (Dressman et al., 1998). Typically used media are Simulated Gastric Fluid (SGF) and Simulated Intestinal Fluid (SIF) (United States Pharmacopeia [USP], 2011). SGF is a hydrochloric acid solution, pH 1.2, containing large amounts of pepsin which differs from physiological conditions. Since pepsin is a protease, it is of minor importance for studying the fate of lipid-based drug delivery systems. SIF is a phosphate buffer, pH 6.8, containing large amounts of pancreatin, which is important for the digestion of lipid-based drug delivery systems. However, the

usefulness of pancreatin concentrations much higher than those encountered physiologically under fasted conditions is questionable. In 1998, Galia et al. introduced two media, simulating conditions in the proximal small intestine in the fasted as well as fed state (Galia et al., 1998). These media were used extensively in industrial and academic work. It was demonstrated that experiments performed in biorelevant media are suitable for in vitro/in vivo correlations (Dressman and Reppas, 2000; Nicolaides et al., 1999). The composition of these media was later modified to reduce costs and preparation time. In addition to the existing intestinal media, Vertzoni et al. created Fasted Stated Simulated Gastric Fluid (FaSSGF) for a better simulation of the physiological conditions than the gastric fluids of the USP (Vertzoni et al., 2005). As the comparison with human gastro-intestinal contents showed, there was still a need for improvement (Kalantzi et al., 2006). In 2008, Jantratid et al. introduced modified biorelevant media which were claimed to be of higher physiological relevance and better stability than the previous versions. Jantratid et al. developed an adjusted Fasted State Simulated Intestinal Fluid (FaSSIF V2) and "snapshot" media for simulating the fed state in the gastro-intestinal tract. "Early", "middle", and "late" Fed State Simulated Gastric Fluid (FeSSGF) as well as Fed State Simulated Intestinal Fluid (FeSSIF) simulate variable time points after meal intake. Although the biorelevant media are well adjusted to physiological conditions, discussions about the optimal composition are still ongoing und further adaptions are expected.

2.5.2 In vitro testing of oral dosage forms

2.5.2.1 USP dissolution equipments

In 1950, the USP introduced disintegration tests. Since it was recognized that only dissolved drug is available for absorption, it became clear that disintegration tests are

not suited for reliable prediction of in vivo/in vitro correlations. As a consequence, dissolution testing started in 1968, and the USP I apparatus was introduced (Cohen et al., 1990).

This was the onset of the development of various UPS apparatus. USP I and USP II apparatus are the most widely used equipments for testing the performance of oral drug delivery systems. Test media are placed in a standardized beaker under constant temperature and adjustable stirring rates. The only difference between USP I and USP II is the stirring device. Using USP I apparatus, capsules or tablets for testing are placed in a rotating basket. In contrast, in the USP II apparatus, the drug is placed in the reaction vessel and if the dosage form floats, it can be weighted with a sinker. A paddle is used as a stirrer. A suitable pH as well as an appropriate stirring speed has to be selected in both devices.

The USP I and USP II apparatus allow dissolution testing in one single reaction medium at defined pH. From a physiological point of view, the volumes of these dissolution tests are too large. Schiller et al. showed that the volumes in the stomach and small intestine are much lower (Schiller et al., 2005). Under fasted conditions, the volumes are in the range of 13 ml to 72 ml in the stomach and 45 ml to 319 ml in the small intestine. The volume in the stomach under fed conditions is much larger (534 ml to 859 ml). The volume in the small intestine is in the range of 20 ml to 156 ml.

The improved USP III apparatus was introduced in 1991. The reciprocating glass cylinders allow the simulation of a process in a moving medium. The hydrodynamics of the USP III are more favorable than those of the USP I and II (Jantratid et al., 2008). In addition, the USP III enables an easy change of the reaction medium for a better simulation of the physiological conditions. In the USP IV, employing the

flow-through method, the sample is placed in a flow-through cell, where the media can pass at different flow rates and where sink conditions are maintained. In an "open-loop" configuration, the cell is floated with fresh medium, and the volumes can be infinite. Using a "closed loop", the amount of medium is fixed and is recirculated through the flow-through cell. The volume of the medium can vary from a few milliliters to several liters if necessary. The advantages of the flow-through method over the methods utilized by USP I/II are different hydrodynamics and mixing effects. Contrary to the USP I and USP II, coning or dead zones are eliminated.

However, these compendial dissolution tests are limited in the predictability of physiological conditions. Therefore, additional tests were introduced by other groups and by us to improve the imitation potential.

2.5.2.2 Biopharmaceutical transfer tests

To improve predictability, drug transfer tests were introduced. An example of such a test is the artificial stomach duodenal model (ASD) (Vatier et al., 1990; Vatier et al., 1998). Drug is first dispersed in the "stomach chamber" and afterwards transferred into the "duodenum chamber", where the concentration of solubilized drug is monitored by ultraviolet visible (UV/Vis) spectroscopy. The model was successfully used in dog studies in both the fasted and fed states (Carino et al., 2006). However, caution is warranted if drug bioavailability is influenced by permeability and metabolism. In 2001, Kostewicz et al. came up with a biopharmaceutical test in which the drug is first dissolved in the simulated stomach medium and then transferred to the more neutral simulated upper intestine (Kostewicz et al., 2001). For simulating variable gastric emptying states, they used different transfer rates and to mimic motility, they varied the stirring rates. Another test was introduced by Kobayashi et al., which simulates not only drug transfer from the simulated stomach into the

simulated intestine but also the absorption step (Kobayashi et al., 2001). Three years later, Gu et al. developed a multicompartment dissolution system containing a simulated stomach compartment, an artificial intestinal compartment, and a simulated absorption compartment (Gu et al., 2004).

All these tests are closer to the physiological conditions than the compendial dissolution tests. However, in these biopharmaceutical transfer tests, a digestion step that is especially important for lipid-based formulations is still missing. Components of such formulations can typically be digested and therefore a digestion step should be considered in an in vitro test.

2.5.2.3   Lipolysis tests

Once a drug enters the upper intestine, digestion of the formulation starts. Lipolysis in the intestine is a complex process. Basic aspects of this biochemical process were excellently reviewed by Verger and Haas in 1976. They showed that lipases are special esterases that do not follow the Michaelis-Menten kinetics due to the interfacial catalysis. Lipolysis is influenced by the stereospecificity of the enzyme, the quality, and form of the reaction interface (monolayer, bilayer, micelles), the size of the substrate droplets, the orientation of the substrate molecules at the interface, the chain lengths of the substrates, and the presence of inhibitors that can be physiological or artificial substances.

Several groups have come up with lipolysis tests, simulating digestion processes in the intestine (Fernandez et al., 2009; MacGregor et al., 1997; Reymond and Sucker, 1987; Sek et al., 2002; Zangenberg et al., 2001). Comparison of the different in vitro lipolysis tests shows many experimental differences, such as duration of the tests as well as sampling times, for example. However, the most important differences comprise the use of media at different pH, varying amounts of formulation added, and

different activities of lipases. Another critical point is the addition of Ca^{2+}-ions, both with respect to the final concentration and the method of addition. Some groups added Ca^{2+}-ions as a bolus at the beginning of the experiments, while others added the ions continuously during the experiment. This experimental difference changes the reaction conditions significantly (Zangenberg et al., 2001). During digestion, liberated free fatty acids accumulate at the interface of the micelles and can sterically hinder the attachment of the lipase, resulting in a reduction of the lipolysis rate. Ca^{2+}-ions are added to form calcium soaps with the free fatty acids, which then precipitate and thus are removed from the surface of the micelles. If the Ca^{2+}-concentration is higher than the amount of free fatty acids, they can precipitate fatty acids incorporated in the mixed micelles and bile acids. Both reactions lead to a change of the micelle composition and consequently to an altered dissolution capacity (Larsen et al., 2008). Thus, Ca^{2+}-ions are needed to increase lipase activity (Alvarez and Stella, 1989).

Fernandez et al. established a new lipolysis test containing a gastric phase (Fernandez et al., 2009). This constitutes an eligible reaction step, since it is known that gastric lipases hydrolyze approx. 10% to 20% of the triglycerides (Fatouros and Muellertz, 2007). Another lipolysis test is in development by the group of Muellertz et al. They intend to combine a lipolysis test with drug absorption, using Caco-2 cell monolayers (Larsen et al., 2011).

At present, standard procedures for lipolysis testing do not exist. Comparison of the outcomes of different experiments is therefore rather difficult. Even though the experimental conditions are still under evaluation, lipolysis tests already demonstrated suitability with respect to the in vivo situation. Dahan and Hoffman demonstrated excellent correlation between in vitro data and bioavailability data of progesterone and vitamin D3 in rats (Dahan and Hoffman, 2006). In another experiment, Fatouros

et al. showed that in vitro results from lipolysis tests for probucol in three different formulations were in good agreement with in vivo results in fed minipigs (Fatouros et al., 2008).

2.6 Analytical tools: needs and challenges for monitoring drug precipitation in biorelevant media

Appropriate simulation of physiological conditions is one goal in the development of novel in vitro tests. In addition, the process of drug dissolution should be better understood, and reliable monitoring tools are indispensible. Especially drug precipitation in biorelevant media requires suitable analytical tools for close monitoring of precipitation. In chemical and pharmaceutical industry, various analytical technologies have been introduced, mainly in the context of process analytical technology with the aim to monitor manufacturing processes. In contrast, analytical tools to investigate biopharmaceutical in vitro processes are rarely used.

Process analytical tools can be used in different measurement modes such as offline, atline, online, inline, or non-invasive (Yu et al., 2004). With offline analytical methods, the sample is removed from the reaction mixture and is analyzed in a separate place, whereas with atline analysis, the sample is analyzed in a place close to the manufacturing site. Offline and atline methods have the disadvantages that the samples are analyzed with a time delay and may therefore have been altered. In online analytics, the samples are redirected to the analytical tool and immediately returned into the reaction mixture after analysis. Inline measurements provide real-time analysis by placing the sensor directly into the samples. An obvious disadvantage of this mode is that the process may be disturbed by contact with the probe.

Process analytics are used in several areas, e.g. in crystallization studies of new active pharmaceutical ingredients. UV/Vis spectroscopy, infrared spectroscopy, near-

infrared spectroscopy, Raman spectroscopy, FBRM, endoscopy, or chemical imaging techniques are used (Bugay, 2001; Gao et al., 2009; Simon et al., 2009; Stephenson et al., 2001).

It would be beneficial to use such analytical tools for drug precipitation monitoring in biorelevant media. As mentioned, monitoring the fate of the drugs under simulated physiological conditions is a rather unexplored field. However, the knowledge available based on the use of monitoring tools in different fields is advantageous. To obtain real-time results and to avoid errors in measurements due to subsequent treatments, inline or non-invasive analytical tools are favored. However, some media, e.g. Fasted State Simulated Intestinal Fluid (FaSSIF), are turbid, which can be a problem in the detection of very small precipitates since the detection is covered by the signals of the medium. The possibility of a "blind spot" in the analysis of the precipitates must to be borne in mind. Another disadvantage is the fact that biorelevant media hamper the detection of different polymorphs in the reaction mixture. Therefore, not every method is suitable as an analytical tool for biorelevant media. The tool has to be selected very carefully and research is needed to evaluate the most suited analytical tools for drug precipitation in biorelevant media.

3 COMPARISON OF DIFFERENT IN VITRO TESTS TO ASSESS ORAL LIPID-BASED FORMULATIONS USING A POORLY SOLUBLE ACIDIC DRUG

3.1 Introduction

In the following chapter we compared the behavior of formulations in dissolution tests as well as a lipolysis test. Oral lipid-based systems are often assessed using compendial dissolution equipment. Since the drug is generally dissolved in the formulation, the test primarily characterizes dispersion of the formulation and partitioning of the drug into the aqueous medium. In some cases, precipitation may occur and the tests can show the extent of drug redissolution. The suitability of the existing dissolution tests for lipid-based systems is currently not fully explored and is therefore an area of ongoing research.

Another area of current interest is to study the digestion of lipid-based systems by means of an in vitro lipolysis test. As mentioned before different in vitro lipolysis models are known (Cuiné et al., 2007; Fernandez et al., 2007; Zangenberg et al., 2001), which mainly differ by the way of how the calcium ions are added. Harmonization of the test protocols and a better understanding of these in vitro tests using lipid-based formulations are crucial for a rational and efficient formulation development.

In the present work, we used three formulations of type 3 of which one was semisolid and the others were liquid. These SMEDDS comprised oils, surfactants, cosolvents, as well as the model drug indomethacin, a weakly acidic BCS class II compound. Employing the USP II apparatus, we used 0.1 N HCl, phosphate buffer pH 6.8, and biorelevant media (Vertzoni et al., 2004; Vertzoni et al., 2005). The results were

compared with those of a dynamic USP IV method as well as with the outcome of a lipolysis test in biorelevant media.

3.2 Materials and Methods

3.2.1 Materials

Indomethacin ($pK_{a \ indomethacin}$ = 4.5 [Dollery, 1998]), sodium taurocholate, 4-bromophenylboronic acid, calcium chloride dihydrate, porcine pancreatin, hog pepsin, potassium chloride, potassium dihydrogen phosphate, potassium phosphate dibasic anhydrous, sodium chloride, 0.2 N hydrochloric acid, and 0.2 N sodium hydroxide were purchased from Sigma-Aldrich GmbH, Switzerland. Hydrochloric acid (1 N), hydroxide solution (1 N), monobasic potassium phosphate, and sodium hydroxide were obtained from Riedel-de Haën AG, Germany. Gelucire®44/14, Labrafil®M-2125 CS, and Transcutol®HP were supplied from Gattefossé GmbH, France. Ethanol 96 %, Imwitor®742, Miglyol®812, pepsin, and phosphoric acid 85 % were purchased from Hänseler AG, Switzerland. Cremophor®RH 40 and Solutol®HS 15 were obtained from BASF AG, Switzerland. Acetonitrile HPLC grade was supplied from Mallinckrodt Baker, Inc., United States, and phopsphatidylcholine was obtained from Lipoid GmbH, Germany.

3.2.2 Methods

3.2.2.1 Aqueous buffer systems and simulated gastro-intestinal fluids

Equilibrium solubility of indomethacin was determined in different aqueous buffer systems and simulated gastro-intestinal fluids.

The different citrate buffer solutions and phosphate buffer solutions were manufactured as described (Geigy, 1973). Phosphate buffer pH 6.8, containing NaCl, was prepared according to the European Pharmacopeia (Ph.Eur.), 2008. Table 3-1 shows the composition of various biorelevant media.

	SGF	SIF	FaSSGF	FaSSIF	FeSSIF
NaTC (mM)	-	-	$8*10^{-2}$	3	15
Lecithin (mM)	-	-	$2*10^{-2}$	0.75	3.75
KCl (mM)	-	-	-	-	204
KH_2PO_4 (mM)	-	50	-	-	-
Maleic anhydride (mM)	-	-	-	25	-
NaCl (mM)	34	-	34	109	-
NaOH (mM)	-	15.4	-	45	-
Pancreatin (g)	-	10	-	-	-
Pepsin (µM)	93	-	1.24	-	-
pH	1.2	6.8	1.6	6.5	5

SGF: Simulated Gastric Fluid, SIF: Simulated Intestinal Fluid, FaSSGF: Fasted State Simulated Gastric Fluid, FaSSIF: Fasted State Simulated Intestinal Fluid, FeSSIF: Fed State Simulated Intestinal Fluid

Table 3-1: Compositions of biorelevant media

3.2.2.2   Preparation of pancreatin suspension

Porcine pancreatin (3478 mg) was suspended in 20 ml FaSSIF. After stirring the suspension at room temperature (15 min, $25 \pm 0.5°C$), the suspension was centrifuged with an Eppendorf Centrifuge 5415C (15 min, 14000 rpm) from Vaudaux-Eppendorf AG, Switzerland. The clear supernatant was collected and pH was adjusted using 1 N NaOH. The resulting solution exhibited an enzyme activity of 10000 tributyrin units (TBU) per ml, whereas 1 TBU is the amount of enzyme that liberates 1 µmol of titratable fatty acid from tributyrin per minute. The solution was freshly prepared each day.

3.2.2.3   Preparation of self-microemulsifying drug delivery systems

Gelucire®44/14, Cremophor®RH 40, and Solutol®HS 15 were melted, and Labrafil®M-2125 CS was warmed up to eliminate flocculation. Afterwards,

formulations were prepared according to the following compositions: formulation 1 [Gelucire®44/14: Transcutol®HP: Labrafil®M-2125 CS, 76: 19: 5, w/w], formulation 2 [Cremophor®RH 40: Imwitor®742: Miglyol®812: EtOH, 34: 25.5: 25.5: 15, w/w], formulation 3 [Solutol®HS 15: Imwitor®742: Miglyol®812: EtOH, 34: 25.5: 25.5: 15, w/w]. Indomethacin was added (50 mg/ml). Hard gelatine capsules (size 0) from Capsugel Inc., Belgium, were filled with 0.5 ml formulation to achieve a dose of 25 mg API per capsule. For the experiments with pure indomethacin, 25 mg of API were manually filled in each capsule.

3.2.2.4 Saturation solubility

Saturation solubility of indomethacin was determined in aqueous and physiologically representative media as well as in the three formulations. Sample with drug excess (n = 3) were equilibrated for 24 h in the corresponding media using a constant stirring (785 rpm) at $37 \pm 0.5°C$. Aliquots were taken after 24 h of equilibration, centrifuged with an Eppendorf Centrifuge 5415C (15 min, 14000 rpm) from Vaudaux-Eppendorf AG, Switzerland, and the concentration of the clear supernatant was determined by HPLC.

3.2.2.5 Dynamic laser light backscattering

Dynamic laser light scattering is a technology in which a time correlation function of the scattered intensity is measured. The decay of this correlation function with time was used to calculate the diffusion coefficient of the particles, D. This property shares a mathematical relationship (Stokes-Einstein equation) with the hydrodynamic radius, R of a particle:

$$R = \frac{k_b T}{6\pi\eta D} \qquad (3.1)$$

Where k_b is the Boltzmann constant, T the absolute temperature, and η is the viscosity of the continuous phase. The dispersion technology software 5.0 (Malvern

Instruments Ltd., United Kingdom) calculated for each measurement a Z-average value together with the polydispersity index (PDI).

The instrument was a Zeta Sizer Nano ZS (Malvern Instruments Ltd., United Kingdom) having a 4 mW He-Ne Laser with a wavelength of 633 nm and the scattering signal was recorded at an angle of 173°. Measurements were conducted at ambient temperature.

3.2.2.6 Dispersion/precipitation tests

Dispersion/precipitation tests were conducted using the paddle method in an USP I/II apparatus (DT 600, ERWEKA GmbH, Germany). The dissolution media used were 0.1 N HCl, phosphate buffer Ph.Eur. pH 6.8, containing NaCl, FaSSGF, and FaSSIF. The volume of the media was 500 ml, the velocity of stirring 100 rpm, and the temperature 37 ± 0.5°C. Samples (1 ml) were taken (n = 3) after 5, 10, 15 and 30 min, and after 1, 2, 4, and 6 h. After filtering the sample through a regenerated cellulose membrane filter with 0.45 μm pore size (SUN-SRi, United States), the concentration of dissolved compound was determined by HPLC.

The flow-through tests were carried out with an USP IV apparatus (CE 7 smart, SOTAX AG, Switzerland) and performed as an open-loop setting. Each dissolution cell (internal diameter 22.6 mm) was charged with a ruby bead in the apex of the cone and glass beads above to generate a laminar flow. A dynamic media change was performed based on a physiologically motivated pH-cascade. pH-values and times were selected according to the pharmacokinetic modeling program Gastro Plus™ (Simulations Plus, Inc., United States): 0.1 N HCl (15 min), phosphate buffer pH 6.0 (16 min), and phosphate buffer pH 6.8 (3 h 02 min). The flow rate was 8 ml/min. Samples were collected (n = 3) at predefined times, filtered, and subsequently assayed by HPLC.

3.2.2.7 Lipolysis test

An aliquot of formulation (0.5 ml) was dispersed in 36 ml of FaSSIF at 37°C in a double-walled glass vessel. The solution was equilibrated for 15 min. By the addition of 4 ml pancreatin extract (1000 TBU/ml final concentration) and 5 mM calcium chloride dihydrate the lipolysis was started. Using 0.2 N NaOH the fatty acids released were titrated. Samples (4.4 ml) were taken (n = 3) after 5, 10, 15, 30, 45, and 60 min. After sampling, lipase was inhibited by adding 40 µl 4-bromophenylboronic acid (0.2 g/ml methanol). The samples were centrifuged at 20°C at 34000 rpm for 90 min in a Beckman L7 Ultracentifuge (Beckman Instruments, Inc., United States). The centrifuge tubes were Polyallomer Bell-Top Quick-Seal™ Tubes, size 16 x 38 mm (Beckman Instruments, Inc., United States). Aqueous phase was collected to determine the concentration of indomethacin via HPLC.

3.2.2.8 HPLC assay

HPLC was performed on a LiChrospher®60, RP select B 125-4 (5 µm) column (Merck KGaA, Germany). The mobile phase consisted of 50 mM phosphoric acid and acetonitrile (40:60 v/v), the flow rate was 1 ml/min, and the detection wavelength was 260 nm (Lunn and Schmuff, 1997-2000).

3.3 Results and Discussion

3.3.1 Solubility of indomethacin in different aqueous buffer systems, simulated gastro-intestinal fluids, and in formulations

Table 3-2 shows the solubility of indomethacin, a poorly soluble, weakly acidic drug, in different aqueous buffer systems, in simulated gastro-intestinal fluids, and in formulations at 37°C.

Solubility of indomethacin in	pH	Solubility (µg/ml)	Standard deviation (%)
Aqueous buffer systems			
Citrate buffer	4.0	1.55	3.9
Citrate buffer	5.0	8.75	2.2
Citrate buffer	6.0	77.58	2.6
Phosphate buffer	7.0	569.66	8.4
Gastro-intestinal fluids			
SGF	1.2	0.93	7.5
FaSSGF	1.6	1.33	51.9
FeSSIF	5.0	106.14	2.3
FaSSIF	6.5	397.89	0.9
SIF	6.8	516.2	1.6
Formulations			
Formulation 1	-	$71.67*10^3$	2.5
Formulation 2	-	$74.63*10^3$	2.6
Formulation 3	-	$76.47*10^3$	5.7

SGF: Simulated Gastric Fluid, FaSSGF: Fasted State Simulated Gastric Fluid, FeSSIF: Fed State Simulated Intestinal Fluid, FaSSIF: Fasted State Simulated Intestinal Fluid, SIF: Simulated Intestinal Fluid

Table 3-2: Solubility of indomethacin in different aqueous buffer systems, in gastro-intestinal fluid, and in formulations at 37°C after 24 h

As expected for a weak acid, the solubility at lower pH was clearly reduced as compared with the solubility of pH-values above the pK_a. This dominant pH-effect was also observed comparing the solubilities in the simulated gastro-intestinal fluids. Under acidic conditions in simulated gastric fluid, only a small amount of indomethacin was dissolved. The solubility increased in all the other media with higher pH. Solubility of the API at equal pH was higher in the biorelevant media than in simple buffers due to the drug solubilization in mixed micelles (Galia et al., 1998). The effect of bile salt and lecithin was evident comparing the solubilities of citrate buffer at pH 5 and FeSSIF at pH 5, whereas an approximately tenfold increase of

solubility occurred. Finally, we also determined the solubility in the formulations at 37°C to learn about differences. This initial drug solubility can be viewed as a starting solvent capacity of the formulation prior to the dispersion process. Substantial differences in the drug formulation solubility can influence the potential of a system to keep the drug solubilized. The results showed that all lipid-based systems had roughly similar equilibration solubility. All systems had an equal initial situation with respect to drug solubility and it would be the specific dispersion and lipolysis process that could make a difference regarding the fate of the formulations.

3.3.2 Dilution tests

Simple dilution tests primarily aim to characterize lipid-based formulations according to their type of self-emulsification. It is also of interest to check, if potential drug precipitation occurs. The ability to keep the drug solubilized in combination with a small final particle size can be viewed as positive indicators for viable lipid-based formulations (Pouton, 2000). Dilutions tests can therefore help screening initial formulation candidates.

SMEDDS formulation of indomethacin (50 mg/ml)	API	Dilution with water	Particle size (nm)	Standard deviation (%)	Polydispersity index (PDI)
Formulation 1	N	1:10	29.4	3.7	0.7
(semi-solid)	Y		14.2	0.7	0.16
	N	1:20	16.8	0.6	0.23
Gelucire®44/14 76%	Y		13	0.8	0.07
Transcutol®HP 19%	N	1:50	13	0.0	0.05
Labrafil®M-2125 CS 5%	Y		13.2	0.8	0.2
	N	1:100	13.2	0.8	0.07
	Y		62.1	59.7	0.19
Formulation 2	N	1:10	27.6	1.4	0.06
(liquid)	Y		17.8	0.6	0.18
	N	1:20	27.2	0.7	0.03
Cremophor®RH 40 34%	Y		16.4	0.0	0.13
Imwitor®742 25.5%	N	1:50	28.5	0.7	0.02
Miglyol®812 25.5%	Y		17.5	0.6	0.12
Ethanol 15%	N	1:100	28.7	0.3	0.02
	Y		20.6	0.5	0.11
Formulation 3	N	1:10	49.6	3.0	0.23
(liquid)	Y		258.7	0.6	0.58
	N	1:20	34.9	0.6	0.05
Solutol®HS 15 34%	Y		132.8	1.1	0.54
Imwitor®742 25.5%	N	1:50	47.4	1.9	0.2
Miglyol®812 25.5%	Y		22.6	0.9	0.27
Ethanol 15%	N	1:100	23.5	0.8	0.02
	Y		27.4	0.7	0.15

API: Y: yes, N: no

Table 3-3: Particle size of the different SMEDDS in various dilutions, consider that all solutions were clear

Table 3-3 shows that all formulations were SMEDDS, since they spontaneously formed transparent microemulsions upon aqueous dilution with a lipid droplet size of less than 50 nm (Gursoy and Benita, 2004). A previous work studied the evolving particle size of SMEDDS and outlined several influential parameters: the dilution factor, the medium, temperature, and formulation components (Ditner et al., 2009). In this study, the diluted systems without indomethacin reached very small particles already at a low dilution of 1:10. Microemulsions were obviously formed in a broad range along the dilution pathway, which can be called a robust dilution.

Interesting was the interaction of the evolving particle size and the dissolved API. Gershanik already reported that interactions between formulation and indomethacin led to changed particles, which may be the consequence of a modified self-emulsification process in the presence of the drug (Gershanik and Benita, 2000). This drug perturbation of the self-emulsification process resulted with formulations 1 and 2 often in a smaller particle size than obtained with dilution of the pure vehicles. This was, however, different in case of formulation 3. Dilutions at 1:10 and 1:20 provided enlarged particles being rather small droplets of high polydispersity than micellar drug assemblies. However, all of these dilution samples were macroscopically transparent showing no drug precipitation. The specific drug-effects on the particle size did evidently not lead to a macroscopic event like a phase separation or the crushing out of drug. Advanced formulation assessment therefore required the conduct of more refined in vitro methods than simple dilution.

3.3.3 Dispersion/precipitation tests

The dispersion/precipitation tests using the paddle apparatus were performed in different media. Experiments were conducted using 0.1 N HCl as well as phosphate buffer pH 6.8. In addition, the same tests were also performed in biorelevant media FaSSGF and FaSSIF. Figure 3-1, Figure 3-2, Figure 3-3, and Figure 3-4 show the kinetic profiles.
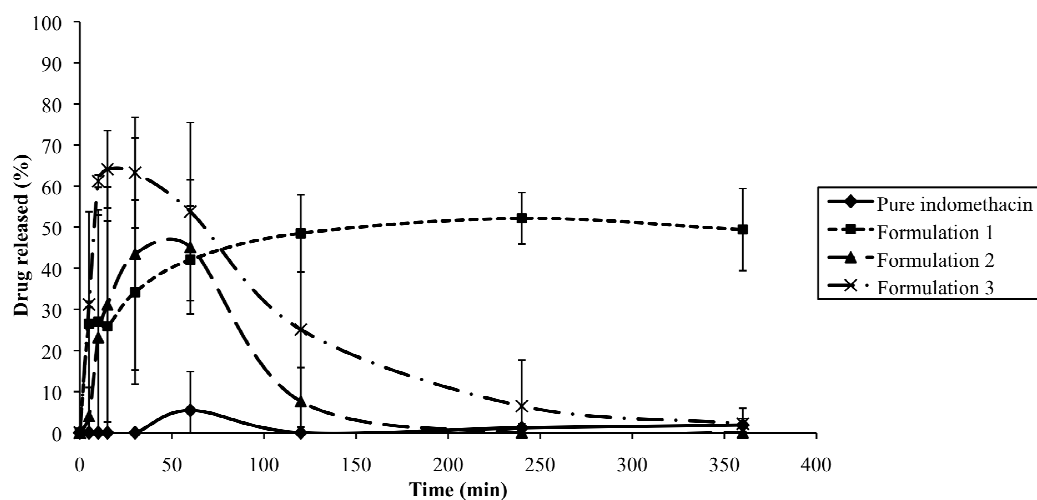
Figure 3-1: USP II dispersion/precipitation at 37°C in 0.1 N HCl using 25 mg pure indomethacin or 25 mg indomethacin in 0.5 ml formulation
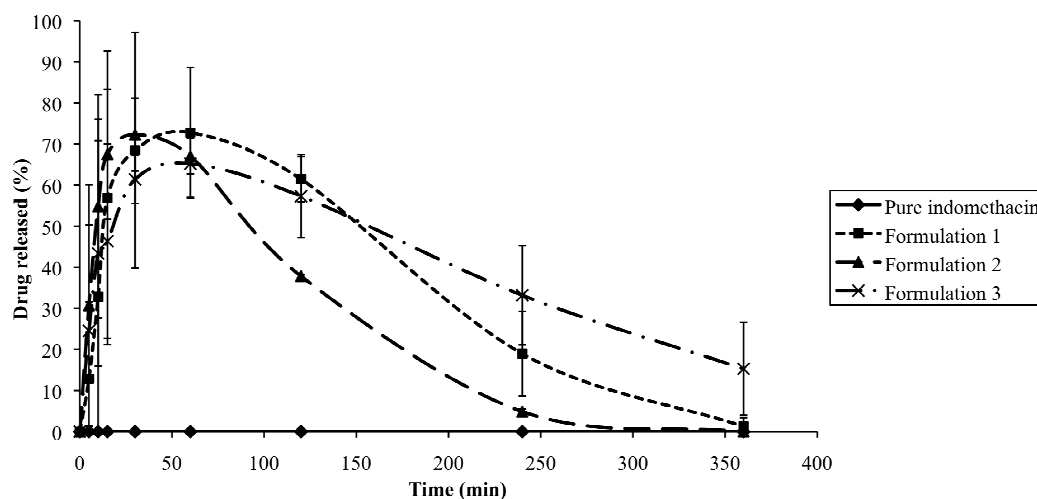
Figure 3-2: USP II dispersion/precipitation at 37°C in FaSSGF pH 1.6 using 25 mg pure indomethacin or 25 mg indomethacin in 0.5 ml formulation

As expected for an acidic drug, the release of indomethacin in 0.1 N HCl was very poor. This was in contrast to the much faster and extensive release of the API from the lipid formulations. However, also the lipid systems displayed differences in this acidic environment. Formulations 2 and 3 displayed a high initial release rate with substantial variability of the drug concentrations. Both delivery systems had declining

drug concentrations after about 30 min and 1 h, which indicated the precipitation of drug. Formulation 1 was able to keep the drug in solution, which could be an advantage over other formulations that would require a redissolution of the drug in the intestine.

It is important to better understand the ability of lipid-based systems to keep a drug in form. As previously reported by Pouton (Pouton, 2000; Pouton, 2008), the presence solubilized and type of cosolvent in the lipid-based formulations can drastically reduce their solvent capacity after aqueous dilution. Formulation 1 contained Transcutol®HP as a different cosolvent than EtOH that was present in formulations 2 and 3. Since EtOH is a small, fast-diffusing molecule, it is possible that a faster depletion of the cosolvent occurred in the swollen micelles of formulations 2 and 3 leading to a reduced ability to keep the drug solubilized.

In FaSSGF, practically no release of indomethacin was observed from the conventional capsules containing the active compound alone (Figure 3-2). In contrast, the maximum dissolved drug from formulations 1 and 3 appeared after 1 h, in case of formulation 2 already after 30 min. Although the drug solubility in FaSSGF was higher than in 0.1 N HCl, all formulations exhibited drug precipitation. In the biorelevant FaSSGF, formulation 1 could not maintain the drug solubilized in contrast to its performance in 0.1 N HCl. After 6 h, only 1.2% of the total amount was dissolved in the biorelevant medium, whereas in the experiment using 0.1 N HCl, 49.4% of indomethacin was still dissolved. It must be concluded that the components of FaSSGF substantially affected the dispersion and precipitation ability of this SMEDDS. The result also underpins the importance of media- and formulation specific effects that define the kinetic course of the dispersion (Charman et al., 1996; Kostewicz et al., 2001). It was remarkable to which extend the lipid formulations

were generally able to achieve a transient supersaturation in comparison with the pure drug. The acidic media were in that respect better suited to detect formulation differences than other media having higher equilibrium drug solubility.
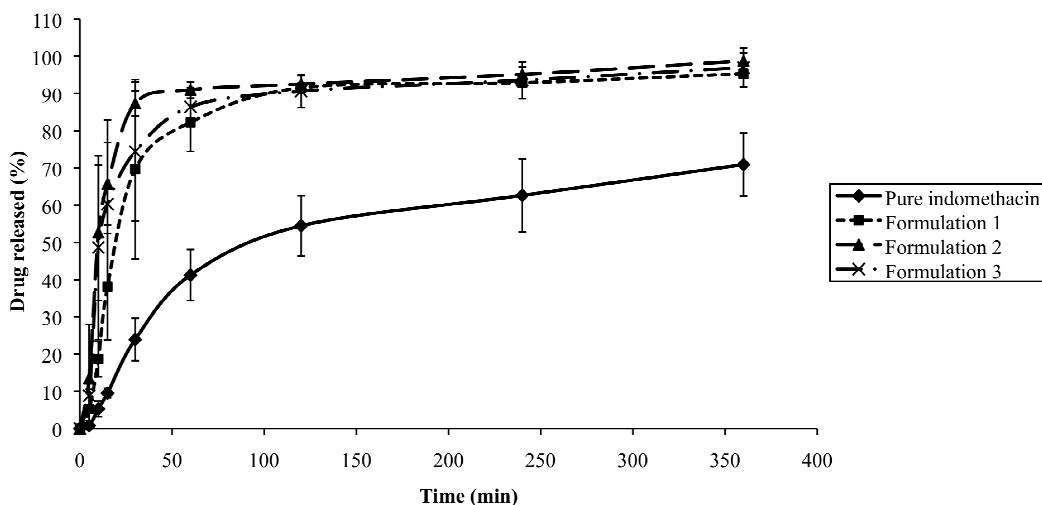
Figure 3-3: USP II dispersion/precipitation at 37°C in phosphate buffer pH 6.8 using 25 mg pure indomethacin or 25 mg indomethacin in 0.5 ml formulation
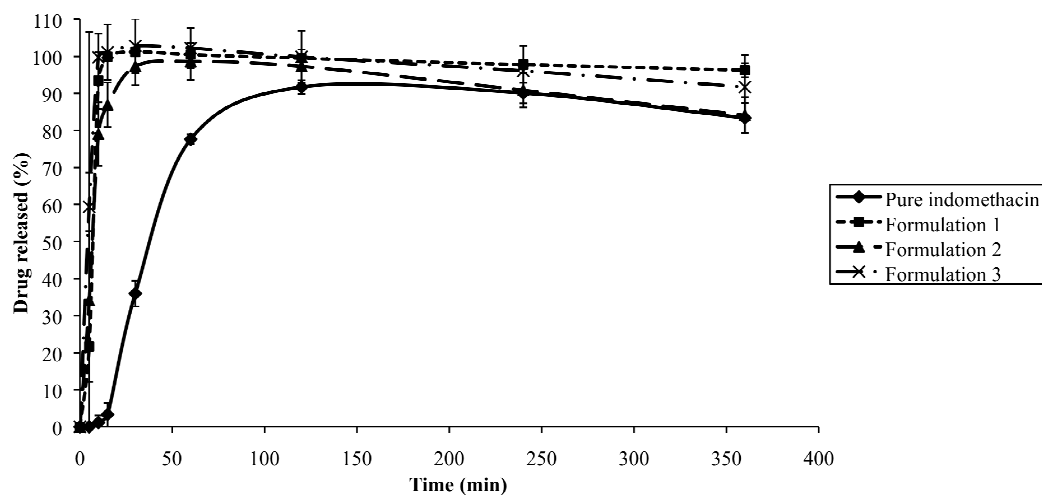
Figure 3-4: USP II dispersion/precipitation at 37°C in FaSSIF pH 6.5 using 25 mg pure indomethacin or 25 mg indomethacin in 0.5 ml formulation

In the experiments at higher pH, the results were less discriminating in comparison to the results in acidic environment. In buffer pH 6.8 (Figure 3-3), the formulations

reached the 90% level of solubilized API quickly (formulation 2 after 1 h, formulations 1 and 3 after 2 h), whereas the solubilized amount of pure indomethacin after 6 h was 70.9%. The results confirmed the difference between the pure drug and the lipid-based systems, but the latter formulations did not reveal substantial differences in this test.

Dispersion/precipitation tests in FaSSIF pH 6.5 (Figure 3-4) showed a maximum of dissolved indomethacin in all formulations after 30 min, the maximum of pure drug appeared 2 h after the beginning of the experiment. Formulations allowed solubilizing nearly the total amount of API (98.6% to 100%), whereas 90.7% of the pure indomethacin went into solution. The increase of the solubility of the pure drug in comparison to the results in phosphate buffer pH 6.8 was due to the bile salt and lecithin in FaSSIF. Like with the phosphate buffer pH 6.8, also FaSSIF pH 6.5 was a medium in which the acidic drug alone reached comparatively high solubility values. Certainly, the expected medium in the intestine is less challenging for an acidic drug than the environment of the stomach. From this physiological viewpoint the question can be raised, what would happen, if the drug first enters an acidic environment followed by media that mimic the intestinal conditions. Such dispersion using a cascade of physiological pH changes was obtained from the USP IV experiments.
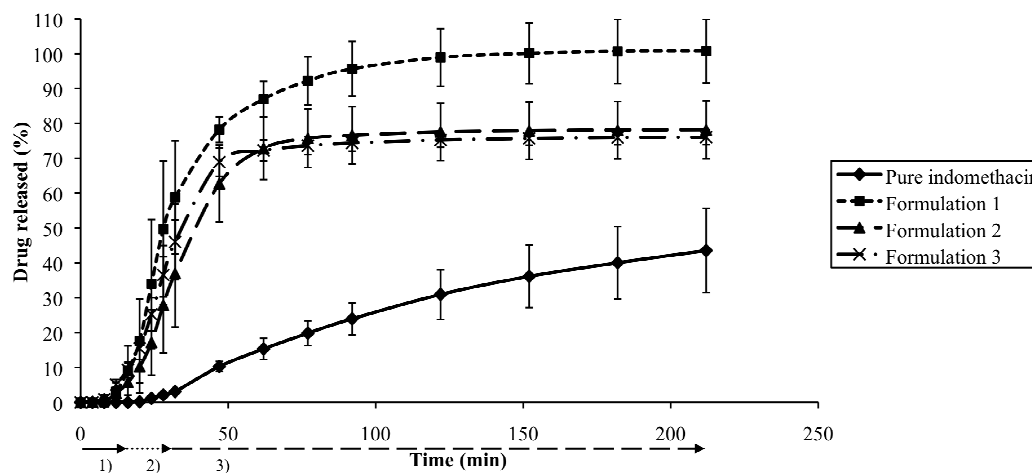
Figure 3-5: USP IV dispersion/precipitation at 37°C applying the pH cascade: 1) 0.1 N HCl (15 min); 2) phosphate buffer pH 6.0 (16 min); 3) phosphate buffer pH 6.8 (182 min) using 25 mg pure indomethacin or 25 mg indomethacin in 0.5 ml formulation

Figure 3-5 shows the results of the physiologically motivated flow-through cell. During the first 20 min, no indomethacin went into solution, if only pure API was used. Afterwards, indomethacin dissolved slowly. Following 3.5 h, 43.5% of the drug was dissolved. Dispersion of lipid-based formulations was in contrast much faster. In the course of the experiment, we observed a clear difference between the dispersion of the formulations. Formulation 1 exhibited a superior kinetic course regarding drug solubilization, whereas the formulations 2 and 3 reached a comparatively lower concentration plateau.

The dissolution investigations using the flow-through method with the USP IV as well as USP II instruments showed a clear difference between the dissolved amount of capsules with pure API and the lipid self-dispersing formulations of indomethacin. During the first 15 min in the USP IV test pure drug/formulations were exposed to 0.1 N HCl as in the experiments using the USP II apparatus. In both cases, no pure

drug went in solution. The rank order within the formulations was similar. Following a continuous change of the medium via pH 6 the drug/formulations were exposed to phosphate buffer at pH 6.8. The release of pure drug was always smaller than that of formulations. Regarding the formulations, a clear difference could be observed using these in vitro tests. The flow-through method was the only experiment in our series, which simulated the important transfer aspect from acidic to more neutral conditions. Due to this fact, that the API as well as the formulations were exposed to acidic and neutral conditions, this results obtained a special significance.

Interestingly, differences between formulations became apparent only under certain experimental test conditions of pH and dynamic media change. Although the effects of these conditions on dissolution of the drug alone are predictable, it is difficult to foresee their possible interactions with the more complex formulation systems. Additionally, the studied formulations differed in practically all of their components, which makes it difficult to clearly interpret their specific behavior. Therefore, the observed effects may be the result of confounding factors originating from the studied drug delivery systems and the experimental conditions. To clearly identify the individual contribution of formulation factors and test conditions on the release behavior, many additional experiments would be needed. Such test factors may include the individual excipients, the additives in the media as well as defined levels of hydrodynamic test conditions. In parallel to such a mechanistic investigation the in vivo relevance of these experimental findings should be demonstrated.

Additionally, the in vivo situation involves the digestion process of formulations. This aspect was considered following lipolysis tests.

3.3.4 Lipolysis in biorelevant media

Figure 3-6 shows the results of drug dispersion using a lipolysis assay. After 5 min of

lipolysis, formulations 1 and 2 reached the maximum of dissolved indomethacin

(69.6% and 75.7%, respectively). The maximum of dissolved amount API of

formulation 3 was obtained after 30 min. We noticed a minimal reduction of dissolved

amount during the continuation of the lipolysis. Pure indomethacin solubilized more

slowly. After an increase to 44.8% during the first 5 min, the dissolved amount raised

to 63.9% at the end.
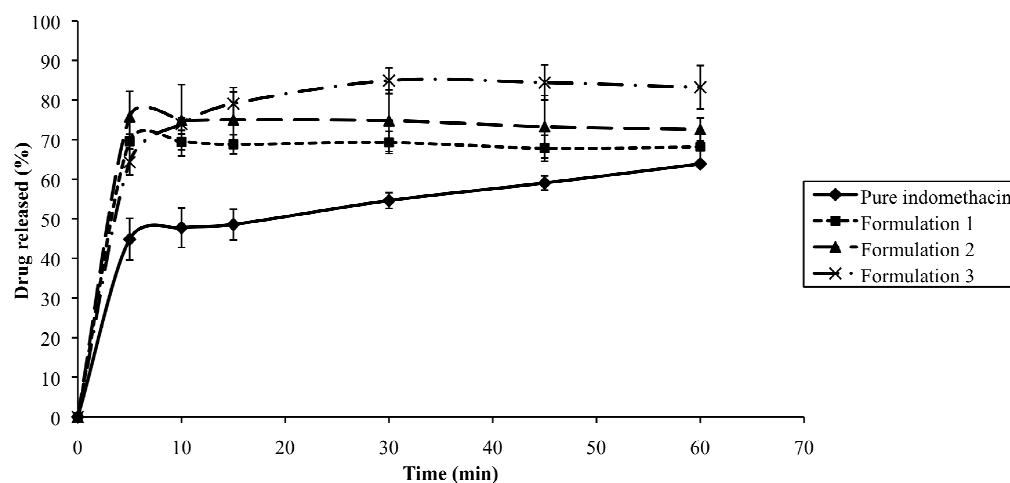
Figure 3-6: Lipolysis at 37°C in FaSSIF pH 6.5 using 25 mg pure indomethacin or 25 mg
indomethacin in 0.5 ml formulation

Once again the lipid-based formulations displayed higher solubilized drug

concentrations than the pure drug in a capsule. However, this concentration gap was

diminished following longer observation times in the experiment. A clear distinction

of the lipid formulations was not exhibited, but some tendencies were observed.

Interestingly, it was not formulation 1 that showed superior drug release, but in this

test formulation 3 had at least following 30 min the highest drug concentrations. The

dispersion behavior of the formulations was obviously affected by the lipolysis.

Effects cannot only happen on the level of the surface-active lipolytic products, but also by means of a lipolysis inhibition of the surfactant (Hutchison, 1994). These specific interactions of the formulation with the lipolysis were shown to be of relevance for the assessment of the formulations. Such effects of formulation digestion are important, as it was the case for considering media of different pH-values.

Regarding the presently used lipolysis test, the different hydrodynamics in comparison to compendial equipment must be mentioned. This aspect shows that currently all lipolysis tests are still research-oriented and there is a need to develop a compendial version in the future. Thus, the design would have to be standardize and the test conditions must be validated.

Even though the present study was focused on the comparison of in vitro tests and indomethacin was selected as model acid, the aspect of in vivo relevance should be discussed. Poorly soluble acids can exhibit incomplete drug absorption (Yazdanian et al., 2004). The reduced absorption can be problematic itself as well as the variability that usually occurs in parallel. As it was shown earlier the effect of incomplete drug absorption of a poorly soluble acid is depending on the dose (Kuentz, 2008). This problem of administering high doses is particularly a problem in the area of toxicological formulations. Poorly soluble drugs therefore provide an especially critical formulation task for the preclinical drug development phase. In case of indomethacin, rat studies at higher doses showed clearly increased absorption of a self-emulsifying system compared with a methyl cellulose suspension (Kim and Ku, 2000). Such in vivo results confirm the potential of lipid-based systems to increase drug absorption of poorly soluble acids. Differences among formulations are expected to be related to their ability to keep the drug in solubilized form. Our in vitro

results were able to show formulation effects in that respect. Furthermore, we found that currently a single compendial test may not be sufficient to fully characterize the dispersion behavior of a lipid formulation.

3.4 Conclusions

Based on the results of the different in vitro tests, we conclude that the combination of different modern in vitro tests provide the means to estimate the potential of new lipid-based formulations for poorly soluble acids. Since the pharmaceutical industry requires a fast and efficient formulation development, it is important to learn about the minimally required formulation tests. The solubilizing capacity of formulations depends on the components of the formulations, the physicochemical properties of the pharmaceutical ingredients, and the environment in the gastro-intestinal tract. The formulations of a poorly soluble acid may be screened by simple dilution tests, but promising candidate formulations must be further explored in dispersion/precipitation experiments. A discriminating acidic medium can be conducted together with a lipolysis test. As an option, the dispersion/precipitation test in the acidic medium can be replaced by a physiologically motivated flow-through test. Further research is needed to develop the most effective in vitro tests for lipid-based systems and also to learn about their relevance for in vivo. A proper in vitro assessment of SMEDDS is not only meaningful for administration in humans, but is also important with respect to preclinical formulations.

4 FENOFIBRATE PRECIPITATION IN THE SIMULATED INTESTINE – IN VITRO STUDY OF POLYSORBATE 80 EFFECTS ON NUCLEATION AND PARTICLE GROWTH IN BIORELEVANT MEDIA USING FBRM

4.1 Introduction

Since the number of poorly water-soluble drug is increasing, a deepened understanding of precipitation processes under physiological conditions is needed. New insights would facilitate the development of suitable formulation principles for drug solubility enhancement in the gastro-intestinal tract. Therefore, for a reliable prediction of the precipitation behavior of a drug, the knowledge about precipitation processes including the whole gastro-intestinal passage has to be improved.

To gain new insights into drug precipitation in biorelevant media, suitable inline tools are required for monitoring number, shape, and size of the arising precipitates. Gao et al. recently pioneered using FBRM in monitoring drug precipitation (Gao et al., 2009). The FBRM technique was used before in scientific applications other than in vitro testing (Chew et al., 2007; Hermanto et al., 2010; Leyssens et al., 2011). This tool appeared to be very promising for in vitro precipitation analysis. However, Gao et al. limited their study to drug precipitation in water, but more physiological conditions would be of more interest.

The aim of this work was to monitor the influence of PS80/EtOH formulations as well as the micelles and vesicles of the biorelevant media on precipitation processes of our BCS II model drug fenofibrate in the simulated intestine, after the passage through the stomach. All the experiments were performed in mixtures of water, FaSSGF, and FaSSIF V2. As analytical inline tool FBRM was used for the first time in biorelevant

media. The findings were complemented with additional measurements using the inline analytical tool Raman spectroscopy.

4.2 Materials and Methods

4.2.1 Materials

Fenofibrate, ammonium acetate, maleic acid, sodium chloride, and sodium hydroxide were purchased from Sigma-Aldrich GmbH, Switzerland. Pepsin and PS80 were obtained from Hänseler AG, Switzerland, sodium taurocholate was purchased from Prodotti Chimici e Alimentari S.p.A., Italy, and the egg lecithin Lipoid E80 was obtained from Lipoid GmbH, Germany. Finally, EtOH and acetonitrile HPLC grade were supplied from Mallinckrodt Baker, Inc., United States.

4.2.2 Methods

4.2.2.1 Preparation of formulations

Six formulations consisting of PS80 and EtOH were prepared. Table 4-1 shows the composition of the formulations, in which fenofibrate was solubilized in the following concentrations: 44.0 mg/ml, 81.6 mg/ml, or 118.8 mg/ml.

Formulation	Polysorbate 80 (ml)	Ethanol (ml)
1	0	0.250
2	0.050	0.200
3	0.083	0.167
4	0.125	0.125
5	0.188	0.063
6	0.250	0

Table 4-1: Compositions of the formulations

4.2.2.2 Preparation of simulated gastro-intestinal fluids

FaSSGF and FaSSIF V2 were used as biorelevant media. They were prepared as previously reported based on the components described in Table 4-2 (Jantratid et al., 2008).

	FaSSGF	FaSSIF V2
Sodium taurocholate (mM)	$8*10^{-2}$	3
Lecithin (mM)	$2*10^{-2}$	0.2
Maleic acid (mM)	-	19.12
Sodium chloride (mM)	34.2	68.62
Sodium hydroxide (mM)	-	34.8
Pepsin (µM)	1.24	-

FaSSGF: Fasted State Simulated Gastric Fluid, FaSSIF V2: Fasted State Simulated Intestinal Fluid V2

Table 4-2: Compositions of biorelevant media

4.2.2.3 Determination of solubilities and definition of supersaturation

To calculate the supersaturation values, the equilibrium solubilities were determined in the formulations, in the pure biorelevant media, and in the biorelevant media with added formulations. Drug excess was added to three samples per mixture that were equilibrated under intensive magnetic stirring at $37 \pm 0.5°C$. Aliquots were taken after 24 h of equilibration and subsequently centrifuged for 15 min at 14000 rpm using an Eppendorf Centrifuge 5415C from Vaudaux-Eppendorf AG, Switzerland. Finally, the clear supernatant was diluted with EtOH (factor 90 in case of pure formulations and factor 1.5 in the samples containing biorelevant media) and the concentrations of these solutions were determined by HPLC. The measurements were performed on a LiChrospher®60, RP select B 125-4 (5 µm) column (Merck KGaA, Germany). The mobile phase consisted of 25 mM ammonium acetate buffer pH 3.5 and acetonitrile (35:65 v/v). Samples of 20 µl were injected and analyzed at flow rate 1 ml/min, and

the detection wavelength was 287 nm (Thi et al., 2009). A calibration line was determined in the concentration range between 0.070 mg/ml and 1.115 mg/ml, which provided a R^2 of higher than 0.99.

Absolute supersaturation SS_{abs} at the beginning of the precipitation monitoring was calculated using equation 4.1:

$$SS = \frac{S}{S_{eq}} \tag{4.1}$$

where S is the corresponding fenofibrate concentration (597 µg/ml, 410 µg/ml, 221 µg/ml) and S_{eq} is the equilibrium solubility in the final mixture (FaSSGF, FaSSIF V2, API, PS80, EtOH, and water).

4.2.2.4   Experimental procedure of the in vitro precipitation test

In a 50 ml beaker, the reaction mixture was prepared as shown in Table 4-3. Detailed determination of the amounts of media and formulations is described in the appendix, section 9.1.1.

Time (min)	Activity
-2	Start medium: 5.5 ml FaSSGF, 37°C
-1	Addition of 11.0 ml water, room temperature
-0.5	Addition of 0.25 ml formulation (options see Table 4-1) containing fenofibrate (44.0 mg/ml, 81.6 mg/ml, or 118.8 mg/ml), room temperature
Start	Addition of 33.0 ml FaSSIF V2, 37°C, and
of the experiment	beginning of precipitation monitoring using FBRM

FaSSGF: Fasted State Simulated Gastric Fluid, FaSSIF V2: Fasted State Simulated Intestinal Fluid V2

Table 4-3: Experimental procedure of the in vitro precipitation test

The solution was mixed with an angular stirrer at 400 rpm and temperature was kept constant at 37°C using EasyMax 102 (Mettler Toledo International, Inc., Switzerland), while precipitation was monitored using a PI-8/91 LASENTEC® FBRM probe (Mettler Toledo International, Inc., Switzerland). Measurements were recorded every two seconds and data were binned into 100 logarithmically-spaced channels in the range from 1 µm to 1000 µm. As additional monitoring tools a Raman spectrometer was used. Raman spectra were determined with a Raman RXN2 spectrometer (Kaiser Optical Systems, Inc., United States). A laser emitting at the wavelength 785 nm and a detector of the type DV 420-OE were used to record spectra over the range from 100 cm^{-1} to 1890 cm^{-1}. To avoid the influence of the daylight on the measurements, the reaction vessel was completely covered with aluminum foil.

4.2.2.5 Analysis of data

Analysis of the variance (ANOVA) was calculated using the program Statgraphics Centurion XV ed. Professional from StatPoint Technologies, Inc., United States. Significance was assumed for those factors that demonstrated a probability p-value of less than 0.05.

4.3 Results and Discussion

4.3.1 Preliminary tests

4.3.1.1 Evolution of FBRM counts/s during preparation of biorelevant media

The FBRM signal was studied during preparation of the biorelevant media. Figure 4-1 indicated that most of the FBRM counts/s were given after the addition of lecithin. Before, the FBRM counts/s were generally low because all other components were well soluble in water. In contrast, lecithin is a water insoluble substance. In case of the preparation of FaSSGF (Figure 4-1a), the slight increase of FBRM counts/s was due to the addition of lecithin that was expected to form vesicles below the critical

concentration of mixed micelles. Regarding the preparation of FaSSIF V2 (Figure 4-1b), it is known that bile salts and lecithins form mixed micelles (Small et al., 1966). However, the elevated FBRM counts/s were most likely due to aggregated vesicles or other larger colloids. It was an interesting finding that the FBRM counts/s of the biorelevant media mixture decreased following addition of the formulation components. This effect will be discussed later in some more details.

a) b)
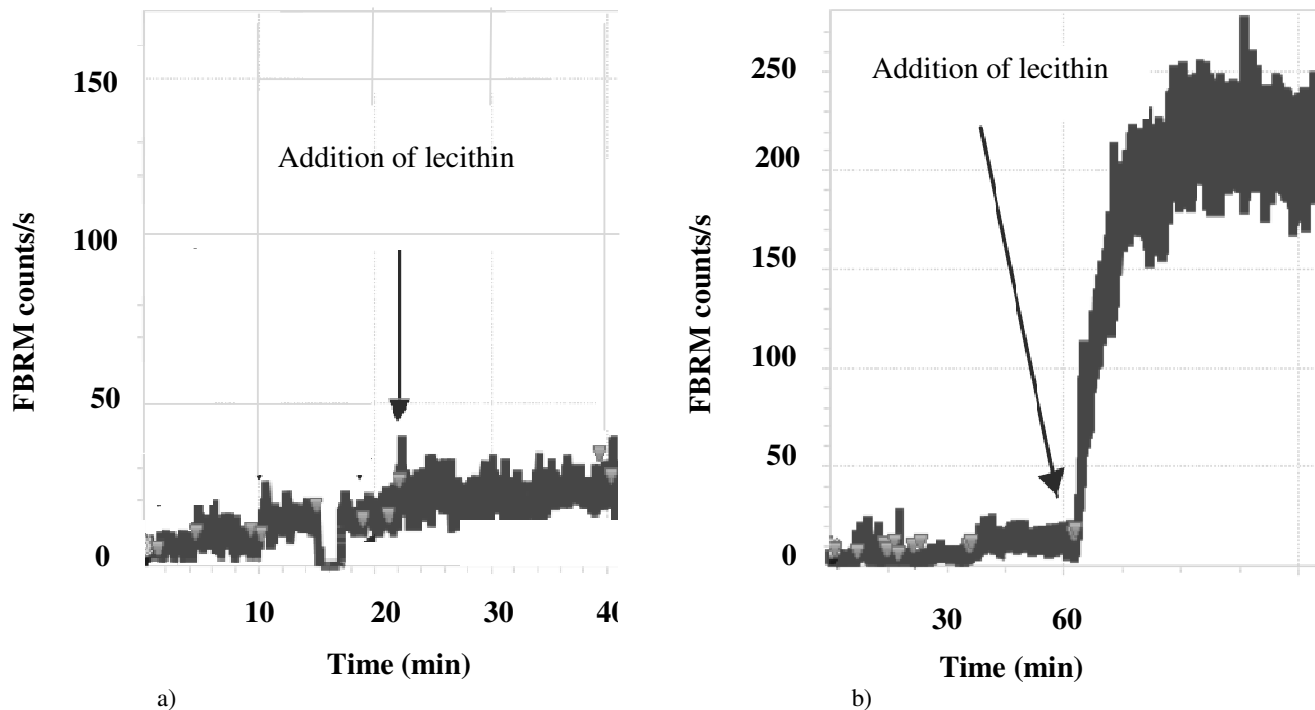
Figure 4-1: FBRM counts/s as a function of time during preparation of 50 ml medium, 37°C: a) FaSSGF, b) FaSSIF V2

As shown in Figure 4-2 the FBRM counts/s of the simulated stomach-intestine-water mixture were conserved after mixing these liquids and they were proportional to the volumetric ratios. Assuming an average FBRM counts/s for the FaSSGF of 190 and for the FaSSIF V2 of 320 (FBRM counts/s in water were 0) and knowing that the volumetric ratio stomach:water:intestine was 1:2:6, then the weighted average of the simulated biorelevant media mixture was about 234 FBRM counts/s which corresponded to the FBRM measurements reported in Figure 4-2. It can be concluded

that the FBRM sensor is a suitable tool to monitor the properties of the biorelevant

media so that reproducible quality of the media was assured for their use in the

following drug precipitation experiments.
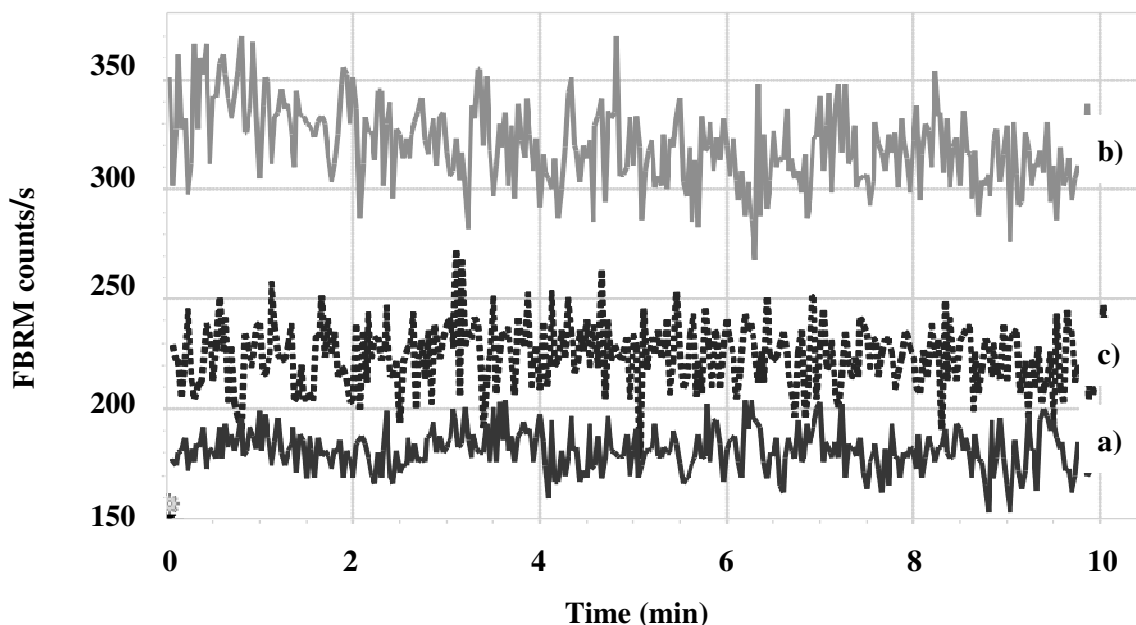
Figure 4-2: FBRM counts/s of the individual biorelevant media, 37°C: a) FaSSGF, b) FaSSIF V2,
c) simulated biorelevant media mixture (composition of the biorelevant media mixture see Table 4-3)

4.3.1.2 Evaluation of the effect of PS80 on the mixture of biorelevant media with respect to the FBRM measurements

Prior to the drug precipitation experiments, the changes in the FBRM signals due to

the addition of pure formulations to the biorelevant media mixture were analyzed.

Figure 4-3 shows that the number of FBRM counts/s specific for the biorelevant

medium was around a 250 FBRM counts/s baseline. Another observation was that,

with one exception, all the biorelevant media samples showed similar number of

FBRM counts/s, which demonstrated the good reproducibility of the medium

preparation. Interesting was the decreasing signal of the FBRM counts/s upon

addition of formulation. The effect was not seen by addition of pure EtOH so the

decreasing numbers of FBRM counts/s were due to PS80 alone.
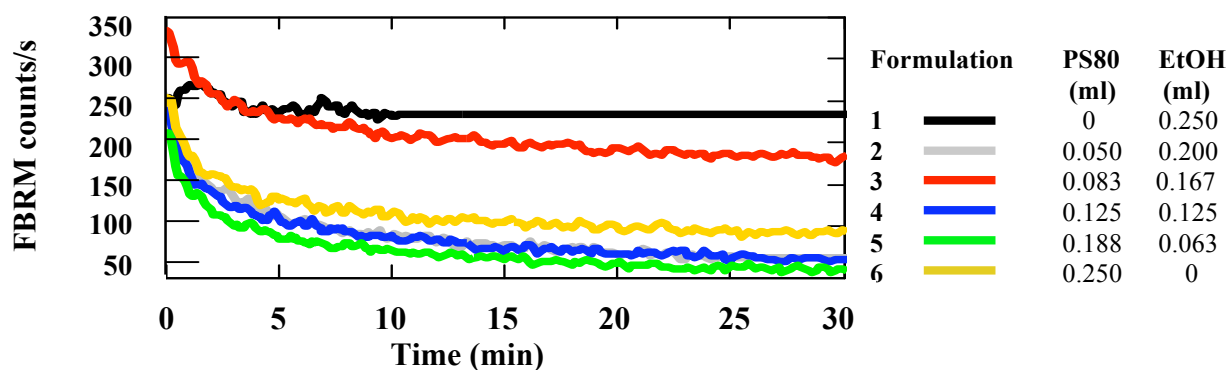
Figure 4-3: Simulated biorelevant media mixture, 37°C: FBRM counts/s of the biorelevant media mixture after addition of 0.25 ml formulation (options see Table 4-1)

To better understand the changes of FBRM counts/s in presence of PS80, Figure 4-4 plots the different chord length distributions (CLDs) before and after the addition of formulation 5 (0.188 ml PS80, 0.063 ml EtOH). It was shown that besides the decrease of the number of FBRM counts/s the mean of the CLD shifted towards larger values. This behavior was observed in all experiments.

PS80 is obviously interacting with the colloidal structures of the biorelevant medium. A reduction of aggregated colloids in favor of mixed micelles could explain the reduction of FBRM counts/s, since it was previously shown that polyoxyethylene chains of polysorbates reduce particle aggregation (Yanasarn et al., 2009). The formed mixed micelles were too small for detection using FBRM. Such interaction of the excipient PS80 with bile salts and lecithins is of interest with respect to drug solubilization. However, changes over time may influence accurate determination of FBRM counts/s in experiments with little precipitation. Experiments with

comparatively high amounts of precipitated drug are expected to be less affected by such changes.
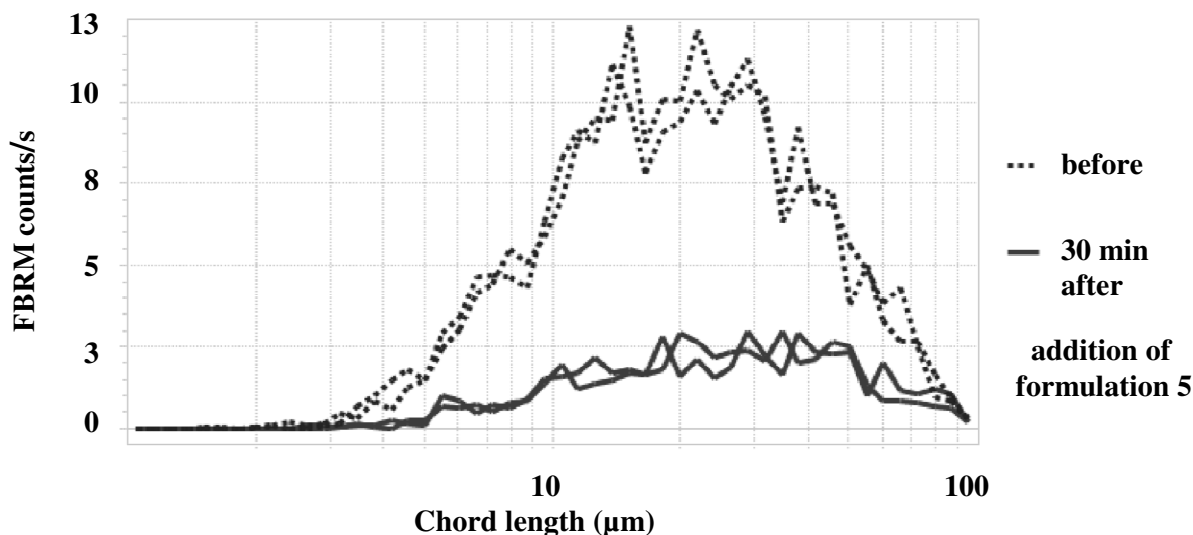
Figure 4-4: Simulated biorelevant media mixture, 37°C: FBRM chord length distributions before and 30 min after the addition of formulation 5 (0.188 ml PS80, 0.063 ml EtOH)

4.3.1.3 Effects of formulations on particles/vesicles of the biorelevant media mixture using Raman spectroscopy

The influence of formulation 5 (0.188 ml PS80, 0.063 ml EtOH) on the biorelevant media mixture was also analyzed using Raman spectroscopy, since it is known that particle size can affect the Raman intensity. It was found that after the addition of the formulation the integrated intensity between 1610 cm^{-1} and 1670 cm^{-1} changed from 2650 to 2735, which is about 3%. In order to investigate whether this change was due to a change of the number of lecithin micelles or due to the spectral characteristics of the PS80/EtOH formulation, the same experiment was conducted in pure water instead of biorelevant medium. It was found that the Raman intensity in the same range was also increased by 3%; therefore, it was concluded that the Raman measurements were only influenced by the addition of PS80/EtOH, while possible changes related to lecithin were not detectable.

4.3.2 Fenofibrate solubility and supersaturation levels

Equilibrium solubilities of fenofibrate were determined systematically in the pure

formulations as well as in the biorelevant media with and without formulations.

Figure 4-5 shows that equilibrium solubilities in the formulations differed

considerably from that in pure EtOH. Fenofibrate equilibrium solubility in pure EtOH

at 37°C was 50.29 ± 3.61 mg/ml. Compared to the value of 1 mg/ml published by

Cayman Chemicals, it was much higher. However, as soon as PS80 (0 ml to 0.25 ml)

was added, equilibrium solubilities at 37°C increased in the range of 101 mg/ml to

127 mg/ml. Among the PS80-containing formulations, increasing amounts of

surfactant were only slightly increasing equilibrium solubilities (Figure 4-5a). In

literature, a broad range from 0.7 mg/ml to 171 mg/ml of fenofibrate solubilities in

PS80 at room temperature was reported (Mongkonwattanaleela et al., 2010; Patel and

Vavia, 2007), while in our experiments an equilibrium solubility of 121 mg/ml was

found.

Solubility in water was found to be $0.4 \pm 0.0 \, \mu g/ml$. This value was close to the

equilibrium solubility at the same temperature of $0.3 \pm 0.0 \, \mu g/ml$ reported by Vogt et

al., 2008. Compared to pure water the micelles of the biorelevant media enhanced

equilibrium solubility at 37°C only slightly up to $0.7 \pm 0.0 \, \mu g/ml$.

As soon as PS80 was added, equilibrium solubilities in the biorelevant media mixture

increased. Figure 4-5b depicts the linearity of the equilibrium solubilities as a function

of the PS80 volumes. The formulations contained varying amounts of PS80 and

EtOH. The latter was either acting at the interface/headgroup region of the micelles or

was expected to reside in the water phase (de Campo et al., 2004). Since the

contribution of EtOH to drug solubility at 37°C was low (see intercept of Figure

4-5b), the effect of EtOH was neglected. The solubility increase was the outcome of

drug solubilization in colloids. However, the approximate linearity of the equilibrium solubilities as a function of the PS80 volumes in the biorelevant media indicated that solubilization was mainly due to micelle formation (Rangel-Yagui et al., 2005). Despite the moderate influence of PS80 on drug solubility in the formulation, the use of relatively high amounts of PS80 was appropriate, because these formulations were able to enhance drug solubility in biorelevant media. Therefore, our mixtures of PS80 and EtOH provided good model systems for in vitro drug precipitation studies.
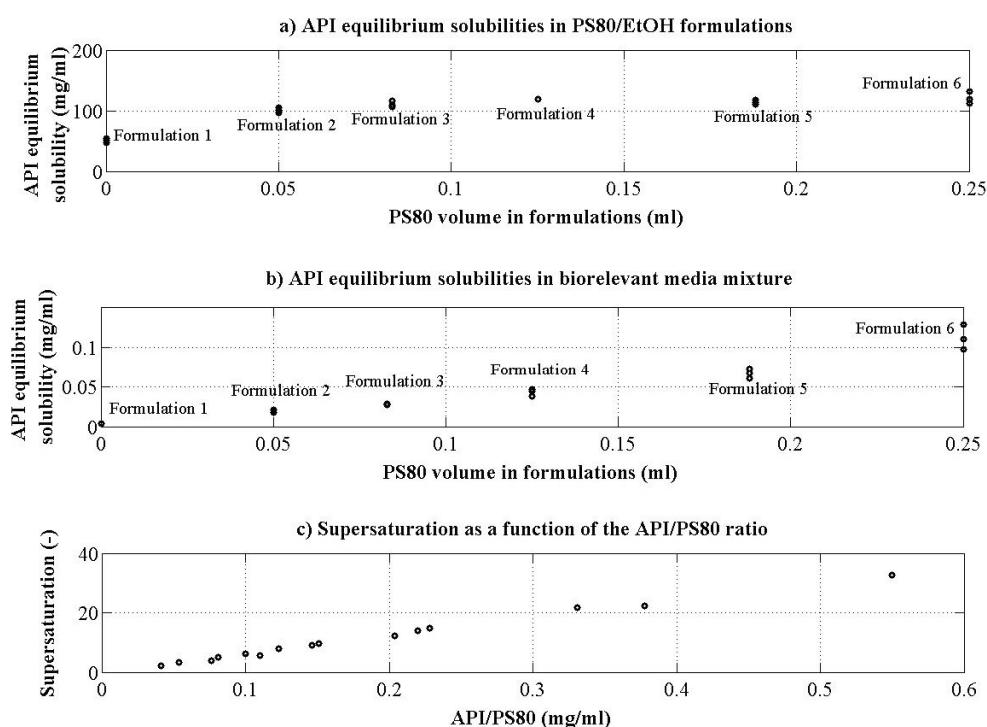
Figure 4-5: a) Fenofibrate equilibrium solubilities at 37°C in formulations (options see Table 4-1), b) Fenofibrate equilibrium solubilities at 37°C in 49.5 ml biorelevant media mixture including 0.25 ml formulation (options see Table 4-1), c) supersaturation as a function of the API/PS80 ratio

In a next step, supersaturation values of the formulations as well as of the formulations in the biorelevant media were calculated, since they are the driving forces of precipitation. A supersaturated solution is in a thermodynamically unstable state. To reach the thermodynamic equilibrium solubility, precipitation occurs

(Brouwers et al., 2008). In our work, supersaturation was influenced by the drug concentration and by the amount of PS80 in the formulation. In Figure 4-5c supersaturation is depicted as a function of the API/PS80 ratio and linearity was demonstrated. An enhancement of PS80 and/or a reduction of the drug concentration resulted in a lower supersaturation and therefore should reduce the precipitation potential. Thus, for the formulation development it seems useful to select a composition with respect to targeting low supersaturation levels.

4.3.3 Fenofibrate precipitation in the simulated intestine monitored using FBRM

4.3.3.1 FBRM analysis of fenofibrate precipitation in simulated intestinal medium

Drug precipitation in biorelevant medium was monitored using FBRM. In all measurements, the probe was placed at exactly the same position, since it was previously shown that the results are sensitive to the location of the probe (Barrett and Glennon, 1999). Three drug concentrations in six formulations, including different amounts of PS80, were tested. The simplicity of the formulation compositions allowed the evaluation of the influence of different amounts of PS80 on fenofibrate precipitation. In addition to the measurements in biorelevant media, the precipitation behavior of formulation 4, including 118.8 mg fenofibrate/ml, was monitored in pure water. Figure 4-6, Figure 4-7, and Figure 4-8 show the FBRM trends of the three drug concentrations in all the formulations in the range from 1 µm to 20 µm as a function of time.
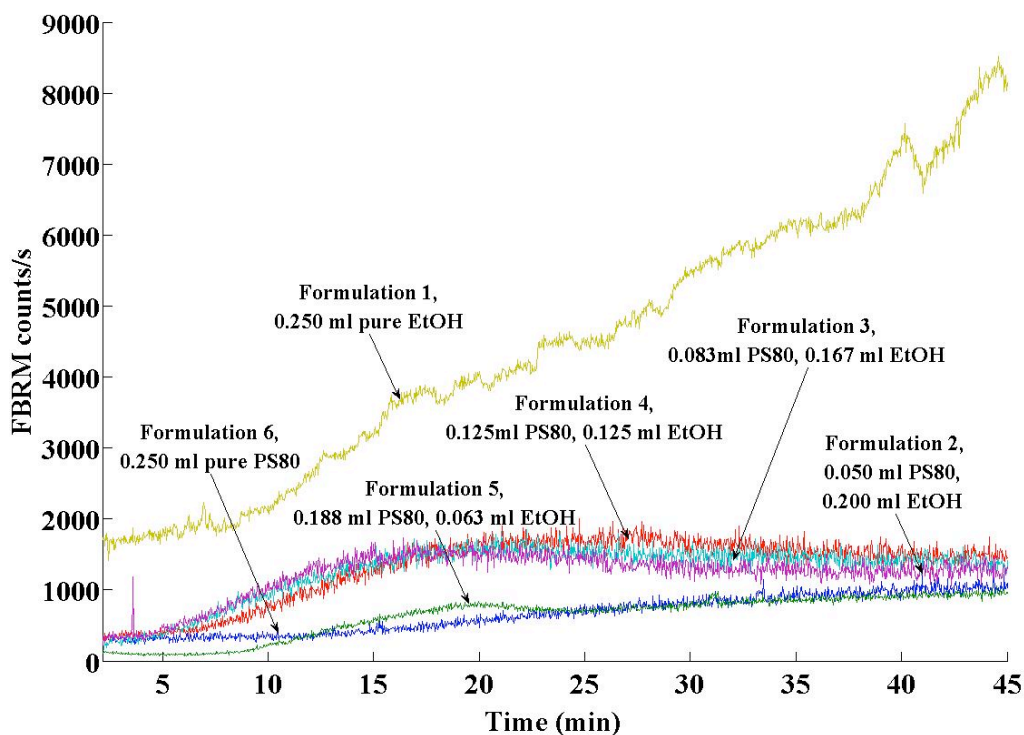
Figure 4-6: 49.5 ml biorelevant media mixture, 37°C: FBRM counts/s in the range from 1 µm to 20 µm as a function of time, 44.0 mg drug/ml formulation
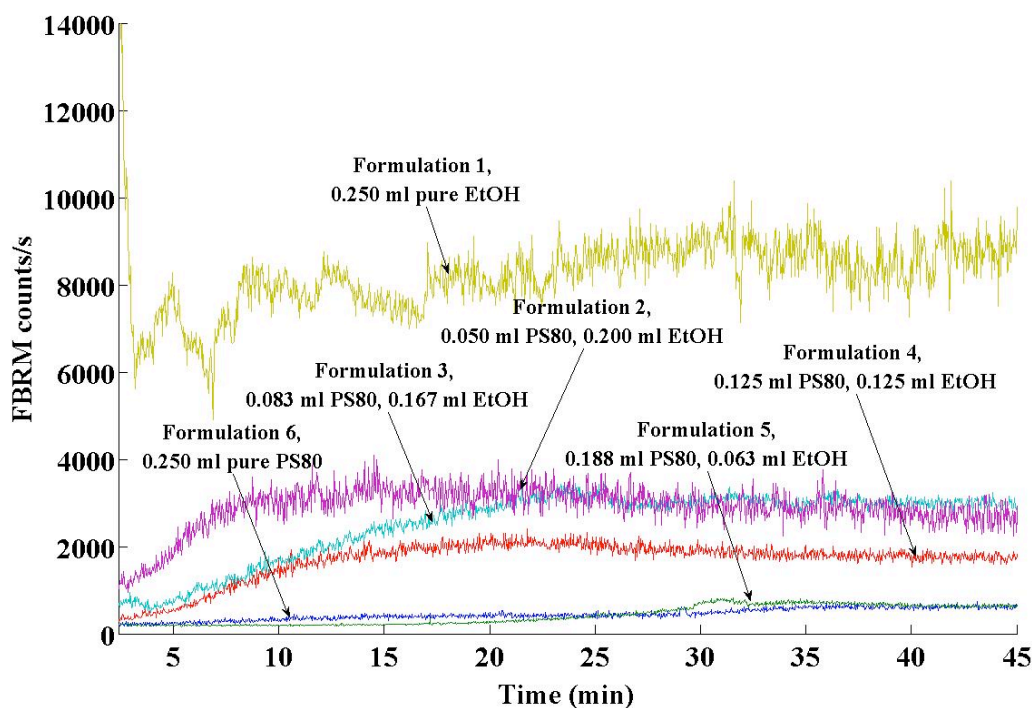
Figure 4-7: 49.5 ml biorelevant media mixture, 37°C: FBRM counts/s in the range from 1 µm to 20 µm as a function of time, 81.6 mg drug/ml formulation
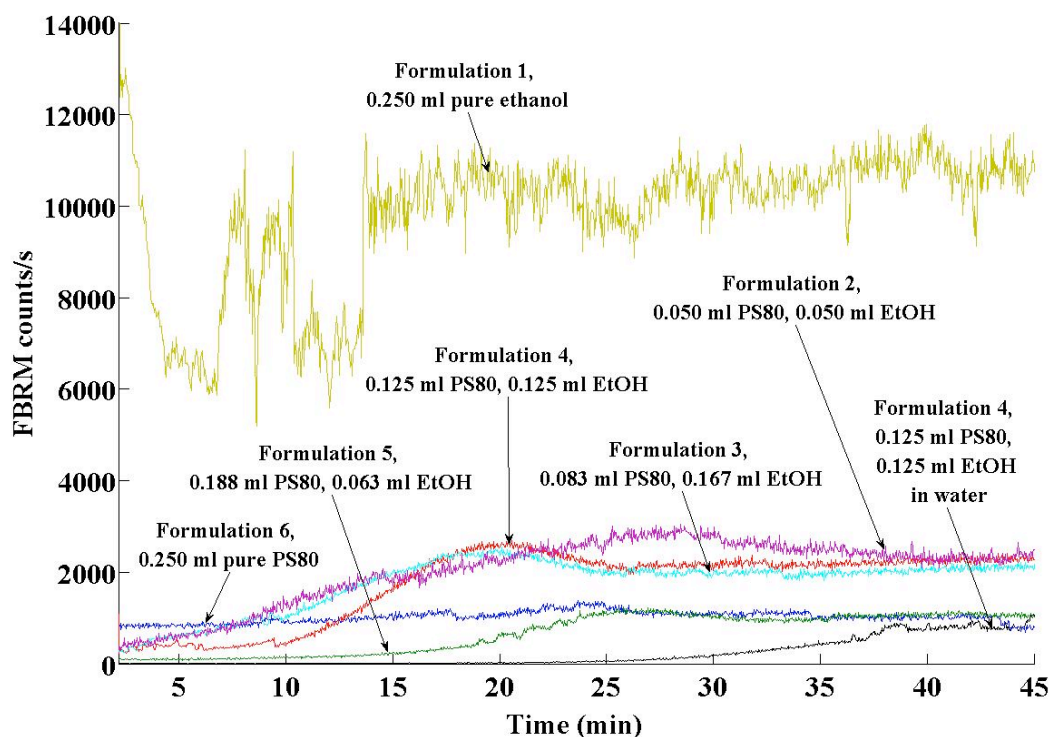
Figure 4-8: 49.5 ml biorelevant media mixture, 37°C: FBRM counts/s in the range from 1 μm to 20 μm as a function of time, 118.8 mg drug/ml formulation

Considering all three drug concentrations, the drug in pure EtOH precipitated extensively (Figure 4-6, Figure 4-7, Figure 4-8). Apparently, EtOH was not able to prevent or prolong precipitation. Moreover, bile salt and lecithin in the biorelevant media were also not able to inhibit or reduce precipitation and particle growth in absence of PS80.

As soon as PS80 was added to the formulation, precipitation still occurred, but to a lesser extent. Interesting was the comparison of drug precipitation in water (black curve) and biorelevant media (red curve) using formulation 4 (0.125 ml PS80, 0.125 ml EtOH, drug load of 118.8 mg/ml). In pure water, induction time was much higher and the number of FBRM counts/s after 45 min was lower (Figure 4-8). In contrast to the pure water, the colloids of the biorelevant media were likely to

promote hetergeneous nucleation. Moreover, it was shown earlier that precipitates were stabilized by adsorbing surfactants (Odian, 2004). It might be that lecithin in biorelevant media were stabilizing the evolving nuclei and therefore were causing accelerated drug precipitation.

Induction time in the biorelevant media mixture was determined considering number of particles in the range of 1 µm to 20 µm. For the evaluation of the influence of drug concentration and formulation composition on the induction times, a multifactorial ANOVA was performed. Drug concentration in the formulations showed no significant influence on the induction time. In contrast, the analysis indicated a significant influence of the formulation composition on the induction time ($p < 0.02$, confidence level of 95 %). It can be concluded that with increasing amounts of PS80, it was possible to enhance the induction time.

One has to keep in mind that nucleation time detection was specific for the FBRM measurements and probably was monitored with some retardation. The FBRM probe is able to detect particles starting from a size of around 1 µm and therefore particles with a size below this limit were not detected (Kee et al., 2011).
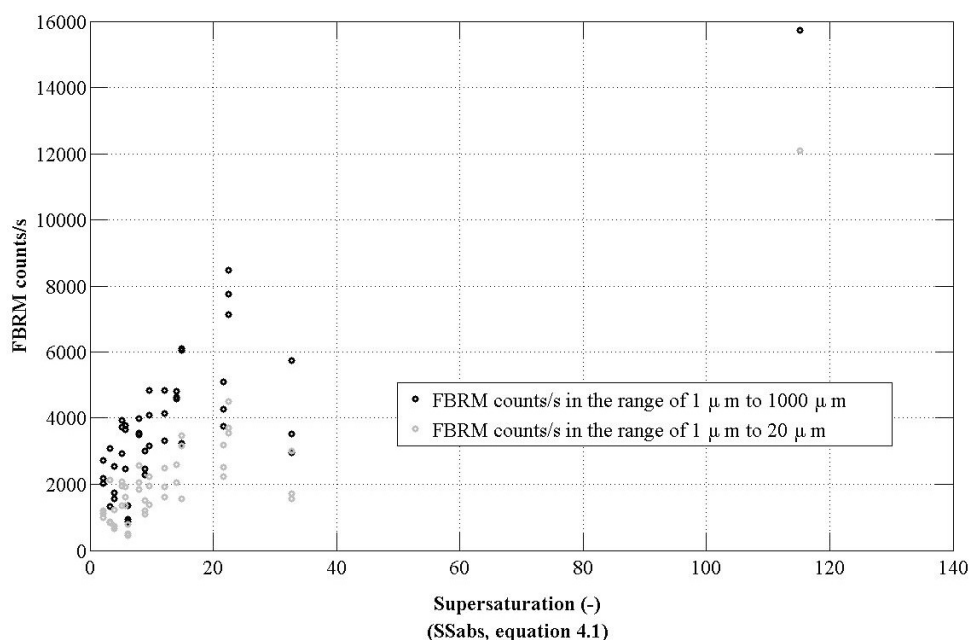
Figure 4-9: Biorelevant media mixture, 37°C: maximum FBRM counts/s as a function of supersaturation

As depicted in Figure 4-9, there was a tendency of increasing number of maximum FBRM counts/s with enhanced supersaturation regarding the FBRM counts/s in the range of 1 µm to 20 µm as well as in the range of 1 µm to 1000 µm. To determine significant influences, a multifactorial ANOVA was performed. Drug concentration had no significant influence on the maximum number of FBRM counts/s, but the amount of PS80 influenced this value significantly ($p < 0.0001$, confidence level of 95 %).

The FBRM counts/s showed no further changes after 60 min and 90 min, indicating an equilibrium state. Such equilibrium did not only mirror drug precipitation processes but also aggregation of the evolving particles.

It was mentioned before that precipitates of poorly water-soluble drugs are often critical for drug absorption. Therefore, it would be desirable to keep drugs in a

solubilized state during the whole gastro-intestinal passage. If precipitation still occurs, it seems preferable to enhance induction time to high levels and to reduce the maximal number of FBRM counts/s significantly. The tested formulations were not able to keep fenofibrate in a solubilized state over the whole simulated gastro-intestinal passage. However, the tested formulations including PS80 were able to enhance drug solubility as well as induction time and to reduce maximal number of counts/s. Based on these results, it appeared possible to enhance fenofibrate absorption under fasted state conditions by oral intake of the drug in PS80/EtOH formulations. However, this assumption would have to be confirmed by in vivo experiments.

4.3.3.2   The use of FBRM for monitoring needle like fenofibrate precipitates

Fenofibrate precipitates appeared needle-shaped and therefore requested a special analytical procedure regarding nucleation and growth processes. Data analysis for the evaluation of the mode and the range of the FBRM counts/s was based on the suggestions of a recent work by Leyssens et al., 2011. To investigate the final shape of particles, offline microscopic images were taken at indicated time intervals shown in Figure 4-10. The next step was to determine the size range of the needles using the offline pictures (Table 4-4). Based on these results, it was possible to select the size ranges for the evaluation of different crystallization parameters.

	Length [µm]	Width [µm]
Sample 1 at 29.5 min		
Crystal 1	406	29
Crystal 2	286	17
Crystal 3	7	5
Sample 2 at 34.5 min		
Crystal 1	19	7
Sample 7 at 180 min		
Crystal 1	11	4

Table 4-4: Dimension of the needle-shaped fenofibrate precipitates

Based on these results, it was concluded that the needle diameter and the number of needles can be monitored by FBRM using the unweighted (no wt) mode of the FBRM counts/s in the 1 µm to 20 µm range (Figure 4-10, experiment in water at 37°C, 0.125 ml PS80, 0.125 ml EtOH, including 118.8 mg/ml API). Furthermore, the needle length was represented by the mode of the square-weighted (sqr wt) FBRM counts/s in the 21 µm to 600 µm range.

As depicted in Figure 4-11, the images taken at 29.5 min (formulation 4, 0.125 ml PS80, 0.125 ml EtOH, drug load of 118.8 mg/ml, added to water at 7 min 38 s) show few large crystals. Due to the large supersaturation these few needles grew to particles in a range from 300 µm to 400 µm in a rather short time. At around 35 min, the images show more small needles besides the big particles, which was considered to be a sign of secondary nucleation. In this case the initial particles provided additional surface area to promote secondary nucleation, which proceeded up to about 40 min. Subsequently, the median in the 21 µm to 600 µm range increased indicating a growth and/or agglomeration driven process. At the same time the FBRM counts/s in the 1 µm to 20 µm range decreased, which was possibly due to dissolution and/or particle growth/agglomeration.

After 50 min the square-weighted median in the 21 µm to 600 µm range became constant, which indicated that the aggregates reached an equilibrium size for the considered size fraction and selected stirring conditions. However, after this time point the median decreased indicating the formation of smaller particles. At the same time, the FBRM counts/s in the 1 µm to 20 µm range increased, while the FBRM counts/s in the square-weighted range of 21 µm to 600 µm decreased, leading to the conclusion that a breakage/disagglomeration took place. This conclusion is also supported by the images taken after 128 min.
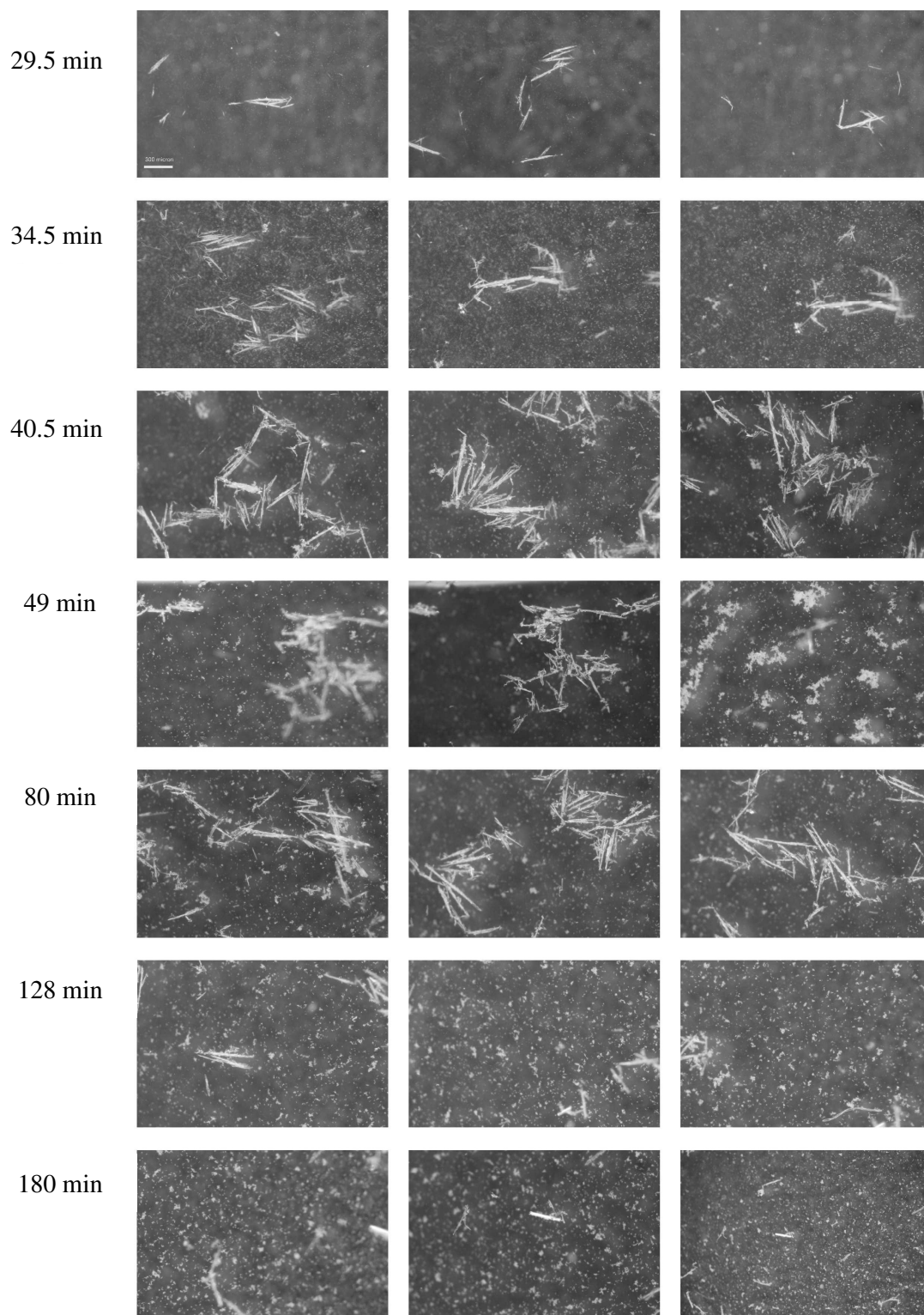
Figure 4-10: Water, 37°C, addition of formulation 4 (0.125 ml PS80 and 0.125 ml EtOH, drug load 118.8 mg/ml) after 7 min 38 s: offline microscopy images taken during experiment
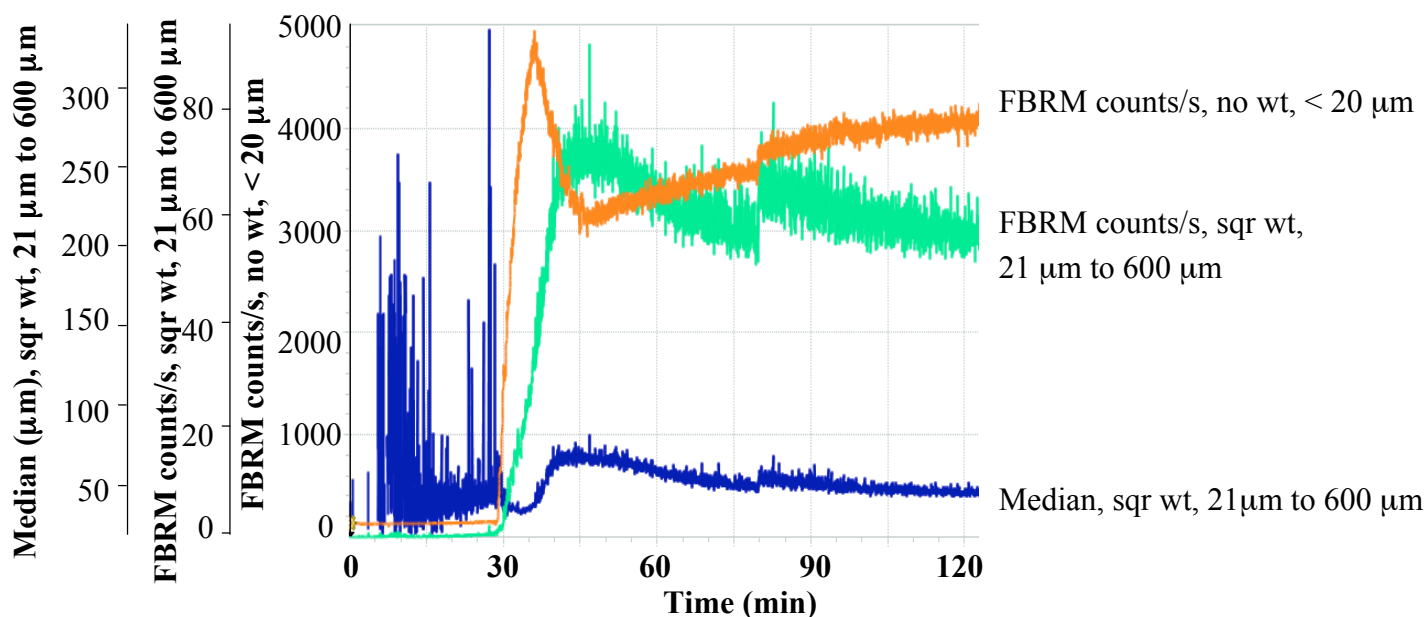
no wt: unweighted mode, sqr wt: square-weighted mode

Figure 4-11: Water, 37°C, addition of formulation 4 (0.125 ml PS80 and 0.125 ml EtOH, drug load 118.8 mg/ml) after 7 min 38 s: FBRM trends for analyzing needle-shaped fenofibrate precipitates

4.3.4 Investigation of possible occurrence of polymorphs during fenofibrate precipitation and the influence of reaction mixture properties on the Raman signal

According to Heinz et al. specific peaks of the Raman spectra between 1660 cm^{-1} and 1560 cm^{-1} can be used to identify the crystalline form of fenofibrate precipitates (Heinz et al., 2009). Figure 4-12 shows the time-evolution of the Raman spectra (water spectrum subtracted from the measurement and PS80 signal was not significant) during the precipitation process and it was concluded that the precipitates were crystalline. Analysis of the full Raman spectra did not show any sign of the appearance of other polymorphs.

To investigate the influence of solid concentration and crystal size on the intensity of the Raman spectra, the integrated intensity value in the range from 1602 cm^{-1} to 1595 cm^{-1} is plotted in Figure 4-13. It was observed that upon the addition of the formulated API at 7 min there was an intensity threshold, which could be due to partial precipitation. This phenomenon could be an indicator for a higher sensitivity of

the Raman probe compared to the FBRM probe, since the latter showed no signal around 7 min. The large peak at 40 min was due to sampling. The reason for the sudden decrease of intensity after 60 min remained unclear, since FBRM data showed no major change in the sample properties. The monotonically increasing trend after 60 min was attributed to enhanced diffuse reflectivity of the reaction mixture, which was the result of small particles generated during the breakage process.
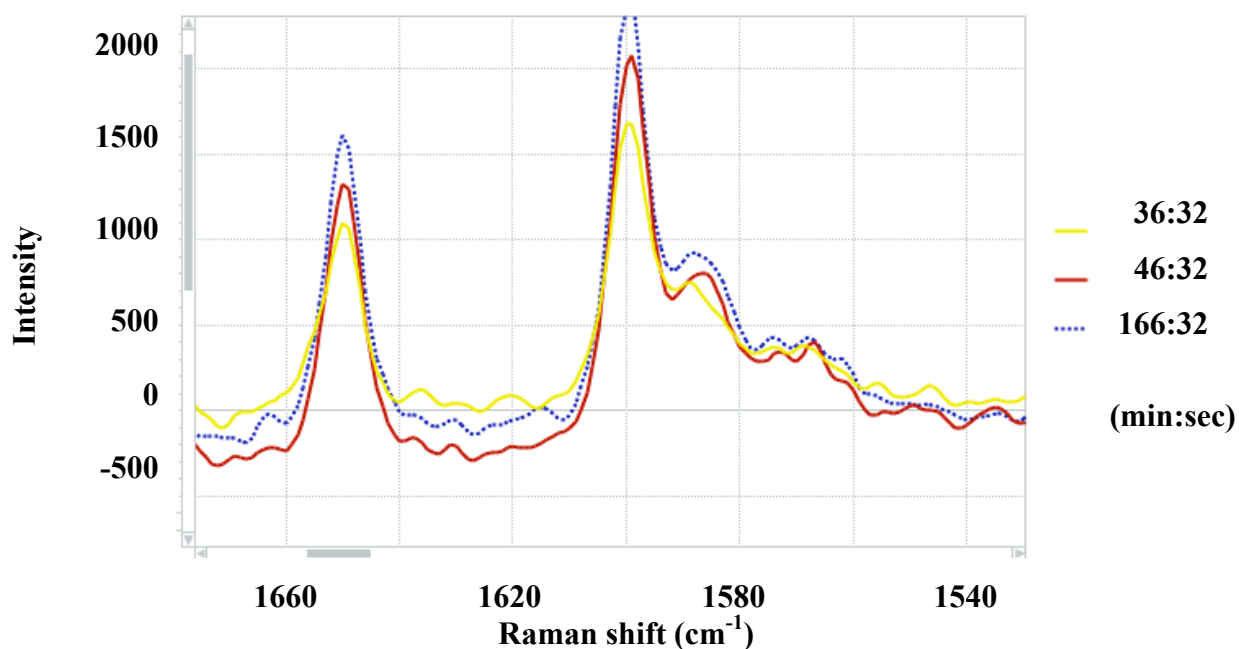
Figure 4-12: Water, 37°C, Raman spectra at three time points for the identification of the solid-state form of fenofibrate precipitates
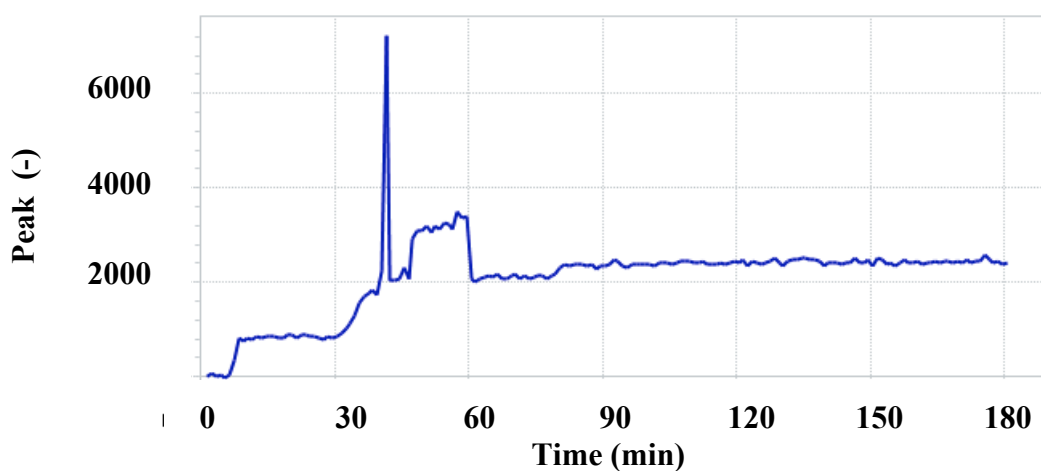
Figure 4-13: Water, 37°C: Integrated Raman spectrum between 1602 cm^{-1} and 1595 cm^{-1}

4.4 Conclusions

The nonionic surfactant PS80 in combination with EtOH was used as a potential precipitation inhibitor of the model drug fenofibrate. Precipitation was monitored in the simulated intestine using inline FBRM. The method was successfully introduced and it was possible to differentiate between heterogeneous nucleation and particle growth. The colloids in the biorelevant medium, interacting with PS80, were promoting drug precipitation compared to the results in pure water. Higher amounts of PS80 in the formulation had a significant influence on induction time and maximal number of FBRM counts/s. Using Raman spectroscopy, polymorphism of the precipitates was ruled out.

FBRM analysis in simulated intestinal media proved to be a suitable tool for in vitro studying excipient effects and to provide a deepened understanding of fenofibrate nucleation and growth processes under simulated physiological conditions. Thus, formulation development can be guided by such novel in vitro tests. However, the obtained ranking of formulations may be confirmed by subsequent in vivo studies.

5   ADVANCING IN VITRO DRUG PRECIPITATION TESTING: NEW PROCESS MONITORING TOOLS AND A KINETIC NUCLEATION AND GROWTH MODEL

5.1 Introduction

New drug candidates in pharmaceutical development are often poorly water-soluble compounds. This leads to challenges in selecting the right formulation principle that on the one hand brings the drug into solution and on the other hand also keeps it in the solubilized state during the entire gastro-intestinal passage. The aqueous solubility is hereby influenced by the physicochemical nature of the compound. Therefore high lipophilicity or comparatively low lipophilicity in combination with a predominant hydrophobicity can result in poor solubility.

Moreover, drug ionization plays an important role. If the pH is below the pKa, the solubility of weak bases is high in comparison to pH-values exceeding the pKa.

Under physiological conditions, drugs move from acidic environment in the stomach to a pH of about 6.5 in the upper intestine, rendering weak bases prone to precipitation under these conditions. This relevant pH-change during the gastro-intestinal passage is influenced by food, concomitant treatment with antacids and age (Badawy et al., 2006; Blum et al., 1991; Charman et al., 1997; Russel et al., 1994).

A biorelevant transfer test is a useful tool to simulate such precipitation processes in vitro. In the literature different transfer tests were reported that describe pumping of the acidic medium containing solubilized drug into the neutral intestinal medium (Gu et al., 2004; Kostewicz et al., 2004; Sugawara et al., 2005; Zhou et al., 2005). Besides this transfer, the composition of the media is an important aspect. Biorelevant media consider drug solubilization in mixed micelles and therefore mimic much better the physiological situation than pure buffer solutions. However, the discussion about best

suited media composition is still ongoing (Jantratid et al., 2008). The choice of technical parameters like the paddle speed or the transfer pump rate has also been debated (Kostewicz et al., 2004). Especially the transfer pump rate is reasonable to vary, since also gastric emptying is subject to variation.

Precipitation is a complex process, involving two different mechanisms. It starts with nucleation from a supersaturated solution followed by growth of the resulting particles. Furthermore processes such as Ostwald ripening or aggregation can occur (Kirwan and Orella, 2002; Lindfors et al., 2008). Such aspects of drug precipitation were studied earlier, but mainly in the framework of drug substance crystallization in chemical synthesis (Shekunov and York, 2000). Here, the LaMer diagram was used as a first approach to predict substance precipitation by focusing on the solubilized amount of drug (Lamer and Dinegar, 1950). In the meantime the understanding of compound supersaturation has evolved and a review article was recently focusing on pharmaceutical systems (Brouwers et al., 2009). Herein, the activation energy for nucleation ΔG^* was described as the driving force of the nucleation process. In the simple case of homogenous nucleation, assuming spherical clusters, it can be calculated using the following equation:

$$\Delta G^* = \frac{16\pi \cdot V_M^{\ 2} \gamma_{ns}^{\ 3}}{3(k_b T \ln(S))^2} \qquad (5.1)$$

Where V_M holds for the molecular volume of the precipitating compound and γ_{ns} is the interfacial energy per unit area between the cluster and the surrounding solvent. The equation further includes the Boltzmann's constant k_b and the degree of supersaturation S. The latter parameter is simply the ratio of the solute concentration in the supersaturated state divided by the equilibrium solubility. This is an important equation for ΔG^*, which displays the key parameters for the nucleation process under

ideal conditions. It must be noted, however, that the presence of polymers or other colloids can change precipitation behavior. Apart from the described ideal case, a heterogeneous precipitation has been described in the literature (Lindfors et al., 2008). This increased level of complexity is one reason for the still limited understanding of the precipitation processes in vivo. Such lack of understanding exists also in the area of modern in vitro precipitation testing. Only recently, Sugano pioneered in using a nucleation and growth model in biopharmaceutical testing (Sugano, 2009). The simulated concentrations, however, could not in all cases adequately predict the experimental concentration-time profiles. As a consequence, there are still open questions with respect to parameters influencing the precipitation mechanisms, starting from the composition of the biorelevant media to the transfer rate of the simulated gastric fluid into the simulated intestinal fluid. Moreover, there is a need for novel analytical tools to monitor the morphology and number of precipitated particles, as well as for the study of subsequent processes like aggregation.

The aim of the present study was to introduce new analytical tools for real-time monitoring in a biopharmaceutical transfer test. Drug precipitation was monitored by online dynamic image analysis and inline disperse Raman spectroscopy. Moreover, a power law modeling approach (Vauck and Mueller, 1994) was adapted for the first time to a biopharmaceutical transfer test. We proposed a kinetic nucleation and growth model that also considered the pump rate used in the test. As model compound dipyridamole was selected. It is a weakly basic BCS II drug, $pKa = 6.4$ (www.roempp.com), which is known for its pH-dependent solubility (Kostewicz et al., 2004; Russell et al., 1994; Zhou et al., 2005).

5.2 Materials and Methods

5.2.1 Materials

Dipyridamole, ammonium acetate, diethylamine, maleic acid, sodium chloride, sodium hydroxide, and sodium oleate were purchased from Sigma-Aldrich GmbH, Switzerland. Pepsin was obtained from Hänseler AG, Switzerland, sodium taurocholate was purchased from Prodotti Chimici e Alimentari S.p.A., Italy, and glycerol monooleate was supplied from Danisco, Denmark. Finally, phopsphatidylcholine was obtained from Lipoid GmbH, Germany.

5.2.2 Methods

5.2.2.1 Preparation of simulated gastro-intestinal fluids

FaSSGF and Fed State Simulated Intestinal Fluid V2 (FeSSIF V2) were used as biorelevant media. They were prepared as previously reported using the compositions described in Table 5-1 (Jantratid et al., 2008).

	FaSSGF	FeSSIF V2
Sodium taurocholate (mM)	$8*10^{-2}$	10
Lecithin (mM)	$2*10^{-2}$	2
Glycerol monooleate (mM)	-	5
Sodium oleate (mM)	-	0.8
Maleic acid (mM)	-	55.02
Sodium chloride (mM)	34.2	125.5
Sodium hydroxide (mM)	-	69.9
Pepsin (μM)	1.24	-
pH	1.6	5.8

FaSSGF: Fasted State Simulated Gastric Fluid, FeSSIF V2: Fed State Simulated Intestinal Fluid

Table 5-1: Compositions of biorelevant media

5.2.2.2   In vitro drug precipitation transfer test

The in vitro transfer test was conducted using an USP II apparatus (DT 600, ERWEKA GmbH, Germany) and dipyridamole was solubilized in 250 ml FaSSGF to reach a drug concentration of 3 mg/ml. This solution was pumped into 500 ml FeSSIF V2 at transfer rates of 4 ml/min and 9 ml/min using a peristaltic pump (Petro Gas Ausrüstungen GmbH, Germany). The media were temperated at $37 \pm 0.5°C$ and stirred with a paddle speed of 100 rpm. Samples (n = 3) of 1 ml were each taken at the different time points, followed by a filtration through a regenerated cellulose membrane, with a pore size of 0.45 μm (SUN-SRi, United States). The samples were then instantly diluted with 1 ml medium and visually checked that no drug precipitation occurred in further analysis. Subsequently, the concentration of dissolved dipyridamole was determined by HPLC. The sample volume taken from the acceptor medium was replaced at each time point with fresh temperature adjusted FeSSIF V2 medium and the entire transfer test was conducted over 3 h. For a visualization of the experimental setup, Figure 5-1 depicts the biopharmaceutical transfer test together with the analytical monitoring tools.
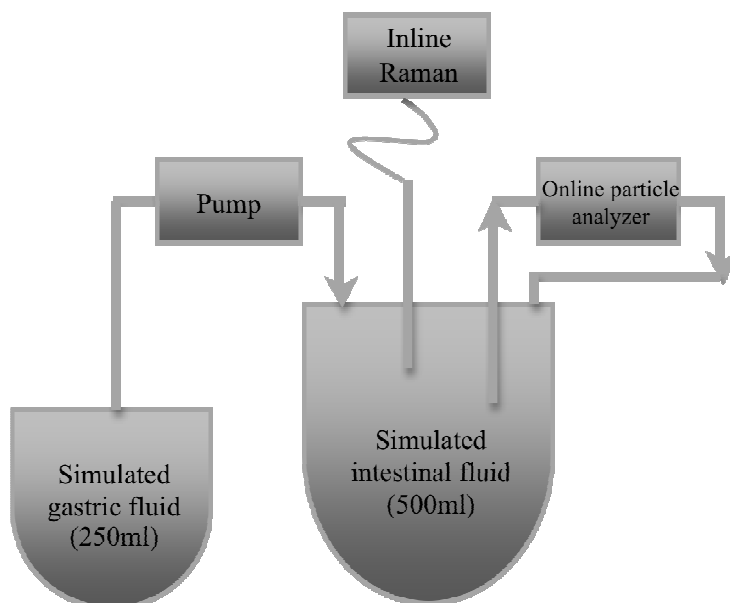
Figure 5-1: Scheme of the transfer test including the inline Raman spectrometer and the dynamic image analysis system as particle analyzer

5.2.2.3 HPLC assay

HPLC measurements were performed on a LiChrospher®60, RP select B 125-4 (5 μm) column (Merck KGaA, Germany). The mobile phase consisted of 0.5% aqueous ammonium acetate solution, 0.2% methanolic diethylene amine solution, and acetonitrile (30:55:15 v/v). Samples of 5 μl were injected and analyzed at a flow rate of 1 ml/min and a detection wavelength of 294 nm (Lunn and Schmuff, 1997-2000).

A new calibration line in the range between 0.089 mg/ml and 1.426 mg/ml was determined for each series of measurements. All calibration lines were in a linear concentration range and exhibited a R^2 of higher than 0.999. The limit of detection was 0.053 ± 0.000 mg/ml (n = 4) of dipyridamole concentration.

5.2.2.4 Dynamic image analysis

Online dynamic image analysis was performed on an XPT-C Particle Analyser (PS Prozesstechnik GmbH, Switzerland). Using a peristaltic pump (Ismatec SA, Switzerland), the acceptor medium was transported through a measuring cell,

equipped with a Flea 2, 1392 x 1032 pixel CCD-camera to analyze the formation of particles/aggregates. The camera performed 70 measurements in a minute, whose average was reported. Data on number, shape and size of the particles or aggregates, respectively were gathered. The number of particles was counted in a total volume of $153 \, mm^3$ and subsequently used to calculate the corresponding particle concentrations. The particle sizes were evaluated as Waddle Disk Diameter (WDD), representing the diameter of a disk with an equal area to the projected area (A) of the observed particle/aggregate:

$$WDD = 2\sqrt{\frac{A}{p}}$$ (5.2)

5.2.2.5   Raman spectroscopy

The in vitro transfer test was monitored in the acceptor phase using a dispersive Raman spectrometer RamanRXN1 Systems (Kaiser Optical Systems, Inc., United States) equipped with a CCD-camera and a fibre optic probe (spot size $0.007 \, mm^2$). A diode laser emitting at 785 nm with a power of 400 mW was used. An exposure time of 20 s every 3 min was chosen to record a spectrum in the range of $100 \, cm^{-1}$ to $3425 \, cm^{-1}$, while averaging every spectrum over 5 scans. To avoid the influence of light on the measurements, the dissolution vessel was completely wrapped in aluminium foil.

5.2.2.6   Mathematical modeling and statistical analysis

We developed a mathematical model that was based on a power law for describing the kinetics of nuclei formation and growth (Vauck and Mueller, 1994). This model took into account the transfer of simulated gastric to intestinal fluid at a set rate. The resulting equations were fitted to the experimental concentration data using EASY-FIT software (K. Schittkowski, University of Bayreuth, Germany). The algorithm of this program was modeling the sum of squared residuals. However, since it was not

possible to estimate all parameters simultaneously, a two-step procedure was applied.

Fitting was performed with fixed exponent values set between a range of 2 to 9 for the

nucleation exponent and we tested values of 1 to 2 for the growth exponent in line

with the reported literature span (Vauck and Mueller, 1994). Each fitting with a given

exponent provided residuals for calculating the root mean square error (RMSE). This

value was subsequently modeled using STATGRAPHICS Centurion, Inc., United

States, to find the best exponent combination for each flow rate separately.

For the statistical treatment of the Raman data, all spectra were corrected for the

baseline. A wavelength range from $504\,\text{cm}^{-1}$ to $2922\,\text{cm}^{-1}$ was selected for a

multivariate analysis of Raman intensities. Accordingly, the response of the model

was the precipitated drug as obtained from the HPLC data. The calculations were

performed using the software IC Quant™ Module 1.0 (Mettler Toledo International,

Inc., Switzerland) to propose an optimal partial least square (PLS) model. This model

exhibited on the one hand a minimal root mean square error of calibration (RMSEC),

while on the other hand the predicted residual sum of squares was minimal as well.

Finally, the standard errors (SE) in the figures and tables were calculated using

Excel V.2003 (Microsoft Corp., United States).

5.3 Results

5.3.1 Solubilities of the model drug dipyridamole

The measured equilibrium solubility of dipyridamole at $37 \pm 0.5°C$ in FaSSGF was

17.2 ± 0.5 mg/ml and 0.068 ± 0.009 mg/ml in FeSSIF V2. The solubility sharply

decreased with increasing pH in line with expectation. This resulted in a low

dipyridamole solubility of 0.017 ± 0.004 mg/ml, in the final medium mixture at the

end of the transfer experiment (FaSSGF : FeSSIF V2 = 1 : 2, pH 5.4), which was

reasonably close to the value in pure FeSSIF V2.

5.3.2 Dynamic image analysis of the in vitro drug precipitation transfer test

The dynamic image analysis revealed that following a lag time, the drug precipitated as complex particles. As shown in Figure 5-2, these particles were either star-like crystals or they were formed through an instantaneous aggregation of elongated primary particles. Both flow rates 4 ml/min and 9 ml/min led to the same habit of the forming particles. We confirmed this form of the particles/aggregates by directly taking samples for light-microscopic analysis. Accordingly, the results were not apparently influenced by the pumping of medium into the camera system of the dynamic image analysis.
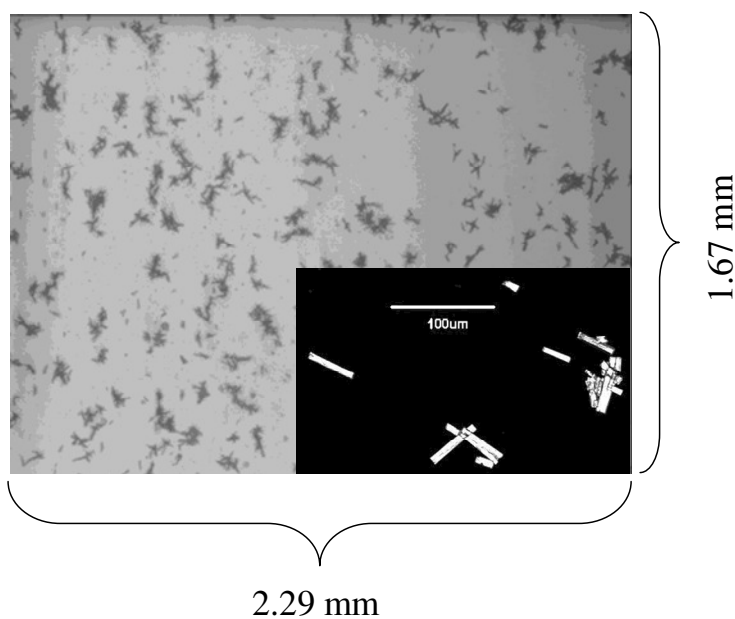
Figure 5-2: Dipyridamole–precipitates after 3 h in the acceptor phase at 37°C, flow rate 9 ml/min, resulting picture of the XPT-C Particle Analyser, including an enlarged image captured with a microscope

Figure 5-3 depicts the time dependent sequence of the particle/aggregate concentration in the acceptor phase. For the high flow rate of 9 ml/min, a lag time of $\cong$ 10 min and a maximum number of particles/aggregates was observed following 20 min. The lower transfer rate on the other hand showed a longer lag time of about 20 min, which was explained by the slower increase in concentration in the acceptor

phase compared to the higher transfer rate. A maximum particle/aggregate number was seen following approximately 30 min. The subsequent decrease in particle counts was probably the result of further particle aggregation and redissolution of a small particle fraction. Finally after one hour, the particle concentrations almost reached an equilibrium showing no differences between the flow rates any more.
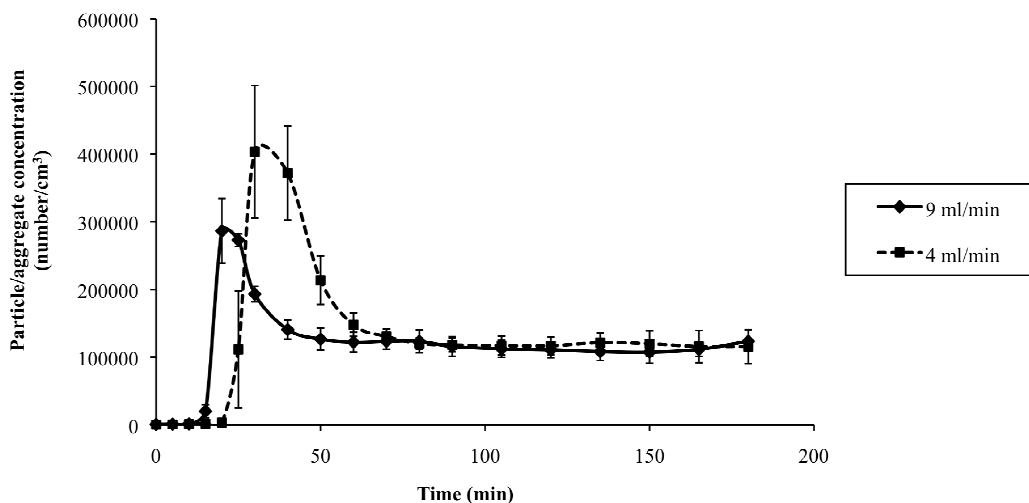
Figure 5-3: Particles/aggregates concentrations of dipyridamole (mean ± SE)
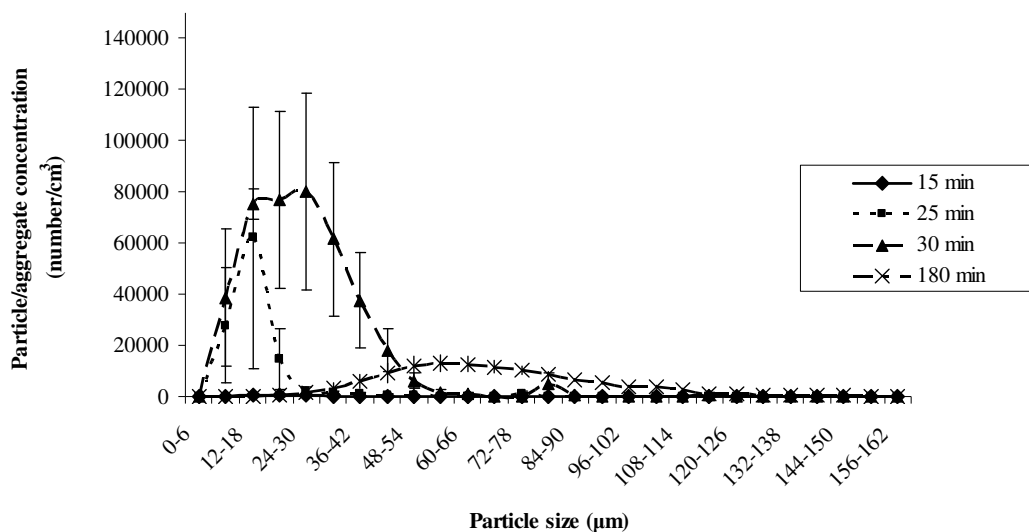
Figure 5-4: Size distribution at flow rate 4 ml/min (mean ± SE)

Figure 5-4 (flow rate 4 ml/min) and Figure 5-5 (flow rate 9 ml/min) show the particle/aggregate size distributions for different time points. Interestingly, not only the mean size, but also the width of the distribution changed over time. Thus, the peak of the size distributions shifted towards larger particle sizes over time. The obtained size distributions were comparatively broad and did not change from 60 min to 180 min. Furthermore, the width of the particle aggregate distribution depended on the transfer rate.
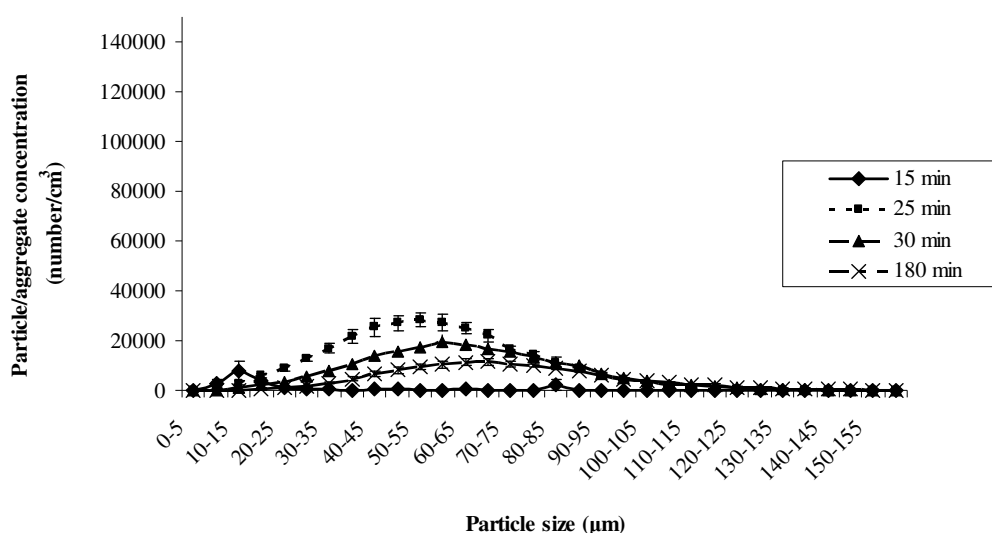
Figure 5-5: Size distribution at flow rate 9 ml/min (mean ± SE)

In a next step, the results of the dynamic image analysis were compared with the concentrations of solubilized dipyridamole in the acceptor phase (Figure 5-6). The concentrations did not increase in a strictly cumulative manner. Decreasing values were observed once a marked crushing out of drug occurred. At the higher flow rate, the peak concentration was reached after 15 min with a value of 0.65 ± 0.05 mg/ml. In contrast the lower flow rate of 4 ml/min, exhibited the maximum concentration of 0.47 ± 0.03 mg/ml after 25 min.
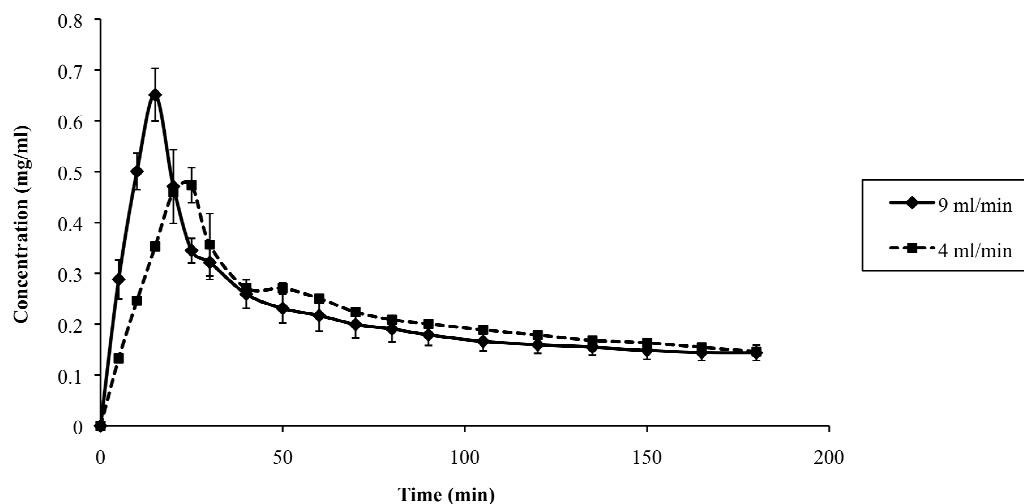
Figure 5-6: Profile of solubilized dipyridamole at flow rate 4 ml/min and 9 ml/min (mean ± SE)

5.3.3 Raman spectroscopy

Raman spectra were inline recorded as a function of time. Figure 5-7 shows the results of a selected wavelength range at the rate of 9 ml/min. Herein the changes of the $1350 \, cm^{-1}$ to $1400 \, cm^{-1}$ signal were of particular interest. Data recording started 40 min prior to the transfer test returning only a small signal at the beginning of the experiment. The significant increase in the signal over the course of the transfer test correlated well with the amount of precipitated drug that was obtained from the HPLC data. Such change of Raman intensities over time was considered as an indicator for the onset of drug precipitation. At flow rate of 9 ml/min we observed the onset of nucleation after 13 min and at the flow rate of 4 ml/min after 23 min.
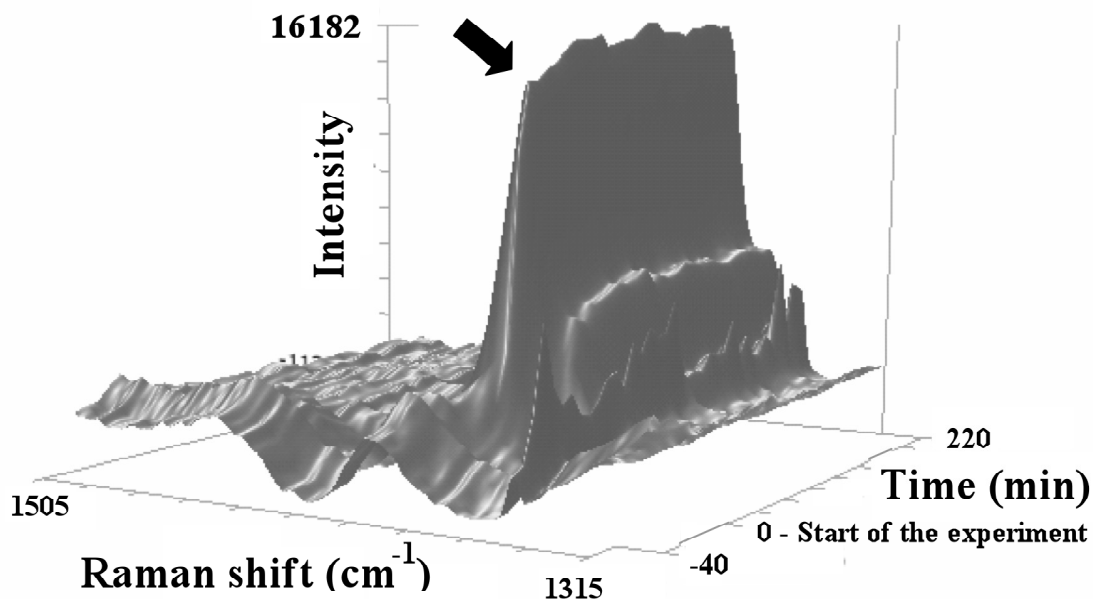
Figure 5-7: 3D plot of a Raman spectrum in the range of 1315 cm^{-1} to 1505 cm^{-1}, flow rate 9 ml/min

To correlate the Raman intensities with the amounts of precipitated drug, we considered a broader range of the Raman spectrum from 504 cm^{-1} to 2922 cm^{-1}. A PLS model was found with four principal components resulting in an R^2 value of 0.995 and the calibration line is depicted in Figure 5-8 using data at the transfer rate of 9 ml/min. The model showed that Raman monitoring provided a sensitive tool for detecting drug precipitation in the acceptor vessel.
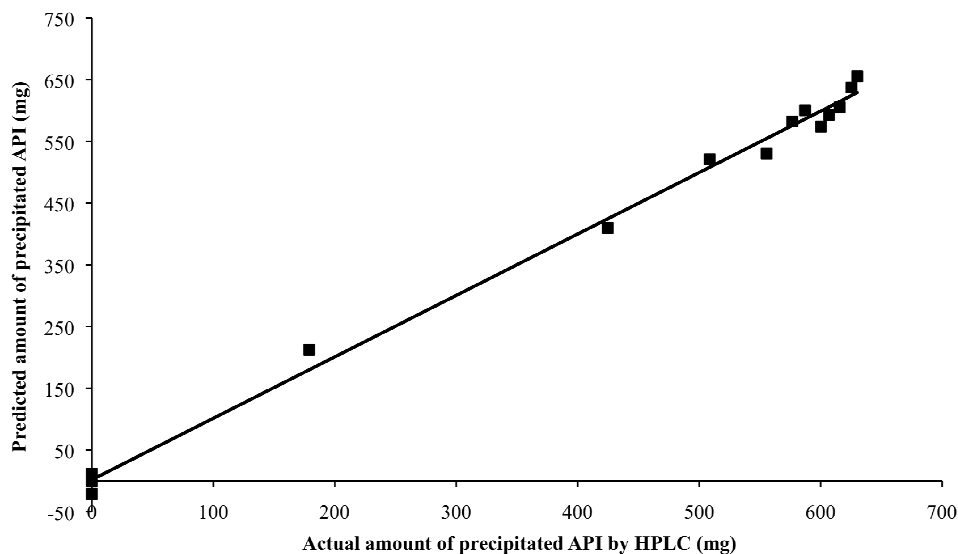
Figure 5-8: Calibration line of the Raman PLS model with the precipitated drug as response variable

5.3.4 Mathematic modeling

It is generally known that precipitation is a two-step process composed of nucleation and particle growth (Kirwan and Orella, 2002). For this reason our model assumptions started with established kinetic crystallisation equations (Vauck and Mueller, 1994). At time $t = 0$ the solubilized amount of drug M_{sol} as well as the precipitated amount M_{pr} are 0. C_i is the effectively solubilized concentration of dipyridamole in the acceptor medium at time point t throughout the entire process and is described by

$$c_i = \frac{M_{sol}}{V_i} \tag{5.3}$$

We divided the entire transfer and precipitation kinetics into four time intervals:

   I. From the beginning to the start of nucleation: $[0, t_{nu}]$

   II. From the start of nucleation to the end of the medium transfer: $[t_{nu}, t_{tr}]$

   III. From the end of the medium transfer to the start of particle growth: $[t_{tr}, t_{gr}]$

   IV. From the beginning of particle growth to infinity: $[t_{gr}, \infty]$

The following equations apply to each time interval:

Interval I $[0, t_{nu}]$:

$$\frac{dM_{sol}}{dt} = F_{tr} \cdot c_g \tag{5.4}$$

$$\frac{dM_{pr}}{dt} = 0 \tag{5.5}$$

$$V_i = V_{i0} + F_{tr} \cdot t \tag{5.6}$$

Where F_{tr} describes the transfer rate used to pump FaSSGF, containing the solubilized drug, into the FeSSIF. The parameter c_g represents the concentration of dissolved dipyridamole in FaSSGF (3 mg/ml).

Interval II $[t_{nu}, t_{tr}]$:

$$\frac{dM_{sol}}{dt} = F_{tr} \cdot c_g - k_{nu} \, (c_i - c_{sat})^n \tag{5.7}$$

$$\frac{dM_{pr}}{dt} = k_{nu} \, (c_i - c_{sat})^n \tag{5.8}$$

$$V_i = V_{i0} + F_{tr} \cdot t \tag{5.6}$$

V_{i0} in the equation represents the initial volume of 500 ml at $t = 0$, whereas V_i stands for the volume at any time point t. The coefficient k_{nu} describes the nucleation constant, c_{sat} (0.017 mg/ml) the saturation concentration, and n represents the nucleation exponent.

Interval III $[t_{tr}, t_{gr}]$:

$$\frac{dM_{sol}}{dt} = - k_{nu} \, (c_i - c_{sat})^n \tag{5.9}$$

$$\frac{dM_{pr}}{dt} = k_{nu} \, (c_i - c_{sat})^n \tag{5.8}$$

$$V_i = V_{i0} + F_{tr} \cdot t_{tr} \tag{5.10}$$

Interval IV [t_{gr}, ∞]:

$$\frac{dM_{sol}}{dt} =- k_{gr}\ (c_i - c_{sat})^g \tag{5.11}$$

$$\frac{dM_{pr}}{dt} = k_{gr}\ (c_i - c_{sat})^g \tag{5.12}$$

$$V_i = V_{i0} + F_{tr} \cdot t_{tr} \tag{5.10}$$

Where k_{gr} is the particle growth constant and g the corresponding particle growth exponent.

The aforementioned set of equations was fitted to the individual concentration profiles. Interestingly, the fits for the different flow rates revealed the same optimum with respect to their exponents. We found 5 for the nucleation exponent and 1.5 for the growth exponent. This consistent finding indicated that the different flow rates obviously produced the same kind of drug precipitation process.
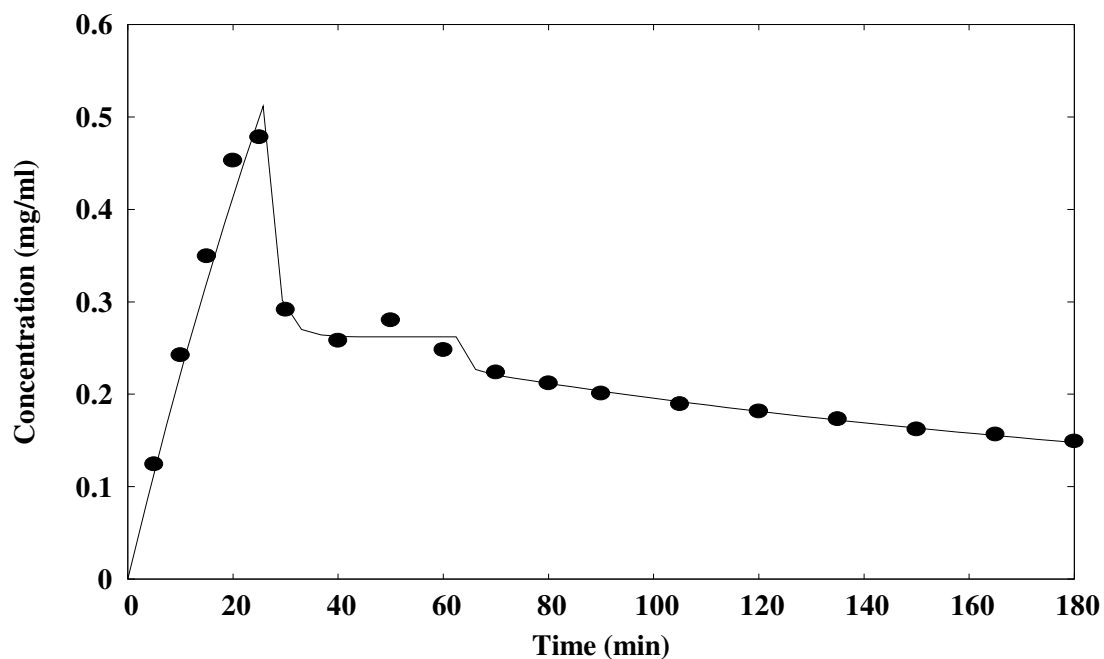
Figure 5-9: Example of dipyridamole concentration profiles (points) together with the mathematical model (solid line) for the flow rate of 4 ml/min
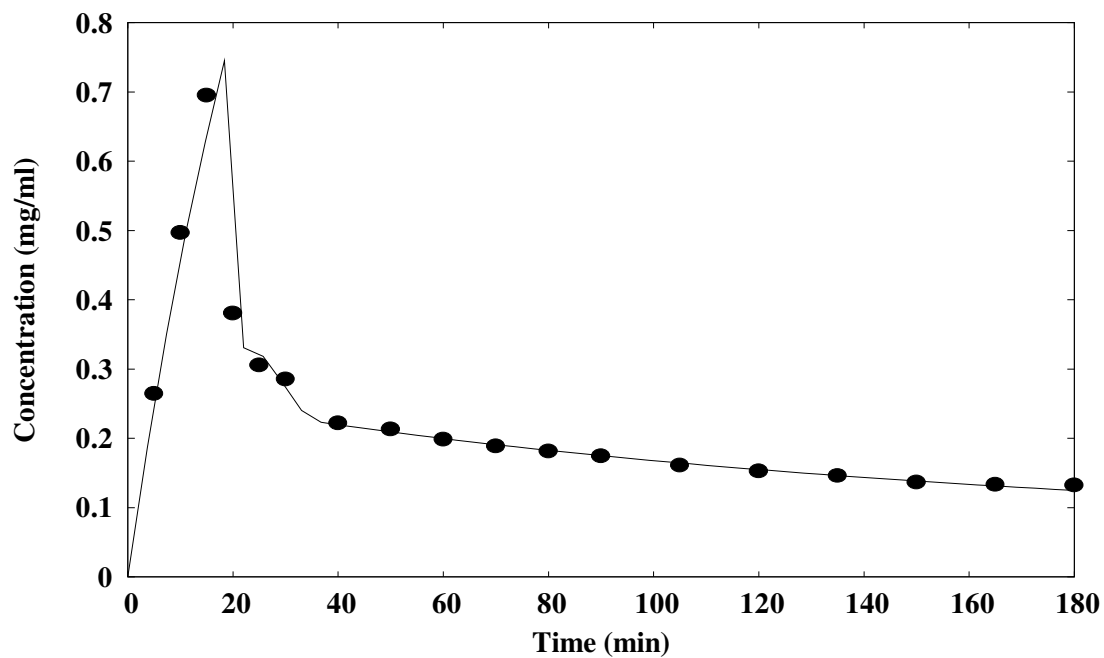
Figure 5-10: Example of dipyridamole concentration profiles (points) together with the mathematical model (solid line) for the flow rate of 9 ml/min

Examples of both flow rates are shown in Figure 5-9 and Figure 5-10. The model excellently agreed with the measured concentration profile over time. Interestingly,

the profiles displayed a shoulder that followed the main peak. This shoulder marked the end of medium transfer into the simulated intestinal acceptor fluid. It was remarkable that the mathematical model was able to agree on this rather subtle effect of the concentration profile. The individual fitting curves resulted in parameter estimates that were averaged as displayed in Table 5-2.

	4 ml/min	**9 ml/min**
n	5	5
gr	1.5	1.5
k_{nu}	11645.69 ± 385.53	6765.74 ± 2135.50
k_{gr}	7.47 ± 0.46	8.46 ± 0.29
t_{nu}	28.06 ± 0.88 min	18.52 ± 0.91 min
t_{gr}	68.01 ± 1.36 min	52.89 ± 17.96 min

n: nucleation exponent, gr: particle growth exponent, k_{nu}: nucleation constant, k_{gr}: particle growth constant, t_{nu}: start time of nucleation, t_{gr}: start time of particle growth

Table 5-2: Estimated values of the fitted kinetic nucleation and growth model for the two transfer rates (mean ± SE)

5.4 Discussion

The in vitro testing was performed using FaSSGF as acidic medium to simulate the gastric environment, whereas the acceptor medium was not only chosen based on the most updated biorelevant media composition, but also for technical reasons. Thus, pure FeSSIF V2 showed the lower background signal in the XPT-C Particle Analyser compared to FaSSIF V2, making it better suited to study in vitro drug precipitation. The combination of FaSSGF and FeSSIF V2 was therefore selected to study in vitro the change in pH, triggered by the transfer from the stomach to the intestine. The media selection had the advantage of a large pH change, but it was on the other hand not possible to study an effect of the fasting versus fed state condition.

Another factor that needed consideration during the in vitro test, was the paddle speed. Previous experiments interestingly showed that this parameter had only a minor effect on the measured profiles in the acceptor phase (Kostewicz et al., 2004). For this reason an arbitrary constant paddle speed of 100 rpm was selected for all experiments. The more important parameter for the in vitro test, however, was the transfer rate. It was not only relevant for the in vitro results, but is also important for the in vivo situation (Kostewicz et al., 2004). As the gastric emptying defines when a dissolved drug in the stomach is transferred to the intestinal fluid, we used different flow rates in vitro that were considered to be relevant for physiological gastric emptying (Kostewicz et al., 2004).

Using dynamic image analysis it was demonstrated that the transfer rate was affecting the precipitation kinetics. A common aspect of the investigated transfer rates was that similar complex particles/aggregates were obtained. The mean particle size and size distribution as well as the concentration profile showed a clear dependence on the transfer rate. Based on particle number and size, the dynamic image analysis agreed with the observed decreasing drug concentration due to precipitation in both cases. Care is however needed, when comparing the size and concentration data on a quantitative basis, since the density of the particles/aggregates is unlikely to stay constant over time. For this reason we did not include the dynamic image analysis data for modeling of the concentration profiles.

The faster transfer rate provided the higher drug concentration peak in the intestinal medium. It could therefore be hypothesized that under such conditions, also the absorption process is promoted in vivo. However, our transfer test did not consider any drug absorption. Unlike the in vivo situation, no permeation step was involved in vitro so that no continuous removal of drug from the bulk solution could be taken into

account. More research is therefore needed to clarify the biorelevance of the current in vitro transfer test.

However, on the level of the in vitro test itself, the new monitoring tools provided insights into the process of in vitro drug precipitation. Disperse Raman spectroscopy hereby showed to be particularly useful. It enabled the definition of precipitation onset and following the amount of precipitated drug. The latter was in good agreement with the concentration data gathered by HPLC analysis. Raman spectroscopy appears to be a valuable tool for the monitoring of biopharmaceutical tests, which was recently also highlighted in another publication (Savolainen et al., 2009). This work studied the in situ solid state of indomethacin and carbamazepin in a flow-through dissolution test. The authors were able to follow changes from the amorphous drug to the crystalline state during the dissolution process. Such changes in the solid-state properties can be of biopharmaceutical relevance and possibly depend on the dissolution medium used. Especially the biorelevant media can hereby influence a solvent-mediated solid-phase transformation (Letho et al., 2009).

For the transfer test it is of interest to see if the drug undergoes changes in solid-state structure during the precipitation process. Even though a drug can potentially precipitate in an amorphous form or as a hydrate, the Raman spectrum of the precipitated model compound dipyridamole revealed no differences compared to its initial crystalline form.

Next to gaining a better understanding of in vitro drug precipitation kinetics by using analytical monitoring tools, mathematical modeling also provided valuable insights. We used power laws to model nucleation as well as the growth of the particles. Based on minimum RMSE values, the best models had the same exponents for both transfer rates. The nucleation exponent of 5, delivered by the model, was well within the

expected range of 3 to 6 (Vauck and Mueller, 1994). It should be modeling that the formation of drug nuclei and the concentration differences in solution showed a highly non-linear relationship. The particle growth exponent, returned by the model, was 1.5. It is interesting to note that this growth exponent was found to be greater than 1. A simple approximation for particle growth would be a first order "inverse dissolution process" according to Noyes Whitney, resulting in a particle growth exponent of 1. Such type of particle growth was previously applied (Sugano, 2009). However, exponents higher than 1, as observed in our experiments, were also inline with previous experimental findings (Vauck and Mueller, 1994). They probably originate from geometric effects, as complex structures of particles and surfaces can be the result of a precipitation/aggregation process (Lin et al., 1989), resulting in deviation from a simple first order model (Macheras and Iliadis, 2002; Valsami and Macheras, 1995). Accordingly, our growth exponent of 1.5 rather that 1 can be the result of a complex particle surface, which defines the true surface area being available for drug dissolution and/or precipitation. This assumption of a complex surface agreed well with the images obtained from online monitoring that demonstrated a complex geometry of the precipitated particles/aggregates. It would be interesting to learn from future tests, how the exponents depend on surface properties of other precipitated drugs than dipyridamole.

The mathematical model was also of a particular interest in the determination of the nucleation onset. This time point is difficult to assess by experimental means, since the initial nuclei are expected to be subvisible as well as instable. Accordingly, the image analysis can only detect particles in a size range of a few micrometers and also Raman spectroscopy has a limited resolution with respect to detecting a small fraction of crystalline drug. Given these limitations, it is remarkable that the calculated

nucleation time (Table 5-2) agreed well with the precipitation onset determined by Raman spectroscopy as well as obtained from dynamic image analysis.

The novel tools, i.e. inline Raman spectroscopy and online dynamic image analysis, as well as HPLC data provided a coherent view on the precipitation process. The in vitro tools allowed a suitable monitoring of the process and the mathematic model facilitated an improved understanding of the in vitro drug precipitation. The obtained model coefficients are expected to be specific for a pharmaceutical compound in a given medium. Determination of these coefficients is of special interest with respect to mechanistic drug absorption modeling. These parameters can be used as input data for physiologically-based pharmacokinetic (PBPK) models. Such mechanistic modeling is today available from a few commercial software packages. However, the mathematical models presently do not consider the precipitation process in its full complexity, i.e. through consideration of a separate nucleation and growth step. Consequently, the PBPK models need to be refined in that respect and our calculated coefficients could then serve as input parameters to obtain mechanistically improved simulations for drug absorption.

5.5 Conclusions

Using a biorelevant transfer test, we examined precipitation of dipyridamole in vitro. Novel analytical methods were introduced together with a mathematical model for nucleation and particle growth. The dynamic image analysis revealed a complex structure of the precipitated particles/aggregates, which was also reflected in the mathematical model by a growth exponent differing from 1. The particle size distribution changed as a function of time and differences between the transfer rates were mainly observed in the initial phase of the precipitation. These observations also

agreed with the findings of the inline Raman spectroscopy that demonstrated to be an excellent tool in monitoring the precipitated drug fraction.

It can be concluded that a simple measurement of drug concentration in the acceptor phase does not provide a complete characterization of in vitro drug precipitation. The underlying processes are highly complex especially in biorelevant media, so that further analytical tools are required. The combined efforts of modeling and advanced analytical monitoring provide important insights into drug nucleation and particle growth. Furthermore these results can be used for a subsequent mechanistic absorption modeling. Physiologically based absorption modeling can facilitate correlations with in vivo findings. Accordingly, we must have a good understanding of the in vitro results to enable meaningful in vivo correlations. This is also the key to better optimizing the in vivo performance of pharmaceutical formulations based on in vitro results.

6 STUDY OF DRUG CONCENTRATION EFFECTS ON IN VITRO LIPOLYSIS KINETICS IN MEDIUM-CHAIN TRIGLYCERIDES BY CONSIDERING OIL VISCOSITY AND SURFACE TENSION

6.1 Introduction

Lipolysis in the intestine is a complex process in which pancreatic lipase is mainly responsible for digestion of triglycerides. The enzyme acts on the oil/water interface, where it exhibits a rather weak adhesion. Therefore substances like proteins or bile salts can easily remove the lipase from the interface and block any further digestion (Embleton and Pouton, 1997). To avoid desorption of the enzyme from the oil/water interface, lipase interacts with the colipase to form a strongly adhering complex. Anchored at the interface, pancreatic lipase catalyzes the hydrolysis of tri- as well as diglycerides resulting in fatty acids and 2-monoglycerides. The latter can undergo a non-enzymatic isomerization to 1-monoglyceride that is digestible by the pancreatic lipase to form glycerol and fatty acid (Embleton and Pouton, 1997).

It was early recognized that surface-active excipients can greatly affect the lipolysis rate (Hutchison, 1994). Some of these lipid-based surfactants were shown to be digested themselves (Fernandez et al., 2007; Fernandez et al., 2008). Moreover a study of Cuiné et al. reported formulations with high amounts of digestible surfactant, which were leading to drug precipitation (Cuiné et al., 2008). Based on these in vitro results, a formulation ranking was determined that was later observed in beagle dogs.

The field of in vitro lipolysis still offers many opportunities for pharmaceutical research and our work focused on a potential drug loading effect. Earlier studies investigated poorly soluble compounds at a single concentration (Christensen et al., 2004; Kaukonen et al., 2004). A next step would be to study drug concentration effects, which to the best of our knowledge has not been explored. We aimed studying

the influence of five poorly soluble model drugs on the in vitro lipolysis rate in medium-chain triglycerides (type I formulation) using three concentration levels. The drug orlistat was furthermore analyzed as reference, due to its known selective direct inhibition of the pancreatic lipase (Hadvàry et al., 1988; Hauptmann et al., 1992). In order to achieve a better mechanistic understanding of drug effects on lipolysis, direct compound effects on physical oil properties were studied. All compounds were first characterized by molecular modeling followed by studying drug effects on oil viscosity and surface tension. In theory, these physical parameters were of relevance for any kind of oil dispersing or surface reaction and therefore of interest for lipolysis testing.

6.2 Materials and methods

6.2.1 Materials

The chemicals danazol, calcium chloride dihydrate, fenofibrate, griseofulvin, maleic acid, porcine pancreatin, probucol, sodium chloride, sodium hydroxide, and 0.2 N sodium hydroxide were purchased from Sigma-Aldrich GmbH, Switzerland. Miglyol®812 was obtained from Hänseler AG, Switzerland. This medium-chain oil comprised triglycerides of 50% to 65% caprylic acid ($C_{8:0}$) and 30% to 45% of capric acid ($C_{10:0}$). A maximal amount of 2% was specified for caproic acid ($C_{6:0}$) as well as for lauric acid ($C_{12:0}$). Finally, the content of myristic acid ($C_{14:0}$) was maximally 1%. Sodium taurocholate (purity > 99% w/w) was purchased from Prodotti Chimici e Alimentari S.p.A., Italy, lecithin (grade EPCS > 98% phospholipids) was obtained from Lipoid GmbH, Germany, and felodipine was supplied by Ramidus AB, Sweden. Finally, orlistat was obtained from AK Scientific, Inc., United States.

6.2.2 Methods

6.2.2.1   Preparation of drug formulations

The different drugs and the medium-chain triglyceride oil were mixed in glass vials using a constant stirring. We targeted a broad concentration range for each drug to assure that transparent oily solutions were obtained. This individual range was then used to define three arbitrary concentrations for each drug. Concentration levels were named as "low", "intermediate", and "high" (Table 6-1) and all samples were visually checked for clarity during 7 days to assure that no drug precipitation occurred.

	Drug concentration in MCT (mg/ml)		
	Low	**Intermediate**	**High**
Danazol	0.31	0.55	1.31
Felodipine	0.19	1.35	2.90
Fenofibrate	2.75	28.50	50.40
Griseofulvin	0.25	0.49	0.74
Probucol	0.69	1.67	5.29
Orlistat	5.00	10.00	20.00

Table 6-1: Drug concentration levels in MCT

6.2.2.2   Molecular modeling

Different molecular parameters were calculated using the program Molecular Modeling Pro®, Version 6.2.6 (ChemSW, Inc., United States). The number of proton donors was determined first together with a three dimensional solubility parameter. The latter value employed the definition by Van Krevelen (1997). HLB values were obtained according to Griffin's definition based on molecular weight. This measure of the molecule's amphiphilic character was complemented with the calculation of the critical packing parameter. The latter estimate was determined by the hydrophobic

molecule volume divided by two parameters. One was a slice area through the hydrophilic head group of the molecule and the other was the longest length of the hydrophobic part of the structure. Since most of the octanol/water coefficients log P were experimentally known, we used the values of the drug bank (www.drugbank.ca) to have a physicochemical reference value.

6.2.2.3   Capillary viscosimetry

Viscosity was measured according to the Ubbelohde capillary method. Thus, a Schott capillary viscosimeter of size II (SI Analytics GmbH, Germany) was held at constant temperature of 37°C. This capillary was filled with formulation to a given meniscus height. Following temperature equilibration, time was determined for the sample to flow between defined meniscus levels. Subsequently, the kinematic viscosity was calculated by taking the capillary constant into consideration. The obtained viscosity value was corresponding to the dynamic viscosity normalized by the density. All concentrations in Table 6-1 were tested in triplicate.

6.2.2.4   Dynamic surface tensiometry

Surface tensions at room temperature were measured using the Sita DynoTester (SITA Messtechnik GmbH, Germany). The measurement principle is based on the bubble pressure method. Air was introduced through an orifice into the liquid samples so that a succession of bubbles was generated. Herein an arbitrary range of frequencies was tested, which provided different surface ages of 25 ms, 250 ms, and 2500 ms. During inflation of a bubble, the pressure increases from base value p_0 to a maximal bubble pressure p_{max}. At the latter, the bubble radius equaled to that of the capillary r. The dynamic surface tension σ_d was then calculated according to the following equation 6.1:

$$\sigma_d = \frac{(p_{max} - p_0)r}{2} \tag{6.1}$$

All the measurements were taken in triplicate.

6.2.2.5   Dynamic lipolysis test

The enzymatic test was performed in the biorelevant medium FaSSIF having a composition that was recently updated to a version 2 (Jantratid et al., 2008). This medium contained 3 mM of sodium taurocholate, 0.2 mM lecithin, 19.12 mM maleic acid, 68.62 mM sodium chloride, and 34.8 mM sodium hydroxide. The pH of this medium was adjusted to 6.5.

The porcine pancreatin was suspended in this biorelevant medium (0.174 mg pancreatin/ml medium). After stirring the dispersion at room temperature (15 min, $25 \pm 0.5°C$), the dispersion was centrifuged using an Eppendorf Centrifuge 5415C (Vaudaux-Eppendorf AG, Switzerland) for 15 min at 14000 rpm. The clear supernatant was collected and adjusted to pH 6.5. The resulting solution exhibited an enzyme activity of 10000 TBU per ml. The solution was freshly prepared each day.

Sample (500 µl) was dispersed in 36 ml medium at 37°C in a double-walled glass vessel. The solution was equilibrated for 15 min using magnetic stirring. Subsequently, lipolysis was started by adding 4 ml pancreatin solution (1000 TBU/ml final concentration) and 5 mM calcium chloride dihydrate. Lipolysis products were then titrated with 0.2 NaOH using a computer controlled Titrando 842 (Metrohm Schweiz AG, Switzerland).

6.2.2.6   Statistical design and analysis of data

All measurements were conducted with n = 3 and results were expressed as mean values ± standard deviations. The program Statgraphics Centurion XV ed. Professional from StatPoint Technologies, Inc., United States, was used for the two-factor ANOVA calculations. For the subsequent contrast analysis, Fisher's least significant difference (LSD) procedure was followed. LSDs were intervals for each

pair of means at the 95% confidence level using Student's t distribution. Significance was assumed for those factors that demonstrated a probability p-value of less than 0.05.

6.3 Results

6.3.1 Physicochemical drug effects in oils

6.3.1.1 Modeling of molecular parameters with potential relevance for drug effects on the oil

The different drugs were characterized by means of molecular modeling. Only selected molecular properties were calculated that were of interest with respect to drug/oil interactions (Table 6-2). Thus, a first molecular parameter was the number of proton donors. Such protons were earlier shown to be relevant for the interaction with ester groups in oils (Cao et al., 2004). In that respect, danazol, felodipine, probucol, and orlistat could facilitate hydrogen bonding. Apart from the number of proton donors, the solubility parameter was calculated. This estimate of the cohesive energy was in case of orlistat remarkably low.

	Number of proton donors	Solubility parameter $(J/cm^3)^{0.5}$	HLB, based on molecular weight	Critical packing parameter	log P
Danazol	1	23.54	3.12	0.38	0.51*
Felodipine	1	23.52	4.82	0.99	3.8*
Fenofibrate	0	22.67	2.55	0.44	5.3*
Griseofulvin	0	24.49	5.89	0.66	2*
Probucol	2	22.79	0.49	0.5	7.03
Orlistat	1	18.37	4.15	0.31	8.92*

*The known experimental log P values were listed according to the drug bank (www.drugbank.ca)

Table 6-2: Compound properties obtained from molecular modeling

The balance of the hydrophilic and lipophilic part of a molecule was estimated by the calculated HLB value. As a result, the compounds differed with respect to their amphiphilic nature. Comparatively high HLB values were calculated for griseofulvin, felodipine, and orlistat. These compounds had the highest potential of surface activity by migrating to the oil surface or the oil/water interface. However, all calculations were based on assumed molecular conformations. Changes in these molecular conformations affect the calculated HLB values so that the estimate is not absolute but depends on the drug environment. Such dependence on the molecular conformation was further given with the calculation of the critical packing parameter. This value described the ratio of polar head group volume to the volume of the lipophilic moiety in the amphiphilic molecule. High values among the test compounds were mainly obtained for felodipine and griseofulvin. The model assumed that these compounds exhibit the tendency to aggregate in planar structures.

6.3.1.2   Drug effects on viscosity and surface tension of the oil

The focus on viscosity had the rational that there is a theoretical relation with molecular diffusion and therefore the potential to interact with oil dispersion or with interfacial catalysis. We measured this parameter by means of capillary viscosimetry. Table 6-3 displays the results for the different drug concentrations.

	Kinematic viscosity ± std. (mm²/s) of different drug concentrations in MCT (value of pure oil: 25.1 ± 0.1)		
	Low	**Intermediate**	**High**
Danazol	25.3 ± 0.1	25.6 ± 0.1	25.6 ± 0.1
Felodipine	25.4 ± 0.2	24.2 ± 0.1	25.6 ± 0.2
Fenofibrate	25.6 ± 0.0	26.6 ± 0.1	27.9 ± 0.1
Griseofulvin	25.5 ± 0.1	25.6 ± 0.1	25.5 ± 0.0
Probucol	25.4 ± 0.0	25.6 ± 0.0	26.7 ± 0.1
Orlistat	26.2 ± 0.1	26.3 ± 0.2	26.8 ± 0.1

Table 6-3: Kinematic viscosity of different drug concentrations in MCT

Kinematic viscosity of the pure Miglyol®812 was 25.1 ± 0.1 mm²/s. This reference viscosity was generally increased in presence of the poorly soluble drugs. A two-factor ANOVA was conducted with the type of drug as first factor and its concentration effect as a second parameter. Both effects were highly significant in this study ($p < 0.0001$, confidence level of 95 %).
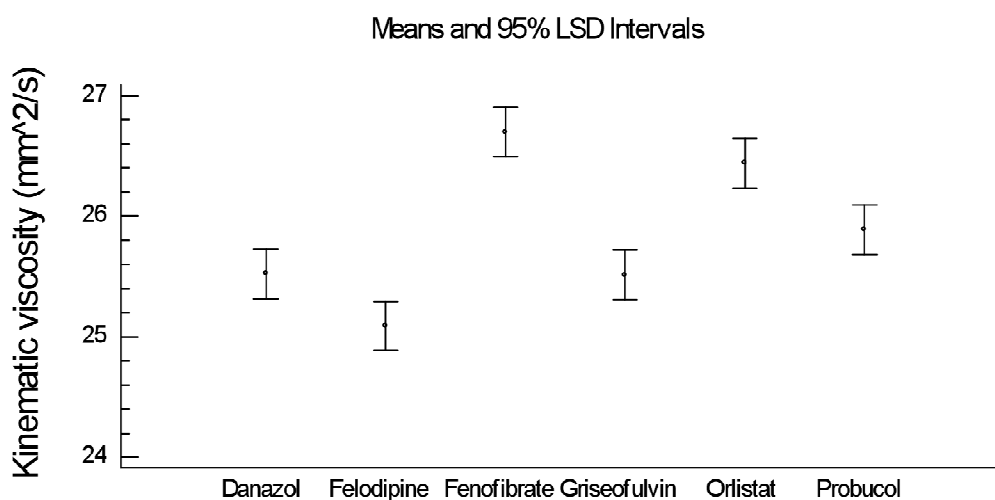
Figure 6-1: ANOVA means plot of drugs and their concentration effects on kinematic viscosity

Comparing the different drugs (Figure 6-1), viscosity increase was most pronounced with fenofibrate and orlistat. Furthermore, probucol increased viscosity of pure oil. The drug effect was depending on concentration and it was most evident at the highest drug load. Despite the statistical significance of the effect, absolute changes in viscosity were rather moderate.

Apart from viscosity, the dynamic surface tension was measured. This measure of surface activity was potentially indicating effects on the specific energy at the oil/water interface, where an interaction with lipolysis is possible. Thus, dynamic surface tension was measured for different surface ages from 25 ms to 2500 ms. Highest surface age produced the best reproducibility and these data were compiled in Table 6-4 (data of surface ages 25 ms and 250 ms are shown in the appendix, section 9.2.1).

	Surface tension ± std. (mN/m) of different drug concentrations in MCT (value of pure oil: 28.5 ± 0.2)		
	Low	**Intermediate**	**High**
Danazol	28.8 ± 0.1	28.5 ± 0.2	28.6 ± 0.3
Felodipine	27.0 ± 0.1	27.0 ± 0.1	28.2 ± 0.2
Fenofibrate	28.8 ± 0.1	28.9 ± 0.1	29.3 ± 0.2
Griseofulvin	28.4 ± 0.1	28.7 ± 0.1	30.9 ± 0.1
Probucol	32.4 ± 0.1	29.0 ± 0.2	29.3 ± 0.7
Orlistat	26.8 ± 0.2	26.8 ± 0.1	26.8 ± 0.0

*Surface age of 2500 ms

Table 6-4: Surface tension of different drug concentrations in MCT

The presence of drug in the oil obviously altered dynamic surface tension of pure oil. Not all compounds affected this value in the same way. A clear reduction in surface tension was, for example, noted for the different concentrations of orlistat. Felodipine demonstrated a similar tendency toward lowering the surface tension. On the other hand the compound probucol increased the average surface tension.

An ANOVA means plot is given as Figure 6-2. There was a highly significant effect between the different groups ($p < 0.0001$, confidence level of 95 %). Confidence bands of felodipine and orlistat supported the first impression that these drugs reduced surface tension of medium-chain triglycerides. The opposite effect was found with griseofulvin and probucol that reached highest surface tensions.

Means and 95% LSD Intervals
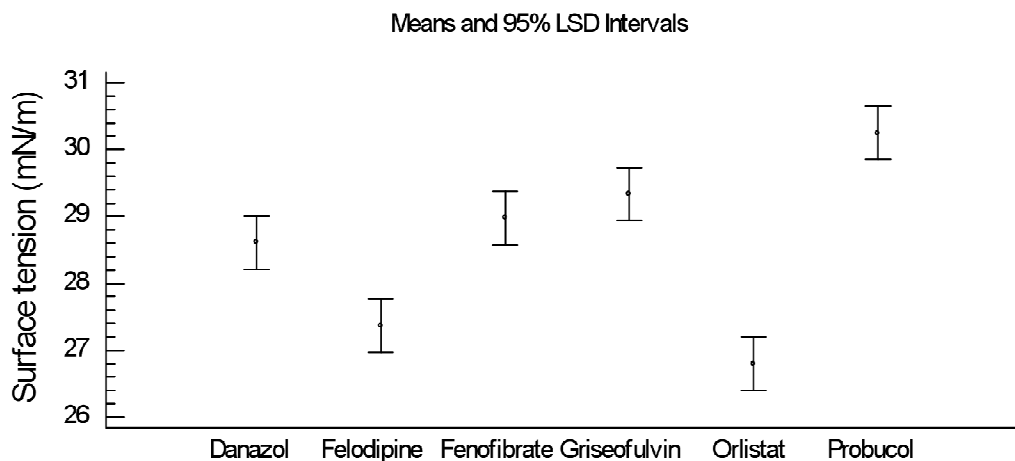
Figure 6-2: ANOVA means plot of drugs and their concentration effects on surface tension

6.3.2 Drug effects on in vitro lipolysis kinetics

Lipolysis testing was conducted at 37°C using biorelevant medium FaSSIF V2 (Jantratid et al., 2008). Released free fatty acids were titrated with 0.2 N NaOH using a computer controlled pH-stat. To identify effects of the biorelevant medium as well as of the pure drugs, blank titrations were performed first. Biorelevant medium

displayed an almost immediate NaOH consumption of 0.39 ± 0.05 ml that was further on kept at a nearly constant level (at 30 min it was 0.40 ± 0.04 ml). Finally we verified that the drugs alone in FaSSIF V2 were as was expected from their neutral character not leading to relevant NaOH consumption.

Pure medium-chain triglycerides were then titrated and the results are shown as reference in Figures 6-3 to 6-8. We determined the lipolysis up to 3 h, which was considered the longest time still physiologically meaningful. The consumed NaOH leveled off so that at 3 h the value of 10.86 ± 0.04 ml was reached. The lipolysis degree during the test was then calculated with reference to this maximal value. Pure oil therefore exhibited a lipolysis degree of $28.31 \pm 2.01\%$ following 30 min and $51.71 \pm 6.46\%$ at 1 h.
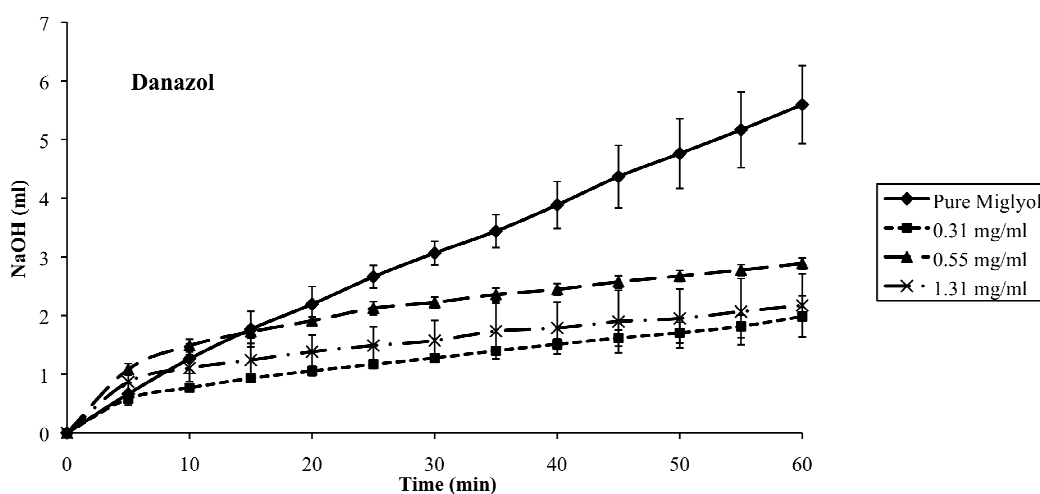
Figure 6-3: NaOH consumption in ml throughout lipolysis of 0.5 ml Miglyol®812 and 0.5 ml Miglyol®812 including three concentrations of danazol
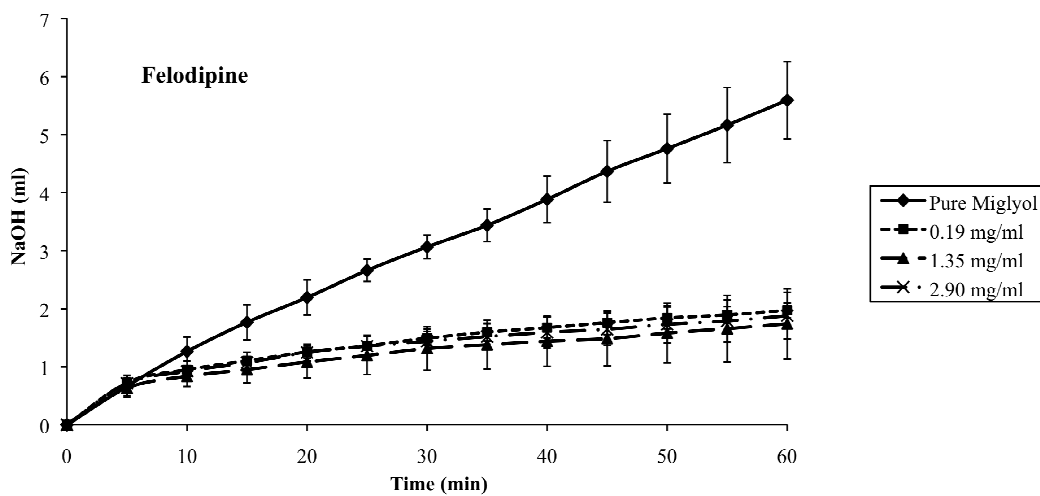
Figure 6-4: NaOH consumption in ml throughout lipolysis of 0.5 ml Miglyol®812 and 0.5 ml Miglyol®812 including three concentrations of felodipine
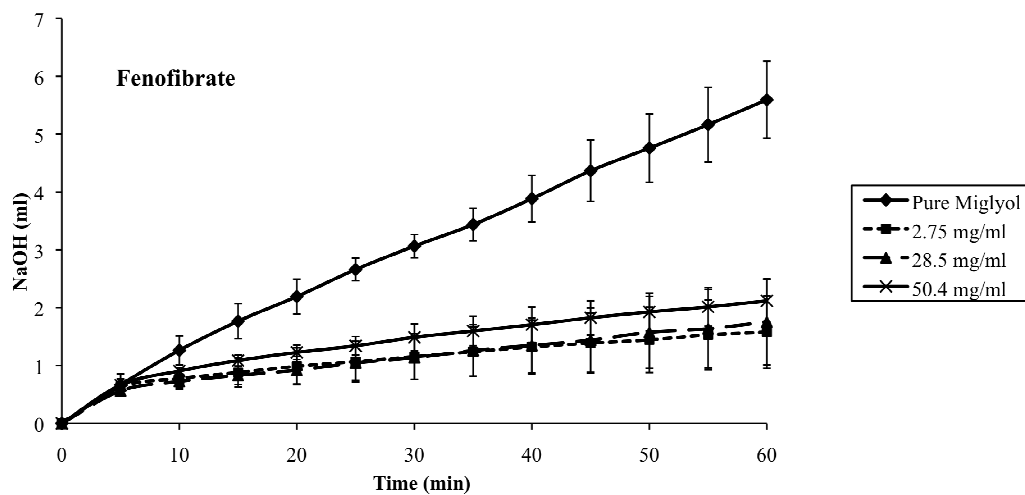
Figure 6-5: NaOH consumption in ml throughout lipolysis of 0.5 ml Miglyol®812 and 0.5 ml Miglyol®812 including three concentrations of fenofibrate
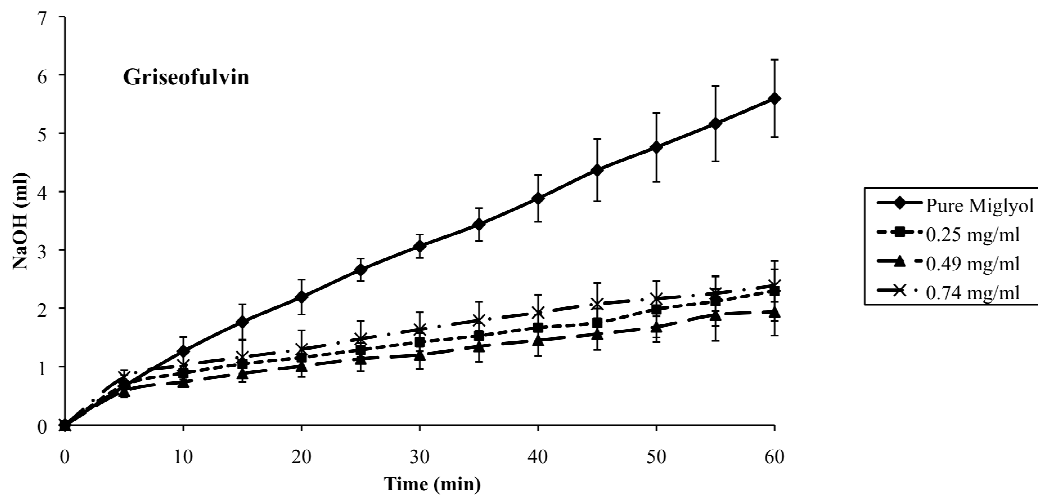
Figure 6-6: NaOH consumption in ml throughout lipolysis of 0.5 ml Miglyol®812 and 0.5 ml Miglyol®812 including three concentrations of griseofulvin
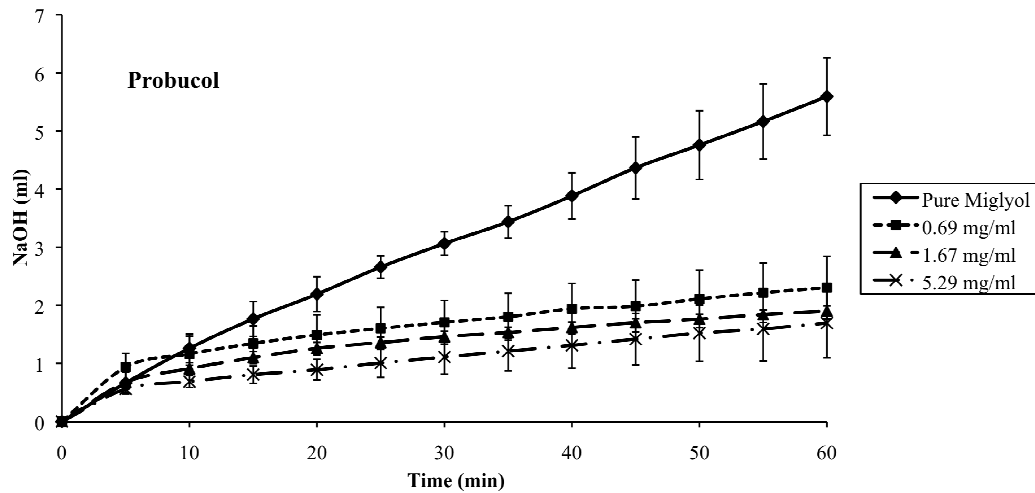
Figure 6-7: NaOH consumption in ml throughout lipolysis of 0.5 ml Miglyol®812 and 0.5 ml Miglyol®812 including three concentrations of probucol
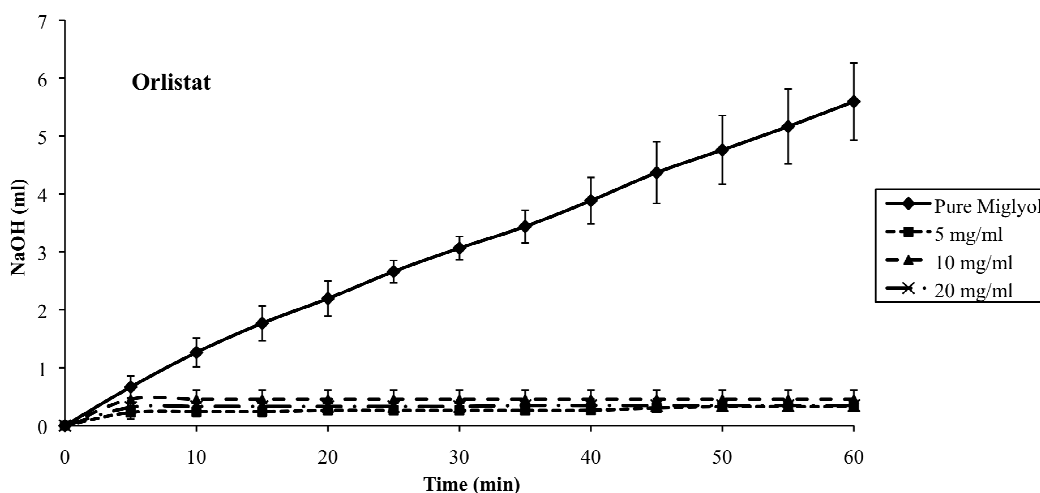
Figure 6-8: NaOH consumption in ml throughout lipolysis of 0.5 ml Miglyol®812 and 0.5 ml Miglyol®812 including three concentrations of orlistat

The results for danazol, felodipine, and fenofibrate are shown in Figure 6-3, Figure 6-4, and Figure 6-5. The drugs interestingly had a strong influence on in vitro lipolysis. The lipolysis extent as well as the rate of the process were clearly lowered. Hereby, the different compounds exhibited a similar effect when compared to the pure oil. A comparison of the low concentration (squares), intermediate concentration (triangles), and high concentration (crosses) did not reveal a clear trend. Thus, no marked effect of concentration was observed.

Instead of relying on absolute values, we opted for calculation of a rate of free fatty acids titrated. Initial time points were neglected and the titration rate was found to be nearly linear between 10 min and 40 min with R^2 values of regression lines higher than 0.9. One exception was orlistat, which was expected because of the very small slope that was displayed for this potent lipolysis inhibitor.

We named the rate in the given time interval as "apparent linear lipolysis rate". It was only an apparent value, since apart from assumed linearity, the rate was based on further approximation. Titrated NaOH volumes were not exactly corresponding to the

released fatty acids, since we cannot assume complete ionization of these lipolysis products. The titrated value was therefore only approximating the released fatty acids. An advantage of this rate definition was, however, its independence from initial NaOH consumption (< 10 min), so the rate was practically unaffected by the blank value from pure medium.

The apparent linear lipolysis rate was determined for the different drug concentrations in medium-chain triglycerides and Figure 6-9 depicts the ANOVA results. We determined for Miglyol[®]812 alone a rate of 17.25 ± 1.45 µmol/min that was substantially higher than the means of the different compound groups. All drugs were obviously reducing the lipolysis rate of the oil. Comparing the different groups demonstrated a significant effect ($p < 0.0001$, confidence level of 95 %).) but this finding was mainly due to orlistat. This inhibitor of the pancreatic lipase was known to block the enzymatic reaction (Hadvàry et al., 1988; Hauptmann et al., 1992; Tiss et al., 2009). The other compounds had clearly overlapping confidence bands. Danazol, felodipine, fenofibrate, griseofulvin, and probucol belonged to a homogeneous group in the contrast analysis of the ANOVA so that their means of the apparent lipolysis rate could not be differentiated.
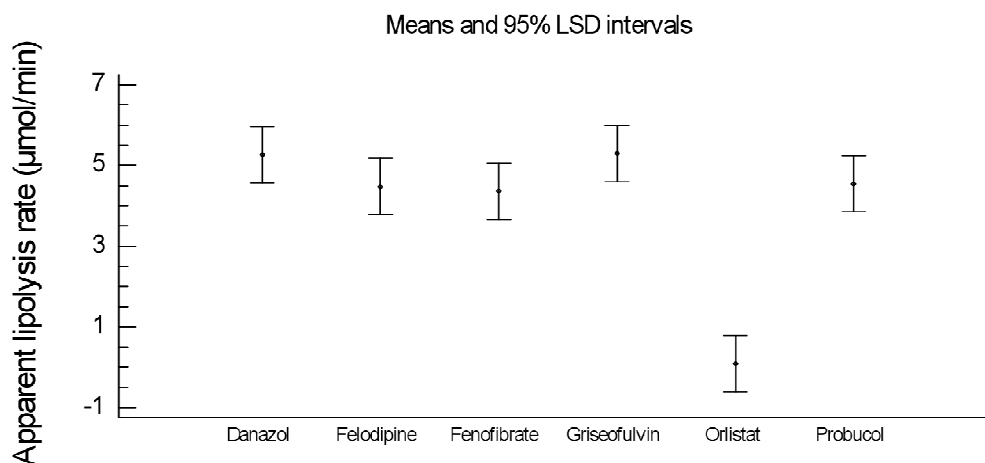
Figure 6-9: ANOVA means plot of drugs and their concentration effects on the apparent lipolysis rate

No distinction was furthermore possible with respect to the different concentration groups. There was no overall effect with clearly overlapping confidence bands. We then inspected the individual compound results more thoroughly. A single-factor ANOVA was conducted for each individual compound to analyze the potential concentration effect on the apparent lipolysis rate, but again no statistical significance was observed.

All the measurements were also performed in long-chain triglycerides. Data are not discussed, but the detailed results can be found in the appendix, section 9.2.2.

6.4 Discussion

It has been a theoretical concern that different drug concentrations in a formulation can first influence the lipolysis kinetics and may secondly lead to different drug solubilization in the evolving degradation phases. For example, different drug distributions in the digestion phases were shown by Kaukonen et al. for different compounds at a given concentration (Kaukonen et al., 2004). More recently, effects of drug distribution were analyzed for anethol trithione with varying lipid formulations

(Han et al., 2009). There is certainly a need to learn about concentration effects of different drugs and this work focused here entirely on the lipolysis kinetics.

Our results did not demonstrate a significant drug concentration effect on the lipolysis kinetics. This lack of a concentration effect could be relevant for different dose strengths of a lipid-based drug delivery system. In contrast, there was a marked effect on lipolysis kinetics observed when comparing the drug-containing oils with the pure medium-chain triglycerides. Drug in oil lowered absolute NaOH consumption as well as inhibited the apparent rates of fatty acid generation if compared to oil alone. This effect could not be solely explained by the fact that dissolved drug replaced some parts of the digestible oil in a constant formulation amount. The concentrations in the formulations were generally below 5% (m/v) and even the highest solubilized drug amount of fenofibrate did similarly affect the apparent lipolysis rate to other drugs in much smaller concentrations in the oil.

To gain a better mechanistic understanding of drug effects on lipolysis, the process must be considered as a heterogeneous enzyme reaction. Such reactions are complex and it was shown early that models of soluble enzymes have limited applicability in describing the kinetics of lipolysis (Panaiotov and Verger, 2000; Verger and Haas, 1976). Thus, lipolysis has become an emerging field of surface enzymology, which provides insights into the biopharmaceutical fate of lipid-based formulations (Aloulu et al., 2006).

A simplified scheme of lipolysis is shown as a flow chart in Figure 6-10. The first step is here dispersion of oil or formulation and this is critical for generation of a high surface area. A study of Goddeeris et al. showed that higher stirring was leading to accelerated lipolysis (Goddeeris et al., 2007). The applied stirring energy is, however, only one parameter that can theoretically impact on oil dispersion. Thus, specific

interfacial energy as well as viscosity are other known parameters that can influence

the dispersion step (Jahnke, 1998). Accordingly, there was an interest how viscosity

or surface activity of drugs in oil were then affecting the lipolysis process.
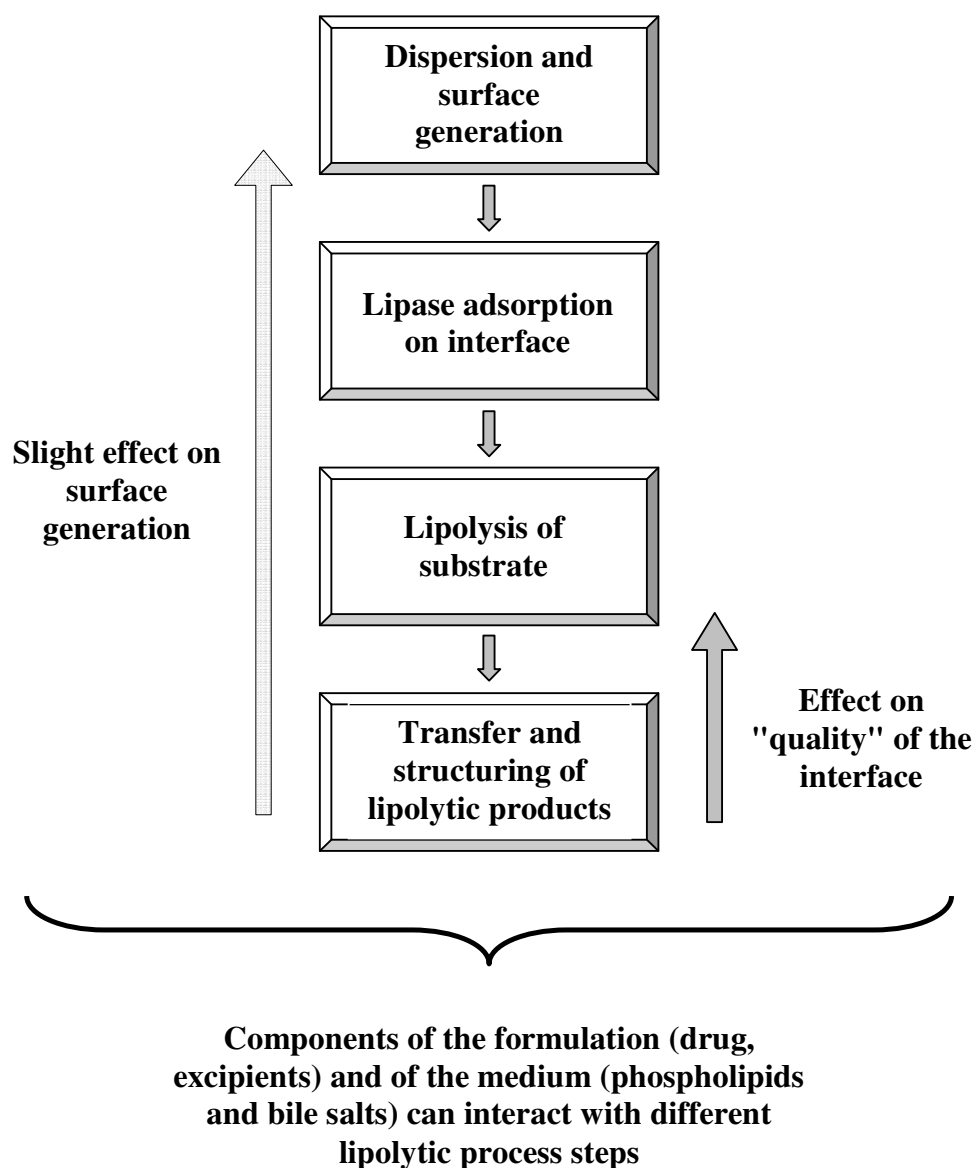
Figure 6-10: Simplified scheme of lipolysis

The drugs increased viscosity overall, but the effects were rather subtle. Some contribution of viscosity to a general lipolysis inhibition cannot be ruled out but a viscosity impact on oil dispersion was not supported by our results.

Some drugs clearly displayed surface activity. An amphiphilic character was already shown by the molecular modeling for danazol, felodipine, fenofibrate, griseofulvin, and orlistat. Subsequently, experimental surface activity was then mainly shown for felodipine and orlistat in medium-chain oil. These compounds were therefore likely to migrate to the oil/water interface and interaction with lipolysis possibly occurs. Such a direct interaction could influence the adsorption of lipase/colipase complex to the oil phase or it could perturb the enzymatic reaction itself. Some direct influence was for that reason expected for felodipine as well as a clear inhibition by orlistat. In the latter case inhibition was mostly based on direct interaction. In contrast, felodipine was not different from other compounds in lowering the apparent lipolysis rate. This result indicated that a predominant effect of the compound's surface activity was consequently not supported by our in vitro lipolysis results.

It is well possible that indirect effects were mainly accounting for the general inhibition of lipolysis. Such an indirect effect can, for example, occur with the fate of the lipolytic products at the interface of the oil droplets. Figure 6-10 shows that lipolytic products are removed from the site of the enzymatic reaction. Thus, soluble short or medium-chain acids are mostly dissolved, while less soluble glycerides form liquid crystalline structures. Such structuring of lipolytic degradation products was investigated in the case of self-emulsifying systems and reviews highlighted the fate of enzymatic products in more detail (Fatouros et al., 2007; Fatouros and Muellertz, 2008; Porter et al., 2007).

The fate of lipolytic degradation products obviously plays a key role in the kinetics of the process. Products residing in the interface generally exert a surface pressure. Comparatively high surface pressure was shown to negatively affect lipolysis (Hall, 1992; Laurent et al., 1994). It can be generally assumed that any production of degradation products affects the "quality of the interface", which is a predominant factor for lipolysis kinetics (Verger and Haas, 1976).

Noteworthy is that generation of surface-active degradation products can feedback on the dispersion process. This effect of a dynamic surface increases during lipolysis, which was experimentally shown by Kierkels et al., even though the importance of this mechanism to overall kinetics remains unclear (Kierkels et al., 1990). It might be less important than the "quality of the interface" with regard to the enzymatic reaction.

It was important to realize that insoluble degradation products of the enzyme reaction can be dissolved by bile salts and phospholipids so that medium composition plays an important role for in vitro testing (Porter and Charman, 2001). Our results supported the view of a critical medium contribution. Thus, medium-chain oil was apparently slower digested in FaSSIF V2 than in another reported test medium (Sek et al., 2002). The kinetic difference was here mainly attributed to different media composition and pH of 7.5, which was higher than pH 6.5 in FaSSIF V2.

The test medium may not only influence lipolysis by solubilization of the hydrolysis products, since components of the medium can also directly interact with the surface catalysis. Due to their surface activity, the phospholipids and bile salts are expected to adsorb to the oil/water interface so that a dynamic equilibrium with mixed micelles and vesicles in solution is attained (Embleton and Pouton, 1997). This equilibrium gives rise to the following hypothesis about indirect drug effects on lipolysis.

All model compounds were poorly soluble so these drugs were prone to inclusion into the colloidal carriers, i.e. mixed micelles and vesicles (Galia et al., 1998; Ilardia-Arana et al., 2006; Schwebel et al., 2010). The solubilized drug is expected to be partially dissolved in the oil as well as in the colloidal medium. However, the latter fraction of solubilized drug was depending on bile salts and phospholipids that were on the other hand in equilibrium with their adsorption on the oil/water interface. Moreover, bile salts and phospholipids were solubilizing lipolytic degradation products so that a competitive situation was given with drug solubilization in the medium.

Given the complexity of the involved mechanisms, it becomes apparent that poorly soluble drugs can interact on several levels with the kinetics of the process (Figure 6-10). Drugs can directly affect the quality of the interface or they can indirectly impact on lipolysis by an interaction with the biorelevant medium. A simple effect of drugs on oil viscosity or surface activity might have contributed to hinder lipolysis, but both factors appeared to play a minor role for in vitro lipolysis kinetics.

6.5 Conclusions

It was shown that a series of poorly soluble drugs exerted a strong effect on in vitro lipolysis kinetics using an updated biorelevant medium. Low drug concentrations were already affecting lipolysis, but no significant effect of drug loading was revealed. This was a promising result from a pharmaceutical viewpoint, since unchanged lipolysis kinetics for different drug loads means that there is possibly no unwanted variability arising different dose strengths.

It was remarkable that the various drugs lowered lipolysis kinetics in a similar way. This was different from how the drugs affected viscosity or surface tension of the model oil. A direct compound effect on the oil could therefore not entirely explain the

observed effects in the digestion test. Probably indirect effects played a role, e.g. drug inclusion into colloids, so that the phospholipids and bile salts of the medium could not equally interact with the oil/water interface as with oil alone. Further testing can address such mechanistic aspects and the drug partitioning into the digestion phases should be studied. A continuous research in this area is required so that lipid-based formulations are in the future developed with an improved understanding of digestion processes.

7 IN VITRO DIGESTION KINETICS OF EXCIPIENTS FOR LIPID-BASED DRUG DELIVERY AND INTRODUCTION OF A RELATIVE LIPOLYSIS HALF LIFE

7.1 Introduction

Previous research on in vitro digestion provided viable information about the fate of triglyceride formulations and solubilized drugs in the intestinal tract (Christensen et al., 2004; Dahan and Hoffmann, 2007; Kaukonen et al., 2004; Porter et al., 2004). Lipolysis of pharmaceutical systems appears to be complex because the excipients are not only enzymatic substrates, but they can also act as inhibitors (MacGregor et al., 1997; Christiansen et al., 2010). Detection of excipient effects requires not only a sensitive in vitro test, but also the in vitro lipolysis should be robust and reliable to become a modern formulation development tool.

Research is needed to make different lipolysis tests better comparable. It is favorable to have kinetic test data that are relative to a standard and therefore bear the potential to be independent of the given experimental conditions. Such a relative kinetic parameter would have to be obtained from a kinetic theory of in vitro lipolysis. In line with these considerations, this work aimed at first studying the lipolysis of nine pharmaceutical excipients and then analyzing the data using a mathematical model. The final goal was to define a relative kinetic parameter by normalizing an obtained lipolysis half life with the corresponding value from the reference oil Miglyol®812.

7.1.1 Theory

Kinetics of lipolysis is complex because it's a heterogeneous catalysis at the oil/water interface. Excellent reviews were written by Aloulou et al. (2006), Panaiotov et al. (1997), as well as Verger and Haas (1976).

An attempt was made to adopt the Michaelis-Menten kinetics as an approximation of lipolysis rate (Laidler and Bunting, 1973):

$$v = v_m' \frac{[S]}{K_m' + [S]} \tag{7.1}$$

The maximal rate v_m' and the Michaelis-Menten constant K_m' are here understood as apparent parameters, since the original model was described for a homogeneous and not for a heterogeneous catalysis. It is therefore unclear, how well the theory can be adapted to lipolysis that takes place at the oil/water interface.

There are alternative kinetic models, which are based on simplifications. Kosugi and Suzuki (1983) proposed a one-substrate, first-order kinetics to describe the lipolysis process under the assumption that the committed step of the entire reaction is the ester hydrolysis. Therefore, one substrate reacts with a water molecule at the oil/water interface to yield product molecules named P and Q. The product concentration [P] or [Q] can be expressed in terms of the concentration of all ester bonds at the start of lipolysis $[S]_0$ minus its value at a given time point [S]:

$$[P] = [Q] = [S]_0 - [S] \tag{7.2}$$

The progress of the lipolysis reaction can be described by the parameter X, which was called lipolysis degree, and represents the ratio between the product and the original substrate concentration:

$$X = \frac{[S]_0 - [S]}{[S]_0} \tag{7.3}$$

Thus, the rate is expressed as a function of the product concentrations using the hydrolysis reaction constant k_1, while assuming reversibility by introducing the constant k_{-1}:

$$v = -\frac{d[S]}{dt} = k_1[S] - k_{-1}[P][Q] \tag{7.4}$$

$$\frac{dX}{dt} = k_1(1-X) - k_{-1}[S]_0 X^2 \tag{7.5}$$

This model was proposed by Knezevic et al. for a lipolysis reaction in general (Knezevic et al., 1998). We consider the underlying assumptions as a first approximation of the kinetics from in vitro lipolysis. However, the late phase of lipolysis probably involves factors that are not considered in the present model. More advanced models would have to include the role of the interface and how it changes in the progress of the reaction. Accumulation of products on the oil surface forms a viscous layer that is expected to influence lipolysis (Embleton and Pouton, 1997). Furthermore not all ester bonds might be kinetically the same so that consecutive reactions can occur, leaving the less accessible ester bonds for the late stage of lipolysis. Different mechanisms therefore lead to a decreasing hydrolysis rate and the present model just holds for a simple approach to model an equilibrium that is reached asymptotically.

At the equilibrium, equation 7.5 becomes zero and X reaches the plateau value X_E.

$$k_1(1-X) - k_{-1}[S]_0 X^2 = 0 \tag{7.6}$$

This equilibrium condition can be used for substituting k_{-1} and to obtain equation 7.7:

$$\frac{dX}{dt} = \frac{k_1 \left[(X_E - 1)X^2 - X_E^2 X + X_E^2 \right]}{X_E^2}$$
(7.7)

This differential equation can be integrated and the mathematical derivation of the equation below was published by Knezevic et al. (1998):

$$X = \frac{\left(1 - (3 - X_E)^{-t/h}\right) X_E}{1 + (1 - X_E)(3 - X_E)^{-t/h}}$$
(7.8)

where h is termed "lipolysis half life" and holds for the time needed to reduce the initial substrate concentration by a factor of two.

In vitro lipolysis testing is a special form of lipase-catalyzed hydrolysis given the comparatively small amount of formulation and the presence of bile salts as well as Ca^{2+}-ions. Under these conditions, complete lipolysis frequently occurs. Accordingly, in this situation we assumed that the lipolysis degree X_E gets close to unity, which greatly simplifies the result:

$$X = 1 - 2^{-t/h}$$
(7.9)

A linear plot can be obtained by rearranging the equation 7.9 to:

$$\ln(1 - X) = -\frac{\ln(2)}{h} t$$
(7.10)

The lipolysis half life h can be inferred from the slope of the ln(1-X) plot . Finally, it makes sense to have relative values of this kinetic measure. Normalization by the value of a standard sample, e.g. Miglyol®812, was used to define the "relative lipolysis half life":

$$h_{rel} = \frac{h(\text{sample})}{h(\text{reference})}$$
(7.11)

7.2 Materials and Methods

7.2.1 Materials

Calcium chloride, maleic acid, porcine pancreatin, sodium chloride, sodium hydroxide, and 0.2 N sodium hydroxide were purchased from Sigma-Aldrich GmbH, Switzerland. Imwitor®742, Miglyol®812, and PS80 were obtained from Hänseler AG, Switzerland. Imwitor®742 is a blend of mono-, di-, and triglycerides, mostly caprylic ($C_{8:0}$) and capric acid ($C_{10:0}$). The fraction of monoglycerides was 44% to 55%. Miglyol®812 is a medium-chain oil consisting of 50% to 65% caprylic acid ($C_{8:0}$) and 30% to 45% of capric acid ($C_{10:0}$). A maximal amount of 2% was specified for caproic acid ($C_{6:0}$) as well as for lauric acid ($C_{12:0}$). Finally, the content of myristic acid ($C_{14:0}$) was maximally 1%. Capryol™90, Lauroglycol™90, Labrafil®M-2125 CS, and Gelucire®44/14 were purchased from Gattefossé GmbH, France. Capryol™90 (propylene glycol monocaprylate) consisted of 99.6% caprylic acid ($C_{8:0}$) and Lauroglycol™90 (propylene glycol monolaurate) contained 99.1% lauric acid ($C_{12:0}$) and 0.1% capric acid ($C_{10:0}$). Labrafil®M-2125 CS is a well-defined mixture of mono-, di-, and triglycerides as well as mono- and di-fatty acid esters of polyethylene glycol. The fatty acid moieties were 52.1% linoleic acid ($C_{18:2}$), 32.2% oleic acid ($C_{18:1}$), and 10.8% palmitic acid ($C_{16:0}$). The amount for stearic acid ($C_{18:0}$) was 2%, for linolenic acid ($C_{18:3}$) 1%, for arachidic acid ($C_{20:0}$) 0.5%, and 0.4% for eicosenoic acid ($C_{20:1}$). Gelucire®44/14 is, similar to Labrafil®M-2125 CS, a well-defined mixture of mono-, di-, and triglycerides as well as mono- and di-fatty acid esters of polyethylene glycol. The amount of lauric acid ($C_{12:0}$) was 44.7%, 18.2% for myristic acid ($C_{14:0}$), 9.6% for palmitic acid ($C_{16:0}$), and 11.7% for stearic acid ($C_{18:0}$). The content of caprylic acid ($C_{8:0}$) was 7.29% and for capric acid ($C_{10:0}$) it was 5.47%. Capmul®MCM was obtained from Abitec Corp., United States. This mixture of medium-chain mono- and

diglycerides contained 82.6% caprylic acid ($C_{8:0}$) and 17.4% capric acid ($C_{10:0}$). Cremophor®RH 40 (Macrogol-Glycerolhydroxystearat Ph.Eur.) was obtained from BASF AG, Switzerland.

Sodium taurocholate was purchased from Prodotti Chimici e Alimentari S.p.A., Italy, and phosophatidylcholine was obtained from Lipoid GmbH, Germany.

7.2.2 Methods

7.2.2.1 Preparation of biorelevant medium and lipase solution

The enzymatic tests were conducted in FaSSIF V2 (Jantratid et al., 2008). This medium was used as reaction medium as well as medium for the suspension of porcine pancreatin (0.174 mg pancreatin/ml medium). Following stirring of the mixture at room temperature (15 min, 25 ± 0.5°C), the dispersion was centrifuged using an Eppendorf 5415C Centrifuge (Vaudaux-Eppendorf AG, Switzerland) for 15 min at 14000 rpm. The clear supernatant was collected and pH 6.5 was adjusted. The resulting solution exhibited an enzyme activity of 10000 TBU/ml. This solution (pancreatic extract) was freshly prepared each day.

7.2.2.2 In vitro lipolysis test

Excipient (500 mg) was dispersed in 36 ml medium at 37°C in a double walled glass vessel. The solution was then equilibrated for 15 min to then start the lipolysis by adding 4 ml pancreatin extract (1000 TBU/ml final concentration) and 5 mM calcium chloride dihydrate. During lipolysis, the pH was kept constant using a Titrando 842 (Metrohm Schweiz AG, Switzerland) that titrated the liberated free fatty acids with 0.2 N NaOH solution.

7.2.2.3 Statistical Design and analysis of data

All measurements were conducted in triplicates and results were expressed as mean values ± standard deviations. For the regression analysis, the program Statgraphics

Centurion XV ed. Professional from StatPoint Technologies, Inc., United States, was used.

7.3 Results

7.3.1.1 NaOH consumption and lipolysis degree

The titrated NaOH volume to keep the pH 6.5 constant was measured. Consumed equivalents of 0.2 N NaOH corresponded to the liberated free fatty acids during the reaction.
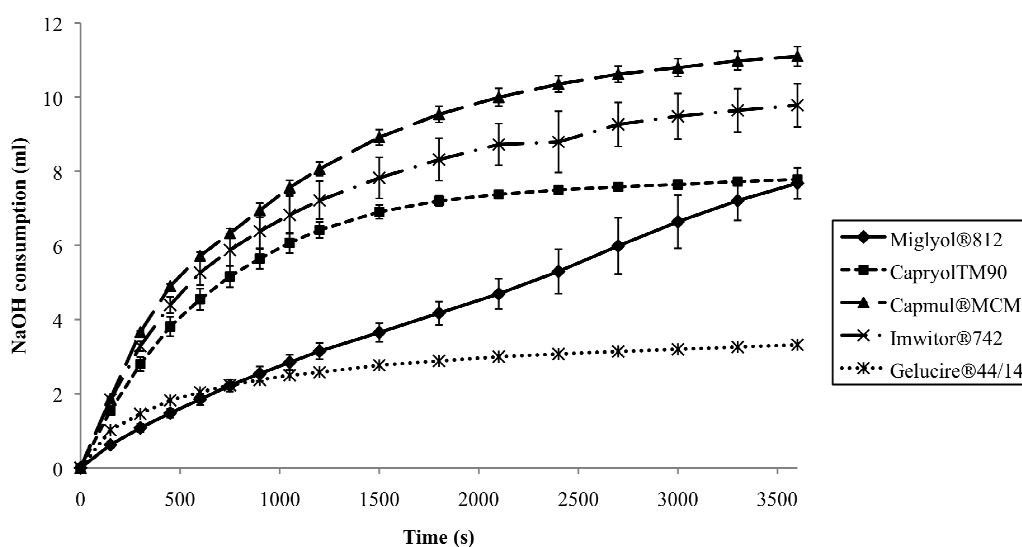
Figure 7-1: Lipolysis profiles of excipients having comparatively high NaOH consumption

Figure 7-1 and Figure 7-2 show lipolysis results of different excipients during the first hour. Pronounced differences were observed in terms of the kinetic profiles. The curves levelled off as a function of time at different values. Fig. 1 depicts a first group of excipients having comparatively high NaOH consumption. This group included mono-, di-, and triglycerides, i.e. Miglyol®812, Capmul®MCM, and Imwitor®742. Further highly digestible excipients in this group were Capryol™90 as well as Gelucire®44/14. All of these excipients obviously released comparatively high

amounts of free fatty acids even though differences were observed with respect to their individual kinetics. Thus, Capmul®MCM and Imwitor®742 had the fastest and the highest NaOH consumption, followed by Capryol™90. Compared with these excipients, the kinetics of medium-chain triglyceride Miglyol®812 was rather slow and the values barely levelled off within the first hour of lipolysis. This was different from Gelucire®44/14 for which the highest NaOH consumption was reached rather quickly. A similar trend was further observed with some of the excipients of the second group (Figure 7-2).
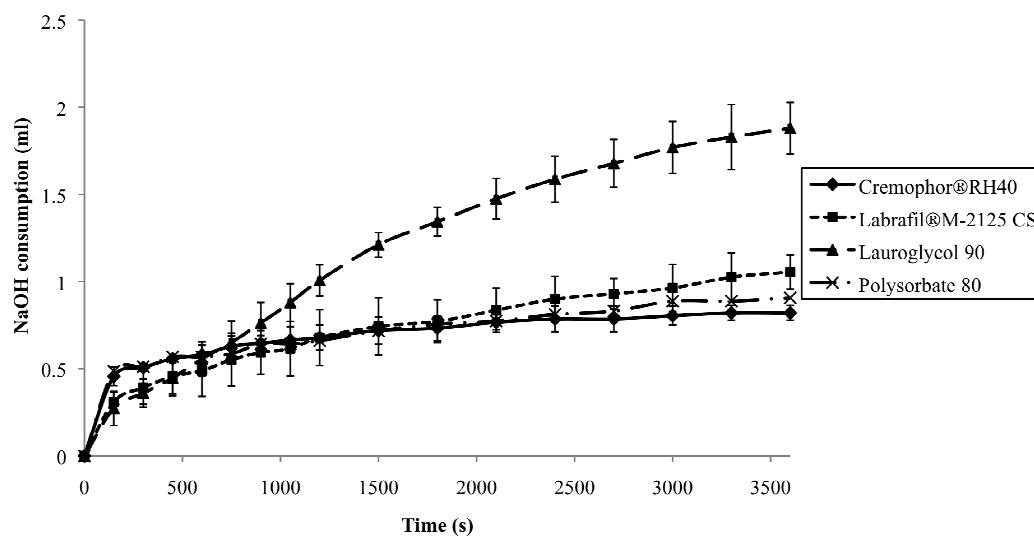
Figure 7-2: Lipolysis profiles of excipients having moderate NaOH consumption

Figure 7-2 displays a group of excipients with moderate NaOH consumption. Interestingly, the excipients curves of Cremophor®RH 40, Labrafil®M-2125 CS, and PS80 levelled off quickly. However, the NaOH consumption was low with a value below 1 ml. Lauroglycol™90 ranked among the second group. It is a propylene glycol monolaurate differing from the PEGylated excipients with respect to lipolysis

results. In fact, steadily increasing values were observed while no plateau was reached within the first minutes of lipolysis.

Differences in absolute NaOH consumption did not directly reflect the lipolysis degree, i.e. how many of the available ester bonds were hydrolyzed. The lipolysis degree can only be calculated referring on the overall number of the available ester bonds. To define the estimated hydrolysis maximum (EHM), we selected the mean saponification value that was inferred from the excipient specifications. Based on this value, a theoretical maximum titration volume was estimated.

Excipient	EHM (ml)	NaOH consumption after 3 h (ml)	Lipolysis degree after 3 h (%)
Miglyol®812	14.95	10.86 ± 0.04	72.6
Capryol™90	12.5	9.02 ± 0.15	72.2
Capmul®MCM	12.05	11.93 ± 0.23	99.0
Imwitor®742	11.8	11.04 ± 0.50	93.6
Lauroglycol™90	9.6	2.40 ± 0.13	25.0
Labrafil®M-2125 CS	7.15	1.42 ± 0.14	19.9
Gelucire®44/14	3.6	3.60 ± 0.14	100.0
Cremophor®RH40	2.45	0.85 ± 0.02	34.7
Polysorbate 80	2.25	1.20 ± 0.11	53.3

Table 7-1: Estimated hydrolysis maximum (EHM) and the experimental lipolysis degree after 3 h for each excipient

Table 7-1 shows the EHM in ml of 0.2 N NaOH solution for all the tested excipients. The EHM was compared to the NaOH consumption after 3 h. This point in time was selected from the physiological consideration that it roughly estimates the upper limit of the residence time that is still reasonable for lipolysis in the small

intestinal tract. Some values after 3 h were in the same range as the EHM and other excipients reached only a fraction thereof. We used the EHM as 100% value to calculate the lipolysis degree that was interesting to consider after the rather long time of 3 h. Excipients that reached more than 70% of total lipolysis were considered as highly digestible. Accordingly, the excipients Miglyol®812, Capmul®MCM, Capryol™90, Imwitor®742, and Gelucire®44/14 displayed almost complete lipolysis of hydrolyzable ester bonds.

7.3.1.2 Kinetic data as ln(1-X) plot and definition of a relative lipolysis half life

According to the model, linearity of the ln(1-X) plot versus time is expected for excipients that are completely digested. Therefore only excipients with a lipolysis degree of > 70% at 3 h were selected for this analysis. Moreover, the evaluation was limited to the initial phase of lipolysis because of the simple model assumptions seemed to be less suitable for the complex equilibrium phase of lipolysis.
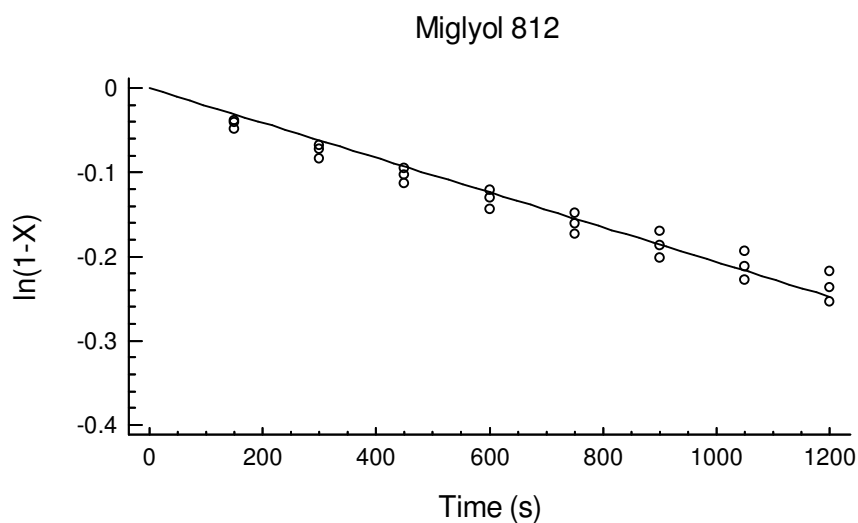
Figure 7-3: ln(1-X) plot for Miglyol®812
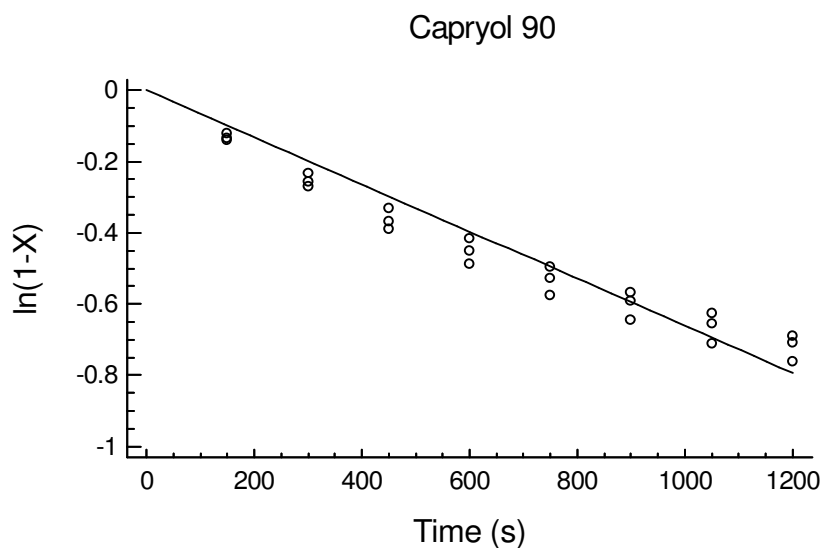
Figure 7-4: ln(1-X) plot for Capryol™90

Figure 7-3 depicts the plot for Miglyol®812 and Figure 7-4 shows the plot Capryol™90. High R^2 values were observed despite the simplicity of the model. Table II lists the slopes of the regression lines as well as the standard errors with 95% confidence intervals. Based on the slope, the lipolysis half life was calculated (Table 7-2).

Excipient	Slope ($*10^{-4}$ s^{-1})	SE ($*10^{-4}$ s^{-1})	95% confidence interval ($*10^{-4}$ s^{-1})	R^2 (%)	Lipolysis half life (s)
Miglyol®812	-2.07	0.04	(-2.14) - (-1.99)	95.2	3349
Capryol™90	-6.61	0.16	(-6.93) - (-6.29)	91.6	1049
Capmul®MCM	-9.70	0.16	(-10.0) - (-9.38)	96.4	715
Imwitor®742	-8.62	0.23	(-9.10) - (-8.14)	89.5	804
Gelucire®44/14[a)]	-8.75	0.34	(-9.45) - (-8.05)	96.9	792

[a)] An intercept was fitted with -0.268 s^{-1} and an SE of 0.026 s^{-1}, SE: standard error

Table 7-2: Statistical evaluation of the linear regression model
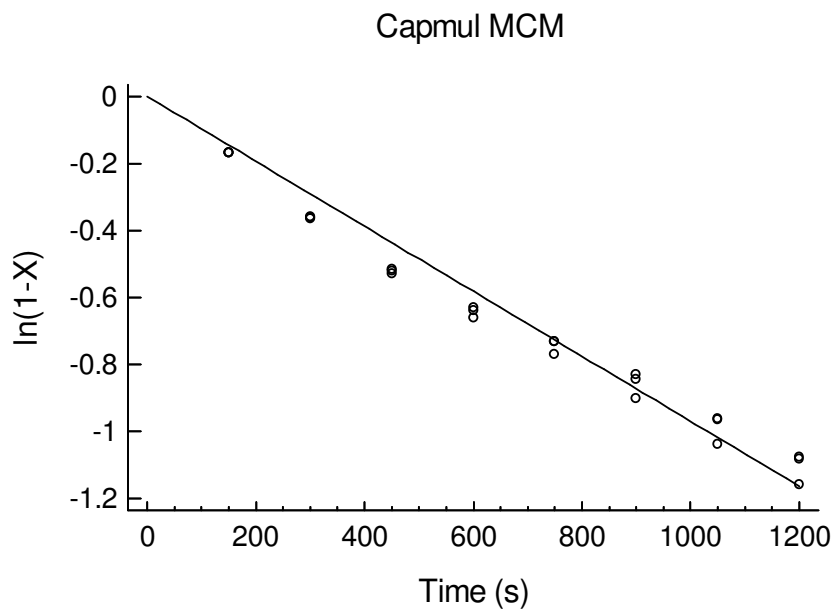
Capmul MCM

Figure 7-5: ln(1-X) plot for Capmul[®]MCM
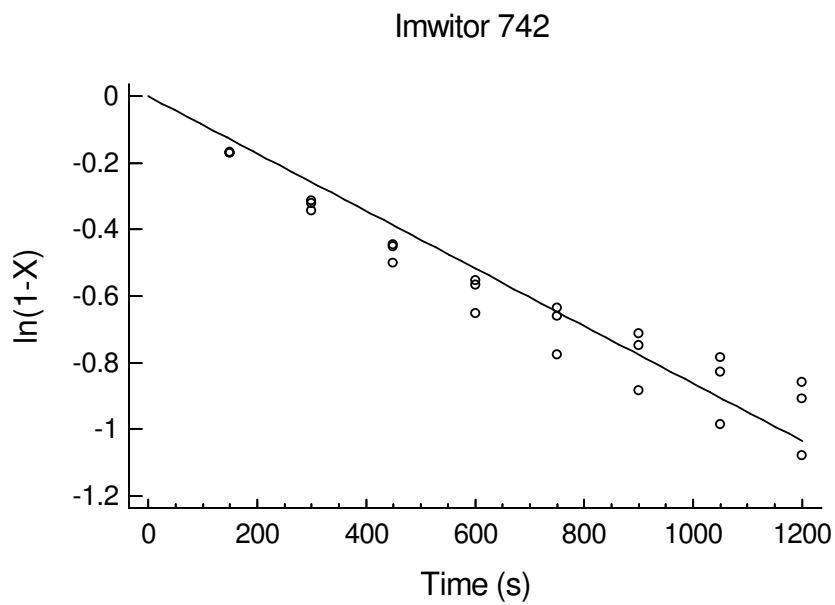
Imwitor 742

Figure 7-6: ln(1-X) plot for Imwitor[®]742

As shown in Figure 7-5 and Figure 7-6, a suitable model fit was further demonstrated for Capmul®MCM and Imwitor®742. It was interesting to note that Gelucire®44/14 needed an assumed intercept for the linear regression. This PEGylated excipient obviously required this intercept as an experimental correction term. It was possibly due to an initial NaOH volume that was consumed apart from the lipolysis reaction. Figure 7-7 displays the ln(1-X) values of Gelucire®44/14 as a function of time. A good first approximation of the initial lipolysis kinetics was attained, which was also reflected by a high correlation coefficient (Table 7-2).
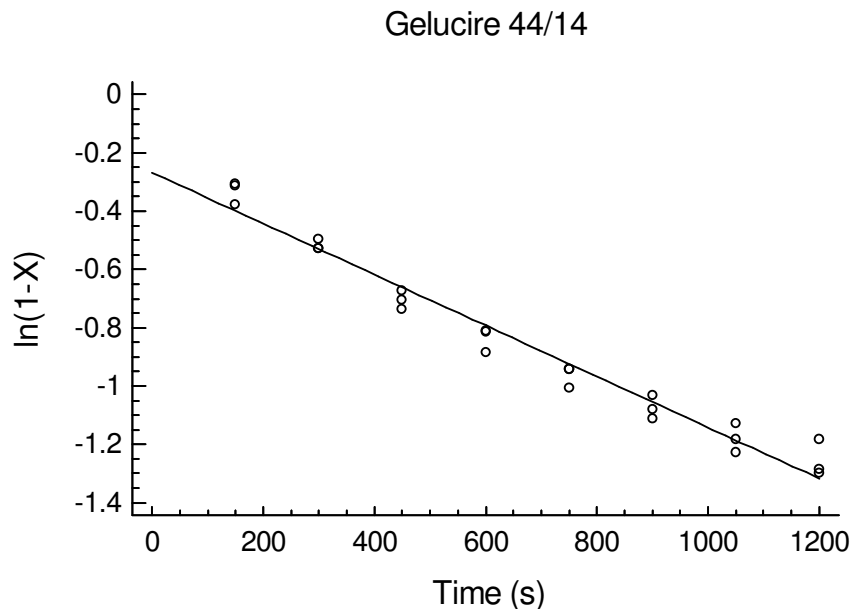
Figure 7-7: ln(1-X) plot for Gelucire®44/14

To obtain a relative kinetic parameter, a reference excipient had to be selected. We used Miglyol®812 as reference for the calculation of the relative lipolysis half life. As shown in Table 7-3, the values ranged from 0.21 in case of Capmul®MCM to 0.31

for Capryol™90. Lipolysis of pure reference oil was obviously substantially slower than that of the other excipients.

Excipient	Lipolysis half life (s)
Miglyol®812 (reference)	1
Capryol™90	0.31
Capmul®MCM	0.21
Imwitor®742	0.24
Gelucire®44/14	0.24

Table 7-3: Lipolysis half life, using Miglyol®812 as reference

7.4 Discussion

The tested excipients ranged from mixtures of mono-, di-, and triglycerides as well as non-ionic PEGylated surfactants. It was interesting to note that excipients with medium-chain-length esters generally displayed high fatty acid titration levels and nearly complete lipolysis. This was true for Miglyol®812, Capryol™90, Capmul®MCM as well as for Imwitor®742. We also found a difference in the digestion kinetics of another chemical group, namely the propylene glycol esters. The monocaprylate Capryol™90 was among the highly digested excipients, whereas the monolaurate ester Lauroglycol™90 showed incomplete lipolysis. Not all lauryl-acid containing excipients were incompletely hydrolyzed as can be seen from the example of Gelucire®44/14. Longer chain derivatives like the oleyl polyglycerides of Labrafil®M-2125 CS, or the PEGylated sorbitant monooleate PS80 further demonstrated that only a low lipolysis degree could be reached. A comparatively low digestion plateau was moreover reached with Cremophor®RH 40, which is a PEGylated hydrogenated castor oil.

Chain length was certainly not the only factor that influenced the lipolysis kinetics. Miglyol®812 was slower hydrolyzed than the other completely digested excipients. There was a clear distinction between the pure triglyceride and the mixtures of mono-, di-, and triglycerides of medium-chain length, i.e. Capmul®MCM and Imwitor®742. These partial glycerides were expected to have a lower specific energy at the water/excipient interface and higher initial surface generation could explain the increased lipolysis rates. However, this aspect of dispersibility and surface generation must be viewed differently if PEGylated surfactants are considered.

Gelucire®44/14 is a PEGylated surfactant that has been widely used in self-emulsifying drug delivery systems and its susceptibility to digestion was reported before (Fernandez et al., 2009). It was still remarkable that the excipient revealed a complete lipolysis. Bulky PEG chains can hinder sterically the lipolysis process. However, the ester bonds in Gelucire®44/14 were obviously well accessible to the enzyme. This was in contrast to the maximal lipolysis degree of Labrafil®M-2125 CS, Cremophor®RH 40, and PS80. Therefore, the effect may not solely depend on the fatty acid chain length. It was earlier reported that Cremophor®RH 40, and PS80 were both inhibiting pancreatic lipase if triglycerides were digested in vitro (Christiansen et al., 2010). This recent finding supported the pioneering work of Gargouri et al. who studied the surfactant effects on inhibition of lipase (Gargouri et al., 1983). Surfactants interfere with the lipolysis of triglycerides and they can be digested themselves. Such digestion of functional excipients typically affects the drug solubilization behaviour. Cuiné et al. showed that formulations with high quantities of digestible surfactant prevented drug precipitation less effectively (Cuiné et al., 2007). These effects must be known in formulation development to avoid drug precipitation in the gastro-intestinal tract due to the loss of surfactants in the course of digestion.

Our study focused on the lipolysis kinetics of single excipients, which might be a start for future research. For this purpose we suggested a new theoretical concept for the analysis of the kinetic data. We have to keep in mind that many simplifications were made. The basic kinetic model only focused on ester hydrolysis as the committed step. All ester bonds were treated equally even though an experimental substrate can have different ester types. Thus, consecutive reactions can be a reason for changing kinetics as a function of time. It is mainly the phase close to the equilibrium that seems to be rather complex. It was mentioned earlier that the effect of accumulated degradation products on the droplet surface can lead to viscous structures. Biophysical analysis of these mesophases has become a research topic in its own right (Fatouros and Muellertz, 2008). The effect of such structures on the lipolysis kinetics is not clear on a mechanistic level and such effects were not considered in the proposed model.

We studied the initial lipolysis phase of those excipients that were extensively hydrolyzed using a ln(1-X) versus time plot. The theoretical linearity was experimentally verified with these additives. It should not be forgotten that neither the excipients nor the pancreatic extract are pure substances, but rather complex mixtures. In light of the simplicity of the underlying theory, it was therefore remarkable that the group of extensively digested excipients indeed exhibited a fair linearity in the ln(1-X) plot. However, there was a trend in the residuals detected, which underlined the model to hold for a first approximation only.

The theoretical concept differentiates between the equilibrium lipolysis degree X_E and complete lipolysis, where this value reaches unity. This is an important differentiation and care is needed when comparing with another lipolysis extent that is defined differently by simply taking the given equilibrium value as 100%. Our results clearly

demonstrated that some excipients had residual ester bonds that were not cleaved during lipolysis. In this respect, the estimated hydrolysis maximum was a helpful concept. It indicated a maximal ester concentration because the used saponification number was determined under harsher hydrolysis conditions as compared to the in vitro lipolysis test.

To consider the maximal concentration of ester bonds, Ali et al. tried a different theoretical approach (Ali et al., 2007). It was assumed that during lipolysis one mole of triglyceride is hydrolyzed to one mole of 2-monoglycerides and two moles of free fatty acids. The equivalents of maximal titration solution can then be calculated by considering the main specified oil components. However, care is needed since the 2-monoglycerides can undergo a non-enzymatic isomerisation to 1-monoglycerides that can be digested by the pancreatic lipase to glycerol and a fatty acid (Embleton and Pouton, 1997). Thus, values of lipolysis degree or lipolysis extent should be carefully compared in the literature by considering the given definitions.

Comparison of lipolysis data from different origins was a main reason to introduce the relative lipolysis half life. By calculating relative values to standard oil, the dependence on the given experimental conditions is lower than if absolute kinetic values are compared. We used the medium-chain triglycerides Miglyol®812 as reference. Even though the oil was arbitrarily selected, the choice was reasonable with our data, since the other excipients were all hydrolyzed much faster so that values below one were obtained. However, based on our knowledge of comparatively slower hydrolysis of long-chain triglycerides, we expect that other oils of longer chain length reach relative lipolysis half lives of greater than one. We certainly need more data and further digestion experiments with other excipients as well as drug delivery systems.

This will ultimately show the usefulness of the relative lipolysis half life in comparing kinetic data from different in vitro lipolysis tests.

7.5 Conclusions

A series of excipients were digested in vitro and a kinetic theory was adapted to describe the obtained lipolysis data. The excipients were classified into partially and entirely digesting additives. In line with the theory, the latter group displayed linear plots of ln(1-X) versus time and the slope was used to estimate a lipolysis half life. A relative lipolysis half life was subsequently defined to normalize the kinetic measure based on the given experimental in vitro conditions. Progress was made in better characterising the in vitro digestion of pharmaceutical excipients. The ln(1-X) versus time plot can be used as a promising tool for the analysis of future in vitro lipolysis results. A proper assessment of the lipolysis kinetics is an important step because it defines the formulation changes over time. If the formulation is changing in the course of lipolysis, the main concern is whether a poorly water-soluble drug can still be kept in solution. Drug precipitation can greatly limit the oral absorption of such drugs and future research should focus on the link between kinetic changes of lipolysis and the kinetics of potential drug precipitation. Only a proper understanding of the in vitro performance can form a solid basis for good correlations with in vivo data of lipid drug delivery systems.

8 OUTLOOK

In this study, we gained new insight into dissolution and lipolysis processes based on in vitro tests using biorelevant media. The factors influencing the processes under physiological conditions are versatile thus rendering detailed insight rather challenging. As a first step, lipolysis tests should be standardized, as was done with dissolution tests. At present, the results of all existing lipolysis tests cannot be compared due to the highly variable experimental procedures. Standardization of in vitro lipolysis tests would simplify the cross-comparison of data, and therefore accelerate the improvement of a systematic understanding of lipolysis.

In future work, experimental settings might be expanded to include gastric processes and absorption steps. Absorption tests using cells already exist, but there is still potential for improvement. Since some cells, e.g. Caco-2 cells, are sensitive to bile salts and surfactants, the usefulness of these cells has yet to be demonstrated. However, for a simulation close to reality and enhancing the predictability of in vivo dissolution of drugs, the inclusion of additional steps is necessary.

We introduced analytical tools such as Raman spectroscopy, particle analyzer, and FBRM. These tools seemed to be able to monitor the precipitation processes in spite of the turbidity of some media. It would be interesting to introduce other tools and to check the ability of process monitoring in biorelevant media.

Our proposed mathematical models are useful for the description of precipitation and lipolysis processes. The model for precipitation was only adopted for a weakly basic

model drug. The usefulness of this model for acidic and neutral drugs has yet to be proven. It would be interesting to see if the model is also able to describe the process of precipitation of other classes of drugs. The usefulness of the model for a drug dissolved in lipid-based formulations remains an open question.

The mathematical model for lipolysis kinetics was applied for different excipients, indicating that the crucial step during lipolysis is not only ester hydrolysis. Additional steps have to be included to improve the validity of the model. Moreover, the model can be adapted to formulations including poorly water-soluble drugs.

9 APPENDIX

9.1 Appendix of chapter 4

9.1.1 Calculation of used amounts of media and API

The used amount of media was based on the assumption, that the patient takes the drug together with 200 ml of water. The volume of the fasted stomach medium was 100 ml. One-third of the fenofibrate was either precipitated or absorbed in the stomach. Therefore only two-third of API in 100 ml stomach medium/water moved into 200 ml intestinal medium. The amounts were scaled down by a factor 6 to a total volume of 50 ml.

Drug concentrations were calculated based on the product Lipanthyl® which contains 100 mg to 267 mg fenofibrate.

9.1.2 FBRM counts/s at the start of the experiment, before nucleation started
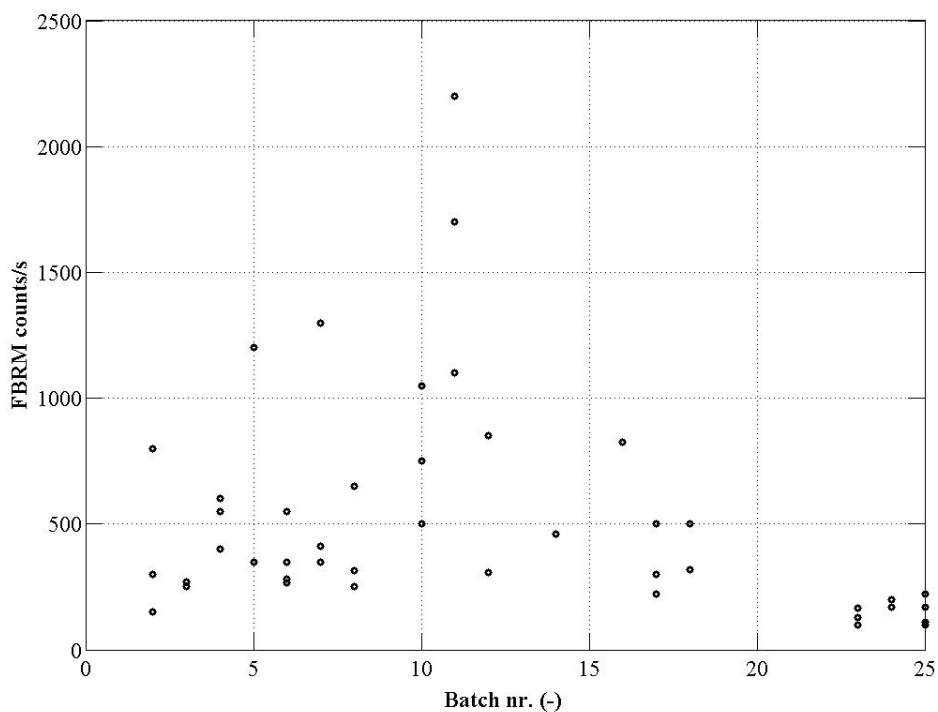
Figure 9-1: Biorelevant media mixture, 37°C: FBRM counts/s at the beginning of the experiment as a function of the biorelevant media batch, before nucleation started

The FBRM counts/s just after the addition of FaSSIF V2 in the range of 1 μm to 20 μm were recorded before nucleation started. The FBRM counts/s were $\neq 0$ and the values showed variations, neither related to the amount of PS80 in the formulation nor to the media batches (Figure 9-1). The latter had no influence in our experiments, because the production of the media was always based on exactly the same procedure. The main reason for the particle number variation was precipitation of fenofibrate in FaSSGF. Not all the formulations were able to keep the drug in a solubilized state during the simulated stomach passage. Previously, equilibrium solubilities in the stomach were measured. A two fold solubility of fenofibrate in FaSSGF resulted compared to the solubility in FaSSIF V2. Therefore it was reasonable, that

precipitation occurred in the simulated stomach. As a consequence, initial precipitates in FaSSGF were moved to the simulated intestine, which resulted in a variable number of the FBRM counts/s before nuleation started.

9.2 Additional results of chapter 6 using medium- and long-chain triglycerides

9.2.1 Additional data using medium-chain triglycerides

	Surface tension ± std. (mN/m) of different drug concentrations in MCT (value of pure oil: 36.13 ± 0.15)		
	Low	**Intermediate**	**High**
Danazol	35.7 ± 0.2	35.4 ± 0.1	35.6 ± 0.1
Felodipine	34.5 ± 0.1	34.6 ± 0.1	35.1 ± 0.2
Fenofibrate	35.8 ± 0.1	36.4 ± 0.1	36.9 ± 0.2
Griseofulvin	35.9 ± 0.1	35.9 ± 0.0	38.6 ± 0.1
Probucol	36.1 ± 0.1	36.0 ± 0.1	36.1 ± 0.1
Orlistat	35.1 ± 0.1	34.8 ± 0.1	34.7 ± 0.1

*Surface age of 25 ms

Table 9-1: Surface tension of different drug concentrations in MCT, surface age 25 ms

Surface tension ± std. (mN/m) of different drug concentrations in MCT
(value of pure oil: 29.57 ± 0.06)

	Low	Intermediate	High
Danazol	29.5 ± 0.0	29.5 ± 0.0	29.5 ± 0.1
Felodipine	27.9 ± 0.1	29.8 ± 0.3	29.3 ± 0.2
Fenofibrate	29.6 ± 0.1	29.8 ± 0.2	30.1 ± 0.1
Griseofulvin	29.6 ± 0.2	29.5 ± 0.1	32.8 ± 0.3
Probucol	32.8 ± 0.2	29.7 ± 0.2	29.5 ± 0.1
Orlistat	28.0 ± 0.2	27.9 ± 0.1	27.8 ± 0.0

*Surface age of 250 ms

Table 9-2: Surface tension of different drug concentrations in MCT, surface age 250 ms

Density ± std. (g/cm^3) of MCT including different drug concentrations
(value of pure oil: 0.938 ± 0)

	Low	Intermediate	High
Danazol	0.938 ± 0	0.938 ± 0	0.938 ± 0
Felodipine	0.938 ± 0	0.938 ± 0	0.938 ± 0
Fenofibrate	0.939 ± 0	0.943 ± 0	0.947 ± 0
Griseofulvin	0.938 ± 0	0.938 ± 0	0.938 ± 0
Probucol	0.938 ± 0	0.938 ± 0	0.938 ± 0
Orlistat	0.938 ± 0	0.938 ± 0	0.938 ± 0

Table 9-3: Density of MCT including different drug concentrations

9.2.2 Additional data using long-chain triglycerides

Drug concentrations in LCT (mg/ml)

	Low	Intermediate	High
Danazol	0.35	0.57	1.31
Felodipine	0.43	1.68	3.33
Fenofibrate	2.50	25.30	50.00
Griseofulvin	0.27	0.57	0.88
Itraconazole	0.17	0.41	0.62
Probucol	1.8	10.32	25.02
Orlistat	5.00	10.00	20.00

Table 9-4: Drug concentration levels in LCT

Kinematic viscosity ± std. (mm^2/s) of different drug concentrations in LCT
(value of pure oil: 72.9 ± 0.1)

	Low	Intermediate	High
Danazol	73.7 ± 0.5	73.4 ± 0.3	71.4 ± 0.4
Felodipine	73.3 ± 0.9	72.5 ± 0.9	72.3 ± 1.3
Fenofibrate	70.6 ± 0.7	74.9 ± 0.2	80.1 ± 1.3
Griseofulvin	72.4 ± 0.8	73.0 ± 1.6	74.1 ± 0.6
Itraconazole	72.9 ± 0.4	72.7 ± 0.3	72.7 ± 0.6
Probucol	73.0 ± 1.8	74.6 ± 0.1	79.8 ± 0.7
Orlistat	73.1 ± 1.9	73.0 ± 1.6	78.2 ± 0.5

Table 9-5: Kinematic viscosity of different drug concentrations in LCT
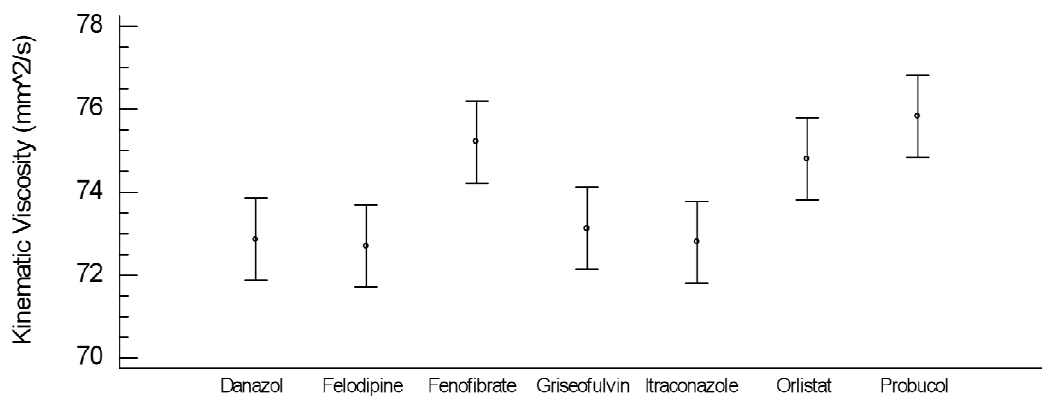
Figure 9-2: ANOVA means plot of drugs and their concentration effects on kinematic viscosity in LCT (means and 95% LSD intervals)

Surface tension ± std. (mN/m) of different drug concentrations in LCT
(value of pure oil: 50.40 ± 0.36)

	Low	Intermediate	High
Danazol	51.0 ± 0.1	51.0 ± 0.5	50.8 ± 0.3
Felodipine	49.5 ± 0.1	49.6 ± 0.3	50.5 ± 0.3
Fenofibrate	52.4 ± 0.2	53.0 ± 1.3	56.3 ± 1.2
Griseofulvin	51.4 ± 0.3	51.9 ± 0.1	51.6 ± 0.1
Itraconazole	51.3 ± 0.3	51.0 ± 0.4	51.2 ± 0.4
Probucol	51.9 ± 0.6	51.3 ± 0.1	51.8 ± 0.2
Orlistat	50.8 ± 0.1	50.5 ± 0.1	51.1 ± 0.3

*Surface age of 25 ms

Table 9-6: Surface tension of different drug concentrations in LCT, surface age 25 ms

**Surface tension ± std. (mN/m) of different drug
concentrations in LCT
(value of pure oil: 34.97 ± 0.12)**

	Low	Intermediate	High
Danazol	35.6 ± 0.1	36.1 ± 0.5	37.0 ± 0.2
Felodipine	33.0 ± 0.0	31.1 ± 0.0	35.1 ± 0.2
Fenofibrate	35.4 ± 0.1	35.9 ± 0.2	36.3 ± 1.0
Griseofulvin	36.8 ± 0.2	35.3 ± 0.1	36.3 ± 0.1
Itraconazole	35.6 ± 0.1	35.2 ± 0.1	35.3 ± 0.0
Probucol	35.8 ± 0.0	35.7 ± 0.0	36.3 ± 0.2
Orlistat	33.3 ± 0.1	35.9 ± 0.0	33.5 ± 0.3

*Surface age of 250 ms

Table 9-7: Surface tension of different drug concentrations in LCT, surface age 250 ms

	Surface tension ± std. (mN/m) of different drug concentrations in LCT **(value of pure oil: 33.2 ± 0.4)**		
	Low	**Intermediate**	**High**
Danazol	32.9 ± 0.1	33.9 ± 0.2	34.5 ± 0.2
Felodipine	30.2 ± 0.2	30.3 ± 0	32.4 ± 0.3
Fenofibrate	32.3 ± 0.1	33.6 ± 0.2	35.2 ± 0.3
Griseofulvin	34.1 ± 0.2	34.3 ± 0.2	33.6 ± 0.2
Itraconazole	34.3 ± 0.1	33.0 ± 0.7	32.4 ± 0.1
Probucol	32.3 ± 0.1	33.8 ± 0.3	33.3 ± 0.2
Orlistat	30.2 ± 0.1	30.2 ± 0.1	30.2 ± 0.1

*Surface age of 2500 ms

Table 9-8: Surface tension of different drug concentrations in LCT, surface age 2500 ms
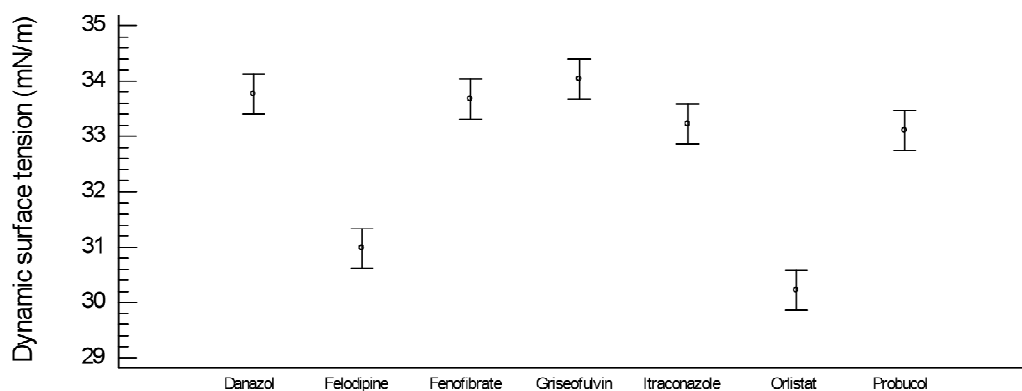
Figure 9-3: ANOVA means plot of drugs and their concentration effects on surface tension in LCT (means and 95% LSD intervals)

Density ± std. (g/cm³) of LCT including different drug concentrations
(value of pure oil: 0.910 ± 0)

	Low	Intermediate	High
Danazol	0.910 ± 0	0.910 ± 0	0.910 ± 0
Felodipine	0.909 ± 0	0.910 ± 0	0.910 ± 0
Fenofibrate	0.910 ± 0	0.915 ± 0	0.921 ± 0
Griseofulvin	0.910 ± 0	0.910 ± 0	0.910 ± 0
Itraconazole	0.910 ± 0	0.910 ± 0	0.910 ± 0
Probucol	0.910 ± 0	0.911 ± 0	0.913 ± 0
Orlistat	0.910 ± 0	0.910 ± 0	0.911 ± 0

Table 9-9: Density of LCT including different drug concentrations
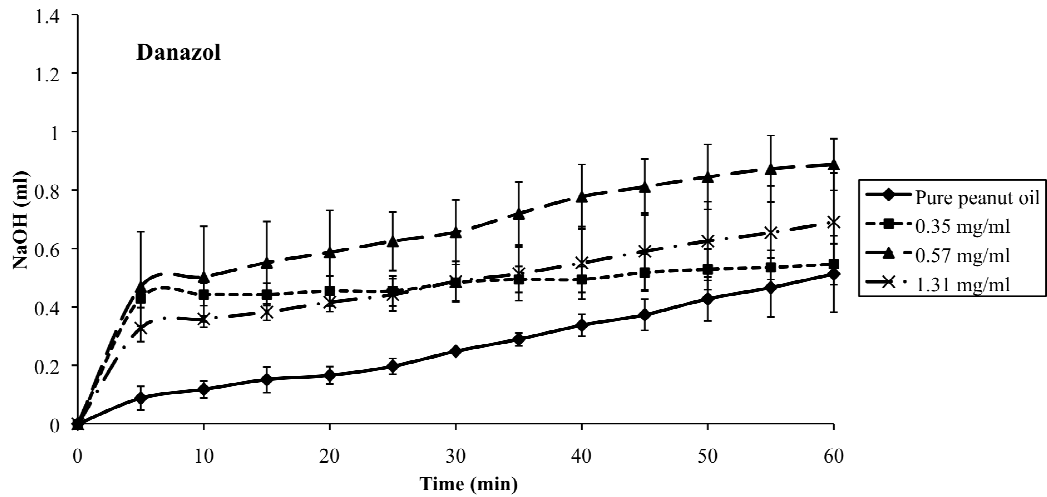
Figure 9-4: NaOH consumption in ml throughout lipolysis of 0.5 ml peanut oil and 0.5 ml peanut oil including three concentrations of danazol
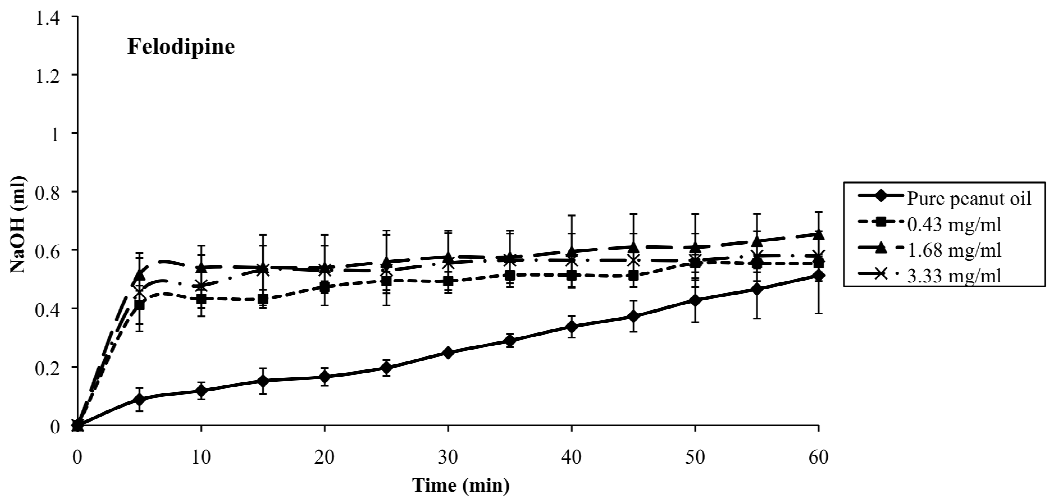
Figure 9-5: NaOH consumption in ml throughout lipolysis of 0.5 ml peanut oil and 0.5 ml peanut oil including three concentrations of felodipine
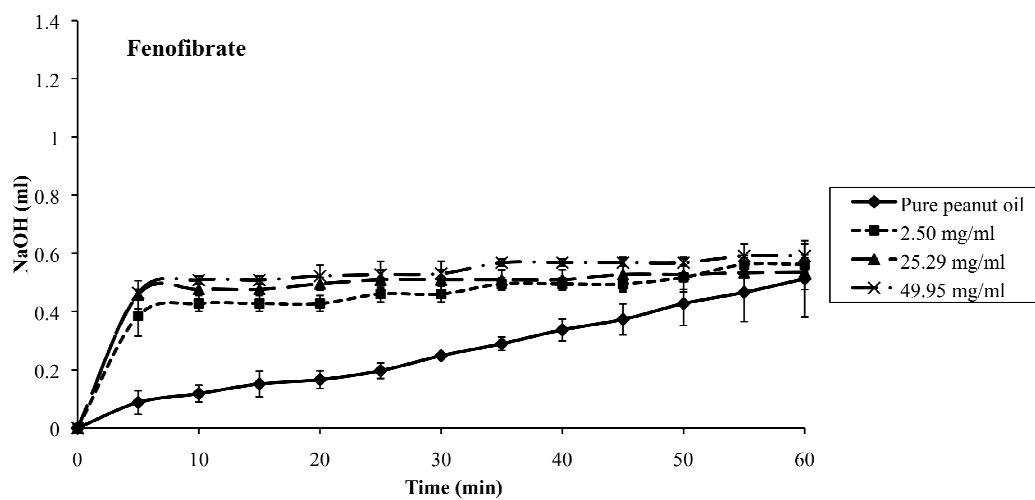
Figure 9-6: NaOH consumption in ml throughout lipolysis of 0.5 ml peanut oil and 0.5 ml peanut oil including three concentrations of fenofibrate
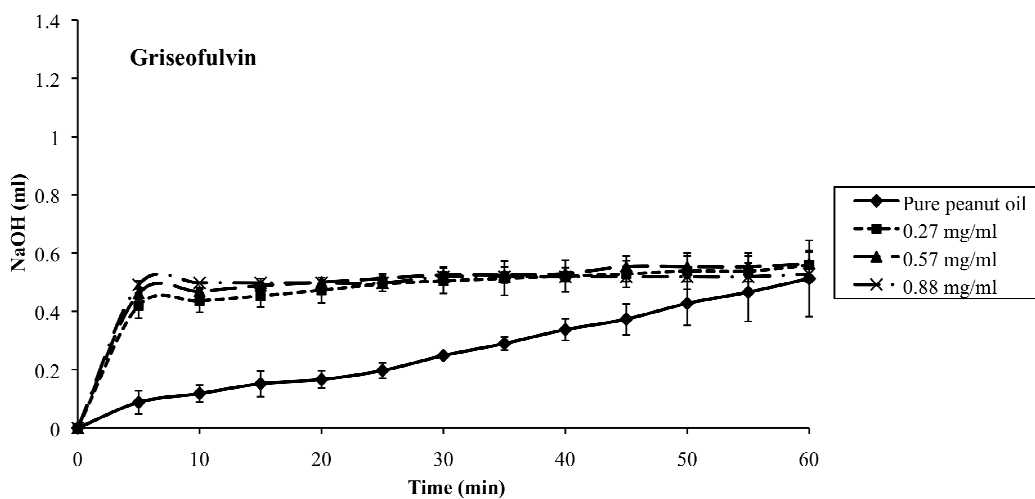
Figure 9-7: NaOH consumption in ml throughout lipolysis of 0.5 ml peanut oil and 0.5 ml peanut oil including three concentrations of griseofulvin

Figure 9-8: NaOH consumption in ml throughout lipolysis of 0.5 ml peanut oil and 0.5 ml peanut oil including three concentrations of itraconazole

Figure 9-9: NaOH consumption in ml throughout lipolysis of 0.5 ml peanut oil and 0.5 ml peanut oil including three concentrations of probucol
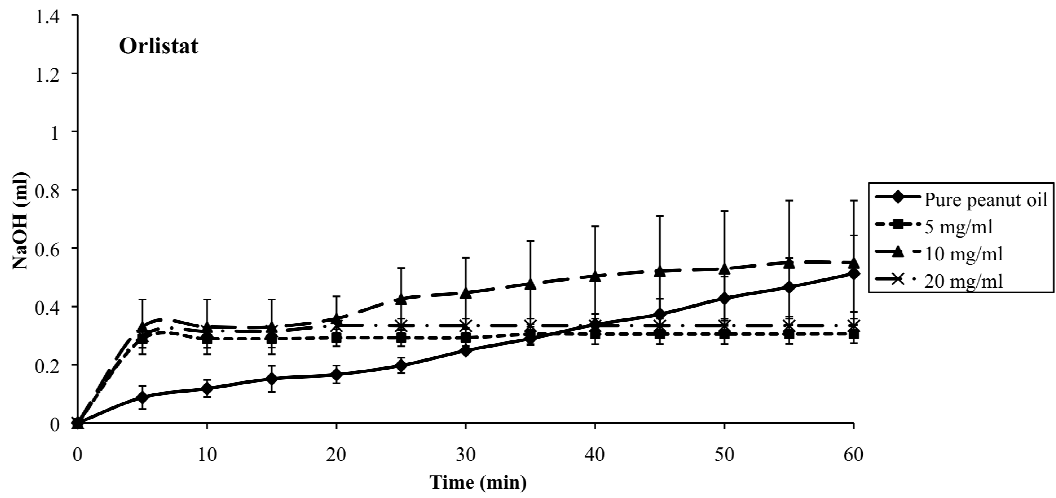
Figure 9-10: NaOH consumption in ml throughout lipolysis of 0.5 ml peanut oil and 0.5 ml peanut oil including three concentrations of orlistat
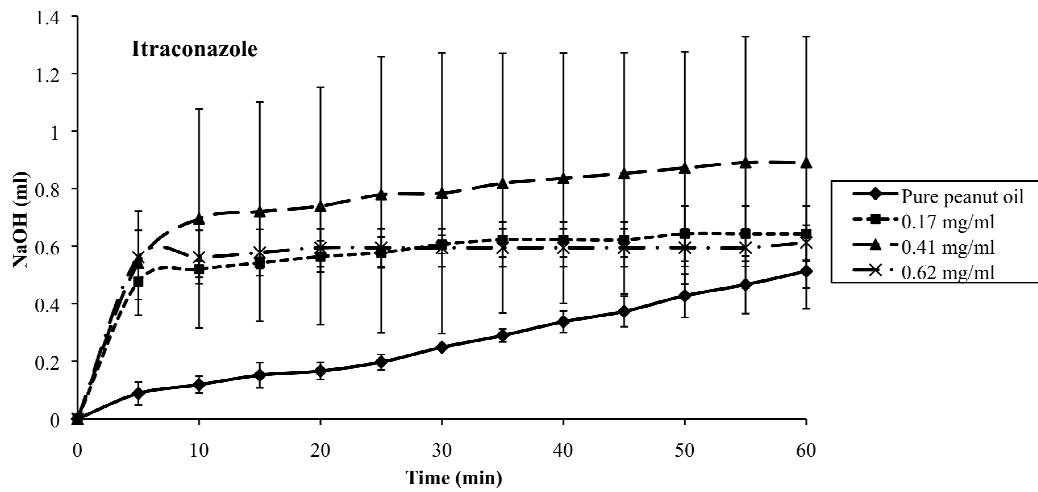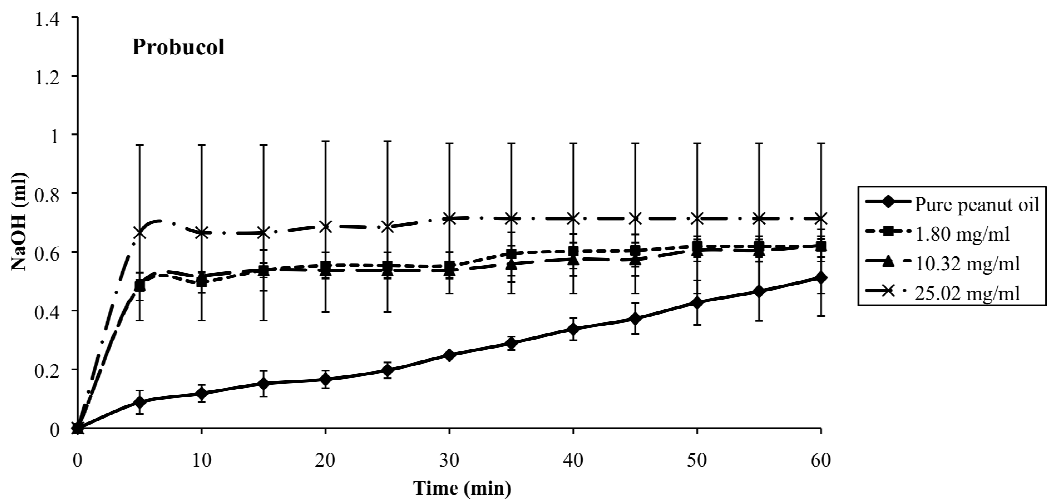
10 REFERENCES

Ali H, Nazzal M, Zaghloul AA, Nazzal S (2007). Comparison between lipolysis and compendial dissolution as alternative techniques for the in vitro characterization of α-tocopherol self-emulsified drug delivery systems (SEDDS). Int J Pharm 352:104-114.

Aloulou A, Rodriguez JA, Fernandez S, van Oosterhout D, Puccinelli D, Carrière F (2006). Exploring the specific features of interfacial enzymology based on lipase studies. Biochim Biophys Acta 1761:995-1013.

Alvarez FJ, Stella VJ (1989). The Role of Calcium Ions and Bile Salts on the Pancreatic Lipase-Catalyzed Hydrolysis of Triglyceride Emulsions Stabilized with Lecithin. Pharm Res 6(6):449-457.

Amidon GL, Lennernas H, Shah VP, Crison JR (1995). A Theoretical Basis for a Biopharmaceutic Drug Classification: The Correlation of In Vitro Drug Product Dissolution and In Vivo Bioavailability. Pharm Res 12:413-420.

Attwood D, Florence AT (1983). Surfactant systems: their chemistry, pharmacy and biology. London: Chapman and Hall.

Badawy SIF, Gray DB, Zhao F, Sun D, Schuster AE, Hussain MA (2006). Formulation of Solid Dosage Forms to Overcome Gastric pH Interaction of the Factor Xa, BMS-561389. Pharm Res 23(5):989-996.

Bakatselou V, Oppenheim RC, Dressman JB (1991). Solubilization and Wetting Effects of Bile Salts in the Dissolution of Steroids. Pharm Res 8(12):1461-1469.

Barker SA, Yap SP, Yuen KH, McCoy CP, Murphy JR, Craig DQM (2003). An investigation into the structure and bioavailability of α-tocopherol dispersions in Gelucire 44/14. J Control Rel 91:477-488.

Barrett P, Glennon B (1999). In-line FBRM Monitoring of Particle Size in Dilute Agitated Suspensions. Part Part Syst Charact 16:207-211.

Blum RA, D'Andrea DT, Florentino BM, Wilton JH, Hilligoss DM, Gardner MJ, Henry EB, Goldstein H, Schentag JJ (1991). Increased Gastric pH and the Bioavailability of Fluconazole and Ketoconazole. Ann Intern Med 114:755-757.

Brewster ME, Vandecruys R, Peeters J, Neeskens P, Verreck G, Loftsson T (2008). Comparative interaction of 2-hydroxypropyl-ß-cyclodextrin with intraconazole: Phase-solubility behavior and stabilization of supersaturated drug solutions. Eur J Pharm Sci 34:94-103.

Brouwers J, Brewster ME, Augstijns P (2009). Supersaturating Drug Delivery Systems: The Answer to Solubility-Limited Oral Bioavailability? J Pharm Sci 98(8):2549-2572.

Bugay DE (2001). Characterization of the solid-state : spectroscopic techniques. Adv Drug Del Rev 48:43-65.

Cao Y, Marra M, Andersen BD (2004). Predictive Relationships for the Effects of Triglyceride Ester Concentration and Water Uptake on Solubility and Partitioning of Small Molecules into Lipid Vehicles. J Pharm Sci 93(11): 2768-2779.

Chambin O, Karbowiak T, Djebili L, Jannin V, Champion D, Pourcelot Y, Cayot P (2009). Influence of drug polarity upon the solid-state structure and release properties of self-emulsifying drug delivery systems in relation with water affinity. Colloid Surface B 71:73-78.

Charman WN, Porter C, Mithani S, Dressman JB (1997). Physicochemical and physiological mechanisms for the effects of food on drug absoprtion: the role of lipids and pH. J Pharm Sci 86(3):269-282.

Chen Y, Xianggen GL, Chen Z, Hang J, Qin B, Chen S, Wang R (2008). Self-microemulsifying drug delivery systems (SMEDDS) of vinpocetine: formulation development and in vivo assessment. Bio Pharm Bull 31(1):118-125.

Chew JW, Chow PS, Tan RBH (2007). Automated In-line Technique Using FBRM to Achieve Consistent Product Quality in Cooling Crystallization. Crys Growth Des 7(8):1416-1422.

Christensen JO, Schultz K, Mollgaard B, Kristensen HG, Muellertz A (2004). Solubilization of poorly water-soluble medium- and long-chain triacylglycerols. Eur J Pharm Sci 23:287-296.

Christiansen A, Backensfeld T, Weitschies W (2010). Effects of non-ionic surfactants on *in vitro* triglyceride digestion and their susceptibility to digestion by pancreatic enzymes. Eur J Pharm Sci 41(2):376-382.

Cohen JL, Hubert BB, Leeson LJ, Rhodes CT, Robinson JR, Roseman TJ, Shefter E (1990). The Development of USP Dissolution and Drug Release Standards. Pharm Res 7(10):983-987.

Cole ET, Cadé D, Benameur H (2008). Challenges and opportunities in the encapsulation of liquid and semi-solid formulations into capsules for oral administration. Adv Drug Del Rev 60:747-756.

Cuiné JF, McEvoy CL, Charman WN, Pouton CW, Edwards GA, Benameur H, Porter CJ (2007). Evaluation of the impact of surfactant digestion on the bioavailability of danazol after oral administration of lipidic self-emulsifying formulations to dog. J Pharm Sci 97(2):995-1012.

Dahan A, Hoffman A (2006). Use of a Dynamic in Vitro Lipolysis Model to Rationalize Oral Formulation Development for Poor Water Soluble Drugs: Correlation with in Vivo Data and the Relationship to Intra-Enterocyte Processes in Rats. Pharm Res 23(9):2165-2174.

Dahan A, Hoffman A (2007). The effect of different lipid-based formulations on the oral absorption of lipophilic drugs: The ability of in vitro lipolysis and consecutive ex vivo intestinal permeability data to predict in vivo bioavailability in rats. Eur J Pharm Biopharm 67:96-105.

Dahan A, Hoffman A (2008). Rationalizing the selection of oral lipid based drug delivery systems by an in vitro lipolysis model for improved oral bioavailability of poorly soluble drugs. J Control Rel 129:1-10.

Dahan A, Miller JM, Amidon GL (2009). Prediction of Solubility and Permeability Class Membership: Provisional BCS Classification of the World's Top Oral Drugs. AAPS J 11(4):740-746.

de Campo L, Yaghmur A, Garti N, Leser ME, Folmer B, Glatter O (2004). Five-component food-grade microemulsion: structural characterization by SANS. J Colloid Interf Sci 274(1):251-267.

Ditner C, Bravo R, Imanidis G, Kuentz M (2009). A systematic dilution study of self-microemulsifying drug delivery systems in artificial intestinal fluid using dynamic laser light backscattering. Drug Dev Ind Pharm 35(2):199-208.

Dollery C (1998). Therapeutic Drugs. 2nd ed., Edinburg London: Churchill Linvingstone. p I41-I43.

Dressman JB, Amidon GL, Reppas C, Shah VP (1998). Dissolution Testing as a Prognostic Tool for Oral Drug Absorption: Immediate Release Dosage Forms. Pharm Res 15(1):11-22.

Dressman JB, Reppas C (2000). In vitro-in vivo correlations for lipophilic, poorly water-soluble drugs. Eur J Pharm Sci 11(2):S73-S80.

Dressman J, Schamp K, Beltz K (2007). Characterizing Release from Lipid-Based Formulations. In: Hauss DJ, Oral Lipid-Based Formulations, Enhancing the Bioavailability of Poorly Water-Soluble Drugs. New York: Informa Healthcare USA, Inc.

Embleton JK, Pouton CW (1997). Structure and function of gastro-intestinal lipases. Adv Drug Del Rev 25:15-32.

Erdemir D, Lee AYL, Myerson AS (2008). Nucleation of Crystals from Solution: Classical and Two-Step Models. Accounts Chem Res 42(5): 621-629.

European Pharmacopeia (2008). 6th ed.

Fatouros DG, Deen GR, Arleth L, Bergenstahl B, Nielsen FS, Flemming SN, Pedersen JK, Muellertz A (2007). Structural Development of Self Nano Emulsifying Drug Delivery Systems (SNEDDS) During In Vitro Digestion Monitored by Small-angle X-ray Scattering. Pharm Res 24(10):1844-1853.

Fatouros DG, Nielsen FS, Douroumis D, Hadjileontiadis LJ, Muellertz A (2008). In vitro-in vivo correlations of self-emulsifying drug delivery systems combining the dynamic lipolysis model and neuro-fuzzy networks. Eur J Pharm Biopharm 69(3):887-898.

Fatouros D, Muellertz A (2008). In vitro lipid digestion models in design of drug delivery systems for enhancing oral bioavailability. Expert Opin Drug Metab Toxicol 4(1):65-76.

Fernandez S, Jannin V, Rodier J, Ritter N, Mahler B, Carrière F (2007). Comparative study on digestive lipase activities on the self emulsifying excipient Labrasol, medium chain glycerides and PEG esters. Biochim Biophys Acta 1771(5):633-640.

Fernandez S, Rodier JD, Ritter N, Mahler B, Demarne F, Carrière F, Jannin V (2008). Lipolysis of the semi-solid self-emulsifying excipient Gelucire[®]44/14 by digestive lipases. Biochim Biophys Acta 1781:367-375.

Fernandez S, Chevrier S, Ritter N, Mahler B, Demarne F, Carrière F, Jannin V (2009). In vitro Gastrointestinal Lipolysis of Four Formulations of Piroxicam and Cinnarizine with the Self Emulsifying Excipients Labrasol[®] and Gelucire[®] 44/14. Pharm Res 26(8):1901-1910.

Fleisher D, Li C, Zhou Y, Pao L, Karim A (1999). Drug, Meal and Formulation Interactions Influencing Drug Absorption After Oral Administration. Clin Pharmacokinet 36(3):233-254.

Galia E, Nicolaides E, Hoerter D, Loebenberg R, Reppas C, Dressman JB (1998). Evaluation of various dissolution media for predicting in vivo performance of class I and II drugs. Pharm Res 15(5):698-705.

Gao P, Akrami A, Alvarez F, Hu J, Ma C, Surapaneni S (2009). Characterization and Optimization of AMG 517 Supersaturable Self-Emulsifying Drug Delivery System (S-SEEDS) for Improved Oral Absorption. J Pharm Sci 98(2):516-528.

Gargouri Y, Julien R, Bois AG, Verger R, Sarda L (1983). Studies on the detergent inhibition of pancreas lipase activity. J Lipid Res 24:1336-1342.

Geigy JR-PA (1973). Wissenschaftliche Tabellen. 7. Auflage, Basel: Documenta Geigy.

Gershanik T, Benita S (2000). Self-dispersing lipid formulations for improving oral absorption of lipophilic drugs. Eur J Phar Biopharm 50(1):179-188.

Gibbs JW (1948). The collected works of J. Willard Gibbs. Vol. I, Thermodynamics, New Haven: Yale University Press.

Goddeeris C, Coacci J, Van de Mooter G (2007). Correlation between digestion of the lipid phase of smedds and the release of the anti-HIV drug UC 781 and the anti-mycotic drug enilconazol from smedds. Eur J Pharm Biopharm 66:173-181.

Gu C, Rao D, Gandhi RB, Hilden J, Raghavan K (2004). Using a Novel Multicompartment Dissolution System to Predict the Effect of Gastric pH on the Oral Absorption of Weak Bases with Poor Intrinsic Solubility. J Pharm Sci 94:199-208.

Guay DRP (1999). Micronized fenofibrate: A new fibric and hyolipidemic agent. Ann Pharmacother 33:1083-1103.

Gursoy RN, Benita S (2004). Self-emulsifying drug delivery systems (SEDDS) for improved oral delivery of lipophilic drugs. Biomed Pharmacother 58:173-182.

Hadvàry P, Lengsfeld H, Wolfer H (1988). Inhibition of pancreatic lipase in vitro by the covalent inhibitor tetrahydrolipstatin. Biochem J 256(2):357-361.

Hall DG (1992). The dependence of lipid monolayer lipolysis on surface pressure. Biochem J 278:73-78.

Han SF, Yao TT, Zhang XX, Gan L, Zhu C, Yu HZ, Gan Y (2009). Lipid-based formulations to enhance oral bioavailability of the poorly water-soluble drug anethol trithione: Effects of lipid composition and formulation. Int J Pharm 379:18-24.

Hauptmann JB, Jeunet FS, Hartmann D (1992). Initial studies in humans with the novel gastrointestinal lipase inhibitor Ro 18-0647 (tetrahydrolipstatin). Am J Clin Nutr 55(1):309S-313S.

Heinz A, Gordon KC, McGoverin CM, Rades T, Strachan CJ (2009). Understanding the solid-state forms of fenofibrate – A spectroscopic and computational study. Eur J Pharm Biopharm 71:100-108.

Hermanto MW, Chow PS, Tan RBH (2010). Implementation of Focused Beam Reflectance Measurement (FBRM) in Antisolvent Crystallization to Achieve Consistent Product Quality. Crys Growth Des 10:3668-3674.

Hernell O, Staggers JE, Carey MC (1990). Physical-Chemical Behavior of Dietary and Biliary Lipids during Intestinal Digestion and Absorption. 2. Phase Analysis and Aggregation States of Luminal Lipids during Duodenal Fat Digestion in Healthy Adult Human Beings. Biochemistry-US 29:2041-2056.

Herzlich BC, Schiano TD, Moussa Z, Zimbalist E, Panagopoulos G, Ast A, Nawabi I (1992). Decreased intrinsic factor secretion in AIDS: relation to parietal cell acid secretory capacity and vitamin B12 malabsorption. Am J Gastroenterol 87:1781-1788.

Holm R, Joergensen EB, Harborg M, Larsen R, Holm P, Muellertz A, Jacobsen J (2011). A novel excipient, 1-perfluorohexyloctane shows limited utility for the oral delivery of poorly water-soluble drugs. Eur J Pharm Sci 42(4):416-422.

Hong JY, Kim JK, Song YK, Park JS, Kim CK (2006). A new self-emulsifying formulation of itraconazole with improved dissolution and oral absorption. J Control Release 110(2):332-338.

Humberstone AJ, Charman WN (1997). Lipid-based vehicles for the oral delivery of poorly water soluble drugs. Adv Drug Del Rev 25:103-128.

Hutchison K (1994). Digestible emulsions and microemulsions for optimum oral delivery of hydrophobic drugs. ed., B.T. Gattefossé. p 67-74.

Ilardia-Arana D, Kristensen HG, Muellertz A (2006). Biorelevant dissolution media: Aggregation of amphiphilies and solubility of estradiol. J Pharm Sci 95(2): 248-255.

Jahnke S (1998). The theory of high-pressure homogenization. In: Mueller RH, Benita S, Boehm B, Emulsions and Nanosuspensions for the Formulation of Poorly Soluble Drugs. p 177-200.

Jantratid E, Janssen N, Reppas C, Dressman JB (2008). Dissolution Media Simulating Conditions in the Proximal Human Gastrointestinal Tract: An Update. Pharm Res 25(7):1663-1676.

Juenemann D, Jantratid E, Wagner C, Reppas C, Vertzoni M, Dressman JB (2011). Biorelevant *in vitro* dissolution testing of products containing micronized or nanosized fenofibrate with a view to predicting plasma profiles. Eur J Pharm Biopharm 77:257-264.

Kalantzi L, Goumas K, Kalioras V, Abrahamsson B, Dressman JB, Reppas C (2006). Characterization of the Human Upper Gastrointestinal Contents Under Conditions Simulating Bioavailability/Bioequivalence Studies. Pharm Res 23(1):165-176.

Kaukonen AM, Boyd BJ, Porter CJH, Charman WN (2004). Drug Solubilization Behavior During in Vitro Digestion of Simple Triglyceride Lipid Solution Formulations. Drug Pharm Res 21(2):245-260.

Kee NCS, Arendt PD, Goh LM, Tan RBH, Braatz RD (2011). Nucleation and growth kinetics estimation for L-phenylalanine hydrate and anhydrate crystallization. CrystEngComm 13:1197-1209.

Kierkels JGT, Vleugels LFW, Kern JH, Meijer EM, Kloosterman M (1990). Lipase kinetics: On-line measurement of the interfacial area of emulsions. Enzyme Microb Technol 12:760-763.

Kim JY, Ku YS (2000). Enhanced absorption of Indomethacin after oral or rectal administration of a self-emulsifying system containing Indomethacin in rats. Int J Pharm 194:81-89.

Kirwan DJ, Orella CJ (2002). Crystallisation in the Pharmaceutical and Bioprocessing Industries. In Myerson AS. Handbook of Industrial Crystallization. 2nd ed., Woburn: Butterworth-Heinemann.

Knezevic ZD, Siler-Marinkovic SS, Mojovic LV (1998). Kinetics of lipase-catalyzed hydrolysis of palm oil in lecithin/isooctane reversed micelles. Appl Microbiol Biotechnol 49:267-271.

Kobayashi M, Sada N, Sugawara M, Iseki K, Miyazaki K (2001). Development of a new system for prediction of drug absorption that takes into account drug dissolution and pH change in the gastro-intestinal tract. Int J Pharm 221:87-94.

Kohri N, Yoshi YY, Xin H, Iseki K, Sato N, Todu S, Miyazaki K (1999). Improving the Oral Bioavailability of Albendazole in Rabbits by the Solid Dispersion Technique. J Pharm Pharmacol 51:159-164.

Kostewicz ES, Brauns U, Becker R, Dressman JB (2001). Forecasting the oral absorption behavior of poorly soluble weak bases using solubility and dissolution studies in biorelevant media. Pharm Res 19:345-349.

Kostewicz ES, Wunderlich M, Brauns U, Becker R, Bock T, Dressman J (2004). Predicting the precipitation of poorly soluble weak bases upon entry in the small intestine. J Pharm Pharmacol 56(1):43-51.

Kosugi Y, Suzuki H (1983). New Parameters for Simulating Progress Curves of the Lipase Reaction. J Ferment Technol 61(3):287-294.

Kuentz M (2008). Drug absorption modeling as a tool to define the strategy in clinical formulation development. AAPS J 10(3):473-479.

Kuentz M (2011). Oral self-emulsifying drug delivery systems, from biopharmaceutical to technical formulation aspects. J Drug Del Sci Tech 21(1):17-26.

Laidler KJ, Bunting PS (1973). The chemical kinetics of enzyme action. 2th ed., Oxford: Clarendon.

Lamer V, Dinegar R (1950). Theory, production and mechanism of formation of monodispersed hydrosols. J Am Chem Soc 72:4847-4854.

Larsen A, Holm R, Pedersen ML, Muellertz A (2008). Lipid-based Formulations for Danazol Containing a Digestible Surfactant, Labrafil M2125CS: *In Vivo* Bioavailability and Dynamic *In Vitro* Lipolysis. Pharm Res 25(12):2769-2777.

Larsen AT, Sassene P, Muellertz A (2011). *In vitro* lipolysis models as a tool for the characterization of oral lipid and surfactant based drug delivery systems. Int J Pharm 417(1-2):245-255.

Laurent S, Ivanova MG, Pioch D, Graille J, Verger R (1994). Interactions between β-cyclodextrin and insoluble glyceride molecular films at the argon/water interface: application to lipase kinetics. Chem Phys of Lipids 70:35-42.

Lehto P, Aaltonen J, Tenho M, Rantanen J, Hirvonen J, Tanninen VP, Peltonen L (2009). Solvent-Mediated Solid Phase Transformation of Carbamazepine: Effects of Simulated Intestinal Fluid and Fasted State Simulated Intestinal Fluid. J Pharm Sci 98(3):985-996.

Leyssens T, Baudry C, Escudero Hernandez ML (2011). Optimization of a Crystallization by Online FBRM Analysis of Needle-Shaped Crystals. Org Process Res Dev 15:413-426.

Lin MY, Lindsay HM, Weitz DA, Ball RC, Klein R, Meakin P (1989). Universality in colloid aggregation. Nature 339:360-362.

Lindfors L, Forssén S, Westergren J, Olsson U (2008). Nucleation and crystal growth in supersaturated solutions of a model drug. J Colloid Interf Sci 325(2):404-413.

Loftsson T, Brewster ME (2010). Pharmaceutical applications of cyclodextrins: basic science and product development. J Pharm Pharmacol 62:1607-1621.

Lunn G, Schmuff NR (1997-2000). HPLC Methods for Pharmaceutical Analysis. New York: Wiley.

MacGregor KJ, Embleton JK, Lacy JE, Perry AE, Solomon J, Seager H, Pouton CW (1997). Influence of lipolysis on drug absorption from the gastro-intestinal tract. Adv Drug Del Rev 25:33-46.

Macheras P, Iliadis A (2002). Modeling in Biopharmaceutics, Pharmacokinetics, and Pharmacodynamics. 1st ed.: Springer Science + Business.

Mohsin K, Long MA, Pouton CW (2009). Design of lipid-based formulations for oral administration of poorly water-soluble drugs: precipitation of drug after dispersion of formulations in aqueous solution. J Pharm Sci 98(10):3582-3595.

Mongkonwattanaleela S, Umprayn K, Chatchawalsaisin J (2010). The Effect of Emulsifiers And Oils On Droplet Size And Drug Loading Capacity Of Self-Emulsifying System. The 11th Graduate Research Conference, Khon Kaen University.

Mullin JW (2001), Crystallization. 4th ed., Woburn: Butterworth-Heinemann.

Myerson AS (2002). Handbook of Industrial Crystallization. 2th ed., Woburn: Butterworth-Heinemann.

Nioclaides E, Galia E, Efthymiopoulos C, Dressman JB, Reppas C (1999). Forecasting the In Vivo Performance of Four Low Solubility Drugs from Their In Vitro Dissolution Data. Pharm Res 16(12):1876-1882.

Odian G (2004). Principles of polymerization. 4th ed., Hoboken: Wiley-Interscience.

O'Driscoll CM (2002). Lipid-based formulations for intestinal lymphatic delivery. Eur J Phar Sci 15(5):405-415.

O'Driscoll CM, Griffin BT (2008). Biopharmaceutical challenges associated with drugs with low aqueous solubility – the potential impact of lipid-based formulation. Adv Drug Del Rev 60:617-624.

Ostwald W (1897). Studien über die Bildung und Umwandlung fester Körper. Z Phys Chem 22:289-330.

Panaiotov I, Ivanova M, Verger R (1997). Interfacial and temporal organization of enzymatic lipolysis. Curr Opin Colloid In 2(5):517-525.

Patel AR, Vavia PR (2007). Preparation and In Vivo Evaluation of SMEDDS (Self-Microemulsifying Drug Delivery System) Containing Fenofibrate. AAPS J 9(3): E344-E352.

Persson EM, Gustafsson A, Carlsson AS, Nilsson RG, Knutson L, Forsell P, Hanisch G, Lennernäs H, Abahamsson B (2005). The Effect of Food on the Dissolution of Poorly Soluble Drugs in Human and in Model Small Intestinal Fluids. Pharm Res 22(12):2141-2151.

Porter CJH, Charman WN (2001). In vitro assessment of oral lipid based formulations. Adv Drug Deliv Rev 50:S127-S147.

Porter CJH, Kaukonen AM, Taillardat- Bertschinger A, Boyd BJ, O'Connor JM, Edwards GA, Charman WN (2004). Use of in vitro lipid digestion data to explain the in vivo performance of triglyceride-based oral lipid formulations of poorly water-soluble drugs: studies of halofantrine. J Pharm Sci 93:1110-1121.

Porter CJH, Trevaskis NL, Charman WN (2007). Lipids and lipid-based formulations: optimizing the oral delivery of lipophilic drugs. Nat Rev Drug Discov 6:231-248.

Porter CW, Pouton CW, Cuine JF, Charman WN (2008). Enhancing intestinal drug solubilisation using lipid-based delivery systems. Adv Drug Del Rev 60(6):673-691.

Pouton CW (1985a). Effects of the inclusion of a model drug on the performance of self-emulsifying formulations. J Pharm Pharmacol 37:p 1P.

Pouton CW (1985b). Self-emulsifying drug delivery systems: assessment of the efficiency of emulsification. Int J Pharm 27:335-348.

Pouton CW (2000). Lipid formulations for oral administration of drugs: non-emulsifying, self-emulsifying and self-microemulsifying drug delivery systems. Eur J Pharm Sci 11(2):S93-S98.

Pouton CW (2006). Formulation of poorly water-soluble drugs for oral administration: physicochemical and physiological issues and the lipid formulation classification system. Eur J Pharm Sci 29(3-4):278-287.

Pouton CW, Porter CJ (2008). Formulation of lipid-based delivery systems for oral administration: materials, methods and strategies. Adv Drug Del Rev 60(6):625-637.

Rabinow BE (2004). Nanosuspensions in drug delivery. Nat Rev Drug Discov 3: 785-796.

Rangel-Yagui CO, Pessoa-Jr A, Costa Tavares L (2005). Micellar solubilization of drugs. J Pharm Pharmaceut Sci 8(2):147-163.

Reymond J, Sucker H (1988). In Vitro Model for Ciclosporin Intestinal Absorption in Lipid Vehicles. Pharm Res 5(10):673-676.

Russel TL, Berardi RR, Barnett JL, O'Sullivan TL, Wagner JG, Dressman JB (1994). pH-Related Changes in the Absorption of Dipyridamole in the Elderly. Pharm Res 11(1):136-143.

Savolainen M, Kogermann K, Heinz A, Aaltonen J, Peltonen L, Strachan C, Yliruusi J (2009). Better understanding of dissolution behaviour of amorphous drugs by in situ solid-state analysis by means of Raman spectroscopy. Eur J Pharm Biopharm 71:71-79.

Schiller C, Froehlich CP, Giessmann W, Siegmund W, Moennikes H, Hosten N, Weitschies W (2005). Intestinal fluid volumes and transit of dosage forms as assessed by magnetic resonance imaging. Aliment Pharmacol Ther 22:971-979.

Schwebel HJ, van Hoogevest P, Leight MLS, Kuentz M (2010). The apparent solubilizing capacity of simulated intestinal fluids for poorly water-soluble drugs. Pharm Dev Technol (online available):1-9.

Sek L, Porter CJH, Kaukonen AM, Charman WN (2002). Evaluation of the in-vitro digestion profiles of long and medium chain glycerides and the phase behaviour of their lipolytic products. J Pharm Pharmacol 54:29-41.

Shafer RB, Levine AS, Marlette JM, Morley JE (1985). Do calories, osmolality, or calcium determine gastric emptying? Am J Physiol 248(4):R479-483.

Shah NH, Carvajal MT, Patel CI, Infeld MH, Malick AW (1994). Self-emulsifying drug delivery systems (SEDDS) with polyglycolyzed glycerides for improving in vitro dissolution and oral absorption of lipophilic drugs. Int J Pharm 106:15-23.

Shekunov BY, York P (2000). Crystallization processes in pharmaceutical technology and drug delivery design. J Cryst Growth 211:122-136.

Simon LL, Nagy ZK, Hungerbuehler K (2009). Comparison of external bulk video imaging with focused beam reflectance measurement and ultra-violet visible spectroscopy for metastable zone identification in food and pharmaceutical crystallization processes. Chem Eng Sci 64:3344-3351.

Small DM (1968). Size and Structure of Bile Salt Micelles. In Molecular Association in Biological and Related Systems; Goddard E, Advances in Chemistry, American Chemical Society: Washington, DC.

Small DM, Bourgès MC, Dervichian DG (1966). The biophysics of lipidic associations. I. The ternary systems lecithin-bile salt-water. Biochim Biophys Acta 125:563-580.

Stephenson GA, Forbes RA, Reutzel-Edens SM (2001). Characterization of the solid state: quantitative issues. Adv Drug Del Rev 48:67-90.

Strickley RG (2004). Solubilizing excipients in oral and injectable formulations. Pharm Res 21(2):201-230.

Strickley RG (2007). Oral lipid-based formulations: enhancing the bioavailability of poorly water soluble drugs. ed., New York: D.J. Hauss Ed., Informa Healthcare, Inc. p 1-31.

Sugano K (2009). A simulation of oral absorption using classical nucleation theory. Int J Pharm 378:142-145.

Sugawara M, Kadomura S, He X, Takekuma Y, Kohri N, Miyazaki K (2005). The use of an in vitro dissolution and absorption system to evaluate oral absorption of two weak bases in pH-independent controlled-release formulations. Eur J Pharm Sci 26(1):1-8.

Thi TD, Speybroeck MV, Barillaro V, Martens J, Annaert P, Augustijns P, Van Humbeeck J, Vermant J, Van den Mooter G (2009). Formulate-ability of ten compounds with different physicochemical profiles in SMEDDS. Eur J Pharm Sci 38:479-488.

Tiss A, Lengsfeld H, Carrière F, Verger R (2009). Inhibition of human pancreatic lipase by tetrahydrolipstatin: Further kinetic studies showing its reversibility. J Mol Cat B: Enzymatic 58:41-47.

Torchilin VP (2001). Structure and design of polymeric surfactant-base drug delivery systems. J Control Rel 73:137-172.

United States Pharmacopeia USP 34-NF 29 (2011). Rockville, MD, The United States Pharmacopeia Convention, Inc.

Valsami G, Macheras P (1995). Determination of fractal reaction dimension in dissolution studies. Eur J Pharm 3:163-169.

Van Krevelen DW (1997). Properties of Polymers: Their Correlation with Chemical Structure; Their Numerical Estimation and Prediction from Additive Group Contributions. Elsevier, Amsterdam, Netherlands, 898.

Vatier J, Vitré MT, Vallot T, Mignon M (1990). Capacité d'induction d'un gradient de pH et activité antiacide des pansements gastro-oesophagiens. Etude pharmacologique in vitro en utilisant le modèle de 'l'estomac artificiel'. Gastroenterol Clin Biol 14:414-422.

Vatier J, Celice-Pingaud C, Farinotti R (1998). A computerized artificial stomach model to assess sodium alginate-induced pH gradient. Int J Pharm 163(1-2):225-229.

Vauck WRA, Mueller HA (1994). Grundoperationen chemischer Verfahrenstechnik. 10 ed., Stuttgart: Deutscher Verlag für Grundstoffindustrie.

Veiga MD, Diaz PJ, Ahsan F (1998). Interactions of Griseofulvin with Cyclodextrins in Solid Binary Systems. J Pharm Sci 87:891-900.

Vekilov PG (2010). The two-step mechanism of nucleation of crystals in solution. Nanoscale 2:2346-2357.

Verger R, Haas GH (1976). Interfacial Enzyme Kinetics of Lipolysis. An Rev Biophys Bioeng 5:77-117.

Vertzoni M, Fotaki N, Kostewicz E, Stippler E, Leuner C, Nicolaides E, Dressman J, Reppas C (2004). Dissolution media simulating the intralumenal composition of the small intestine: physiological issues and practical aspects. J Pharm Pharmacol 56(4):453-462.

Vertzoni M, Dressman J, Butler J, Hempenstall J, Reppas C (2005). Simulation of fasting gastric conditions and its importance for the in vivo dissolution of lipophilic compounds. Eur J Pharm Biopharm 60(3):413-417.

Vogt M, Kunath K, Dressman JB (2008). Dissolution enhancement of fenofibrate by micronization, cogrinding and spray-drying: Comparison with commercial preparations. Eur J Pharm Biopharm 68:283-288.

Wagner JG (1977). Drug bioavailability studies. Hosp Pract 12:119-127.

Welling PG (1977). How food and fluid affect drug absorption. Postgrad Med 62:73-82.

Woo JS, Song YK, Hong JY, Lim S, Kim CK (2008). Reduced food-effect and enhanced bioavailability of a self-microemulsifying formulation of itraconazole in healthy volunteers. Eur J Pharm Sci 33(2):159-165.

Yanasarn N, Sloat B, Cui Z (2009). Nanoparticles engineered from lecithin-in-water emulsions as a potential delivery system for docetaxel. Int J Pharm 379:174-180.

Yazdanian M, Briggs K, Jankovsky C, Hawi A (2004). The 'high solubility' definition of the current FDA Guidance on Biopharmaceutical Classification System may be too strict for acidic drugs. Pharm Res 21(2):293-299.

Yokoyama M (1992). Block copolymers as drug carriers. CRC Crit Rev Ther Drug Carrier Syst 9(3-4):213-248.

Youngberg CA, Berardi RR, Howatt WF, Hyneck ML, Amidon GL, Meyer JH, Dressman JB (1987). Comparison of Gastrointestinal pH in Cystic Fibrosis and Healthy Subjects. Digest Dis Sci 32(5):472-480.

Yu LX, Lionberger RA, Raw AS, D'Costa R, Wu H, Hussain AS (2004). Applications of process analytical technology to crystallizatino processes. Adv Drug Del Rev 56:349-369.

Zangenberg NH, Muellertz A, Kristensen HG, Hovgaard L (2001). A dynamic in vitro lipolysis model. I. Controlling the rate of lipolysis by continuous addition of calcium. Eur J Pharm Sci 14:115-122.

Zangenberg NH, Muellertz A, Kristensen HG, Hovgaard L (2001). A dynamic in vitro lipolysis model. II. Evaluation of the model. Eur J Pharm Sci 14:237-244.

Zhang P, Liu Y, Feng N, Xu J (2008). Preparation and evaluation of self-microemulsifying drug delivery system of oridonin. Int J Pharm 355(1-2):269-276.

Zhou R, Moench P, Heran C, Lu X, Mathias N, Faria TN, Wall DA, Hussain MA, Smith RL, Sun D (2005). pH-Dependent Dissolution in Vitro and Absorption in Vivo of Weakly Basic Drugs: Development of a Canine Model. Pharm Res 22(2):188-192.

11 CURRICULUM VITAE

Yvonne Elisabeth Arnold
Pharmacist

Personal Details

Date of Birth   March 29, 1973
Place of Birth   Zurich
Nationality   Swiss

PhD Thesis

February 2008 -   PhD student at the Institute of Pharmaceutical Technology
November 2011   (University of Basel) and Institute of Pharma Technology (University of Applied Sciences, Muttenz) under supervision of Prof. Dr Georgios Imanidis and Prof. Dr Martin Kuentz, including a research stay at the ETH Zurich, Institute of Bio and Chemical Engineering, Safety and Environmental Technology Group.

Research article (not included in this thesis)
Kuentz MT, Arnold Y (2009). Influence of molecular properties on oral bioavailablilty of lipophilic drugs – Mapping of bulkiness and different measures of polarity. Pharm Dev Technol 14(3):312-320.

Supervision of the following projects

January – July 2009   Master thesis: "Entwicklung eines neuen in Vitro-Tests zur Untersuchung der Präzipitation von Wirkstoffen im Gastrointestinaltrakt"; Barbara Keiser, University of Basel.

Podium presentations

November 2010/   New online/inline analytical tools and a nucleation and growth
January 2011   model for drug precipitation upon transfer from simulated gastric to intestinal fluid. GPEN (Globalization of Pharmaceutics Education Network) Meeting 2010, University of North Carolina, Chapel Hill, North Carolina, United States/ Annual Research Meeting 2011, University of Basel, Switzerland.

April 2010   In vitro tests as useful tools to predict the solubilization behavior of poorly soluble drugs incorporated in lipid-based formulations. University of Applied Sciences, Muttenz, Switzerland.

Poster presentations

September 2011	Monitoring the influence of polysorbate 80 on the precipitation of fenofibrate under physiological conditions using FBRM. ISIC18 (18th International Symposium on Industrial Crystallization), Zurich, Switzerland.
November 2010	In vitro drug precipitation – a nucleation/growth model and new online analytical tools for a better process understanding. FIP Pharmaceutical Sciences World Congress 2010, New Orleans, Louisiana, United States (presented by Prof. Dr Martin Kuentz).
September 2010	In vitro drug precipitation testing of a poorly soluble weak base new online/inline analytical tools and a kinetic nucleation and growth model. Solutions for insoluble drugs, 25ème séminaire en sciences pharmaceutics, Zermatt, Switzerland.
January 2010	Study of different in vitro tests to assess oral lipid-based formulations using a poorly soluble acidic drug. Annual Research Meeting 2010, University of Basel, Switzerland.
June 2009	Comparison of different in-vitro tests to assess oral lipid-based formulations using indomethacin as model acidic drug. PharmSci Fair 2009 – Pharmaceutical Sciences Fair & Exhibition of the European Federation for Pharmaceutical Sciences, Nice, France.

Lectures

Annually	Introduction to Industrial Drug Development, Pharma Technology, and Manufacturing Processes – Generika. Lecture at the University of Applied Sciences of Northwestern Switzerland, Muttenz, Switzerland.

Trainings

October 2008	Sotax USP IV Seminar, Basel, Switzerland
May 2008	Erfolgreich formulieren mit modernen Tablettierhilfsstoffen, JS Pharma Kundenseminar, Basel, Switzerland
March 2008	Capsugel Mini Seminar, Illkirch, France

Education

2004	Staatsexamen to obtain degree of a pharmacist (Eidg. dipl. Apothekerin ETH) at the ETH, Zurich
1992	High school graduation (Maturität, Typus C) at Kantonsschule Zürich-Oerlikon, Zurich

Work Experience

2006 – 2008	Scientific officer at Kantonsapotheke, Zurich
2005 – 2006	Responsible Pharmacist at Linden-Apotheke, Bülach
2001 – 2004	Deputyships as cand. pharm. in several pharmacies: International Airport Pharmacy, Zurich-Airport; Linden-Apotheke, Bülach; Paracelsus-Apotheke, Einsiedeln; Sonnen-Apotheke, Niederglatt
2003	Diploma thesis at Paul Scherrer Institute, Villingen: 'Synthese und in vitro Evaluation von organometallischen Inhibitoren der humanen Thymidinkinase'
2000 -2001	Internship at Paracelsus-Apotheke, Einsiedeln
1992 -1996	Clerk assistant at SWICA Gesundheitsorganisation, Zurich

Additional Skills

Languages	German (native speaker)
	English (fluent)
	French (basic knowledge)
Computer skills	Microsoft Word, Excel, and Power Point
	CorelDRAW, Endnote, Easy Fit, Matlab

As a student and PhD student I have attended lectures and courses given by

Prof. Dr Hansruedi Altdorfer, Prof. Dr Nikolaus Amrhein, Prof. Dr Matthias Baltisberger, Prof. Dr Eric G. Berger, Prof. Dr Alexander A. Borbély, Prof. Dr Urs Boutellier, Prof. Dr Ernesto Carafoli, Prof. Dr Beat Ernst, Prof. Dr Gerd Folkers, PD Dr Herbert Hächler, PD Dr Bruno Gander, Prof. Dr Camille Ganter, Dr Roland Gebert, Prof. Dr Cesare Gessler, Prof. Dr Jörg Heilmann, Prof. Dr Ari Helenius, Dr Richard F. Hurrell, Prof. Dr Georgios Imandis, Dr Sven P. Inäbnit, Prof. Dr Fritz H. Kayser, Prof. Dr Reinhard O. Kissner, Prof. Dr Jana Kohl, PD Dr Stefanie Kraemer, Dr Hans U. Lutz, Dr Stephan Marrer, Prof. Dr Hans P. Merkle, Prof. Dr Hanns Möhler, Prof. Dr Markus Müntener, Prof. Dr Ingo Potrikus, Prof. Dr Paul Pregosin, Dr Christian Richner, Dr Silvia Rogers, Prof. Dr Leonardo Scapozza, Prof. Dr Pius Schubiger, Prof. Dr Otto Sticher, Dr Peter Thurnheer, Dr Michael Ulmschneider, Prof. Dr Dieter J. Vonderschmitt, Dr Penelope Vounatsu, Prof. Dr Kaspar H. Winterhalter, Prof. Dr David P. Wolfer, Prof. Dr Heidi Wunderli-Allenspach